

Workshop on
**RADAR INVESTIGATIONS OF
PLANETARY AND TERRESTRIAL ENVIRONMENTS**

February 7–10, 2005
Houston, Texas

Landsat 7

Jers-1

**WORKSHOP PROGRAM
AND ABSTRACTS**



LPI Contribution No. 1231

WORKSHOP ON
RADAR INVESTIGATIONS OF
PLANETARY AND TERRESTRIAL ENVIRONMENTS

February 7–10, 2005
Houston, Texas

Conveners

Essam Heggy,
Lunar and Planetary Institute
Stephen Clifford,
Lunar and Planetary Institute
Tom Farr,
Jet Propulsion Laboratory
Cynthia Dinwiddie,
Southwest Research Institute
Bob Grimm,
Southwest Research Institute

Sponsored by

Lunar and Planetary Institute
National Aeronautics and Space Administration
Jet Propulsion Laboratory
Southwest Research Institute

Scientific Organizing Committee

Stephen Arcone, <i>U.S. Army Cold Regions Research and Engineering Laboratory</i>	Dick Morris, <i>NASA Johnson Space Center</i>
Jean-Jacques Berthelier, <i>Centre d'étude des Environnements Terrestre et Planétaires</i>	Gary Olhoeft, <i>Colorado School of Mines</i>
Bruce Campbell, <i>Smithsonian Institution</i>	Yuri Ozorovich, <i>Russian Academy of Sciences Space Research Institute</i>
John Grant, <i>Smithsonian Institution</i>	Ali Safaeinili, <i>Jet Propulsion Laboratory</i>
Philippe Paillou, <i>Observatoire Aquitain des Sciences de L'Univers</i>	Wlodek Kofman, <i>Laboratoire de Planétologie de Grenoble</i>

Compiled by Lunar and Planetary Institute, 3600 Bay Area Boulevard, Houston TX 77058-1113. Logistics, administrative, and publications support for the workshop were provided by the Publications and Program Services Department of the LPI. The Lunar and Planetary Institute is operated by the Universities Space Research Association under Cooperative Agreement No. NCC5-679 with the National Aeronautics and Space Administration. Material in this publication may be copied without restraint for library, abstract service, educational, or research purposes; however, republication of any abstract or portion thereof requires the written permission of the authors as well as appropriate acknowledgement of this publication.

Compiled in 2005 by
LUNAR AND PLANETARY INSTITUTE

The Institute is operated by the Universities Space Research Association under Agreement No. NCC5-679 issued through the Solar System Exploration Division of the National Aeronautics and Space Administration.

Any opinions, findings, and conclusions or recommendations expressed in this volume are those of the author(s) and do not necessarily reflect the views of the National Aeronautics and Space Administration.

Material in this volume may be copied without restraint for library, abstract service, education, or personal research purposes; however, republication of any paper or portion thereof requires the written permission of the authors as well as the appropriate acknowledgment of this publication.

Abstracts in this volume may be cited as

Author A. B. (2005) Title of abstract. In *Workshop on Radar Investigations of Planetary and Terrestrial Environments*, p. XX. LPI Contribution No. 1231, Lunar and Planetary Institute, Houston.

This volume is distributed by

ORDER DEPARTMENT
Lunar and Planetary Institute
3600 Bay Area Boulevard
Houston TX 77058-1113, USA
Phone: 281-486-2172
Fax: 281-486-2186
E-mail: order@lpi.usra.edu

Mail orders requestors will be invoiced for the cost of shipping and handling.

Preface

This volume contains abstracts that have been accepted for presentation at the Workshop on Radar Investigations of Planetary and Terrestrial Environments, February 7–10, 2005, Houston, Texas.

Administration and publications support for this meeting were provided by the staff of the Publications and Program Services Department at the Lunar and Planetary Institute.

Contents

Program	1
Salt Kinematics and InSAR <i>P. Aftabi, C. Talbot, and E. Fielding</i>	17
SAR Interferometry as a Tool for Monitoring Coastal Changes in the Nile River Delta of Egypt <i>M. H. Aly, A. G. Klein, and J. R. Giardino</i>	18
Modern Radar Techniques for Geophysical Applications: Two Examples <i>B. J. Arokiasamy, C. Bianchi, U. Sciacca, G. Tutone, A. Zirizzotti, and E. Zuccheretti</i>	19
The WISDOM Experiment on the EXOMARS ESA Mission <i>J. J. Berthelier, S. E. Hamram, R. Ney, and WISDOM Team</i>	21
An Ice Thickness Study Utilizing Ground Penetrating Radar on the Lower Jamapa Glacier of Citlaltépetl (El Pico de Orizaba), Mexico <i>S. B. Brown, B. P. Weissling, and M. J. Lewis</i>	23
Probing the Martian Subsurface with Synthetic Aperture Radar <i>B. A. Campbell</i>	25
Planetary Surface Properties from Radar Polarimetric Observations <i>D. B. Campbell, L. M. Carter, B. A. Campbell, and N. J. Stacy</i>	27
Imaging the Sub-Surface Reflectors : Results from the RANETA/NETLANDER Field Test on the Antarctic Ice Shelf <i>V. Ciarletti, J. J. Berthelier, A. Le Gall, and A. Reineix</i>	28
Strategy for Selection of Mars Geophysical Analogue Sites <i>C. L. Dinwiddie, S. M. Clifford, R. E. Grimm, and E. Heggy</i>	29
Observations of Low Frequency Low Altitude Plasma Oscillations at Mars and Implications for Electromagnetic Sounding of the Subsurface <i>J. R. Easley, P. A. Cloutier, and G. T. Delory</i>	31
Ionospheric Transmission Losses Associated with Mars-orbiting Radar <i>W. M. Farrell</i>	32
A Polarimetric Scattering Model for the 2-Layer Problem <i>A. Freeman, B. A. Campbell, and Y. Oh</i>	33
Radars for Imaging and Sounding of Polar Ice Sheets <i>S. Gogineni, K. Jezek, J. Paden, C. Allen, P. Kanagaratnam, and T. Akins</i>	34
Strata: Ground Penetrating Radar for Mars Rovers <i>J. A. Grant, C. J. Leuschen, A. E. Schutz, J. Rudy, R. S. Bokulic, and K. K. Williams</i>	35
Scattering Limits to Depth of Radar Investigation: Lessons from the Bishop Tuff <i>R. Grimm, E. Heggy, S. Clifford, and C. Dinwiddie</i>	37

The Goldstone Solar System Radar: 1988-2003 Earth-based Mars Radar Observations <i>A. F. C. Haldemann, K. W. Larsen, R. F. Jurgens, and M. A. Slade</i>	39
Mapping Subsurface Stratigraphy and Anamolies in Iron-rich Volcanoclastics Using Ground-penetrating Radar: Potential for Shallow Sounding on Mars <i>E. Heggy, S. Clifford, R. Grimm, S. Gonzalez, D. Bannon, and D. Wyrick</i>	41
Dielectric Map of the Martian Surface <i>E. Heggy and A. Pommerol</i>	43
Surface Clutter Removal in Airborne Radar Sounding Data from the Dry Valleys, Antarctica <i>J. W. Holt, D. D. Blankenship, D. L. Morse, M. E. Peters, and S. D. Kempf</i>	45
Comparing Transient Electromagnetics and Low Frequency Ground Penetrating Radar for Sounding of Subsurface Water in Mars Analog Environments <i>J. A. Jernsletten and E. Heggy</i>	47
The MARSIS Radar, Signal Simulation and Interpretation Using MOLA Topography Data <i>W. Kofman, J. F. Nouvel, A. Hérique, and J.-E. Martelat</i>	49
A Phase Signature for Detecting Wet Structures in the Shallow Subsurface of Mars Using Polarimetric P-band SAR <i>Y. Lasne, Ph. Paillou, and J.-M. Malézieux</i>	50
Experimental Validation of the Mono and Bistatic Operating Mode of a GPR Dedicated to the Martian Subsurface Exploration <i>A. Le Gall, V. Ciarletti, J. J. Berthelier, R. Ney, F. Dolon, and S. Bonaimé</i>	52
Radar Sounding of Convecting Ice Shells in the Presence of Convection: Application to Europa, Ganymede, and Callisto <i>W. B. McKinnon</i>	53
A Tower-based Prototype VHF/UHF Radar for Subsurface Sensing: System Description and Data Inversion Results <i>M. Moghaddam, L. Pierce, A. Tabatabaenejad, and E. Rodriguez</i>	55
Application of Interferometric Radars to Planetary Geologic Studies <i>P. J. Mouginis-Mark, P. Rosen, and A. Freeman</i>	56
A Web-based Collaborative Tool for Mars Analog Data Exploration <i>M. Necsoiu, C. L. Dinwiddie, E. Heggy, and T. G. Farr</i>	58
Propagation of Radar Through the Martian Polar Layered Deposits <i>D. C. Nunes and R. J. Phillips</i>	59
Geoelectrical Markers and Oreols of Subsurface Frozen Structures on Mars for Long-Term Monitoring of Spatial and Temporal Variations and Changes of Martian Cryolitozone Structure on the Base Ground and Satellite Low-Frequency Radar Measurements <i>Y. R. Ozorovich and A. K. Lukomskiy</i>	61
Simulation of P-Band SAR Performances for Mars Exploration <i>Ph. Paillou, Y. Lasne, J.-M. Maleziéux, and E. Heggy</i>	63
High Power Amplifier Design Considerations for Europa Surface Penetrating Radar Application <i>T. Pett, J. Sechler, R. Keller, D. Hill, and M. Cabanas-Holmen</i>	65

SHARAD: Radar Sounder on the 2005 Mars Reconnaissance Orbiter <i>R. J. Phillips, R. Seu, and SHARAD Team</i>	66
The MARSIS Science Mission <i>J. J. Plaut, G. Picardi, and MARSIS Team</i>	68
Complementarity of Radar and Infrared Remote Sensing for the Study of Titan Surface <i>S. Rodriguez, S. Le Mouëlic, J. P. Combe, and C. Sotin</i>	69
Deep Interior Mission: Imaging the Interior of Near-Earth Asteroids Using Radio Reflection Tomography <i>A. Safaeinili, E. Asphaug, E. Rodriguez, E. Gurrola, M. Belton, K. Klaasen, S. Ostro, J. Plaut, and D. Yeoman</i>	71
High-Power Radar Sounders for the Investigation of Jupiter Icy Moons <i>A. Safaeinili, S. Ostro, E. Rodriguez, D. Blankenship, W. Kurth, and D. Kirchner</i>	72
EM Properties of Magnetic Minerals at RADAR Frequencies <i>D. E. Stillman and G. R. Olhoeft</i>	73
Ground-penetrating Radar in Mars Analog Terrains: Testing the Strata Instrument <i>K. K. Williams, J. A. Grant, and A. E. Schutz</i>	75
Invertibility of Radar Layers in the Martian North Polar Cap for Flow and Mass Balance Parameters <i>D. P. Winebrenner, M. A. Fahnestock, and E. D. Waddington</i>	77
Application of an Orbital GPR Model to Detecting Martian Polar Subsurface Features <i>Y. Xu, S. A. Cummer, and W. M. Farrell</i>	79
In-Situ Remote Sensing Reflectance Measurements in Case 2 Water <i>Y. Yan</i>	80

Program

Monday, February 7, 2005
MORNING SESSION I
8:30 a.m. Lecture Hall

WELCOME AND INTRODUCTIONS

PAST, PRESENT, AND POTENTIAL NEAR-FUTURE RADAR INVESTIGATIONS OF MARS

Beatty D. * [INVITED]

The Relationship of Radar Investigations to the Mars Program's Strategic Planning

Haldemann A. F. C. * Larsen K. W. Jurgens R. F. Slade M. A.

The Goldstone Solar System Radar: 1988–2003 Earth-based Mars Radar Observations [#6037]

Plaut J. J. * Picardi G. MARSIS Team [INVITED]

The MARSIS Science Mission [#6024]

Kofman W. * Nouvel J. F. Hérique A. Martelat J.-E.

The MARSIS Radar, Signal Simulation and Interpretation Using MOLA Topography Data [#6002]

10:00 – 10:15 a.m. BREAK

* Denotes Speaker

Monday, February 7, 2005
MORNING SESSION II
PAST, PRESENT, AND POTENTIAL
NEAR-FUTURE RADAR INVESTIGATIONS OF MARS (Continued)
10:15 a.m. Lecture Hall

Phillips R. J. * Seu R. SHARAD Team [INVITED]
SHARAD: Radar Sounder on the 2005 Mars Reconnaissance Orbiter [#6013]

Ciarletti V. * Berthelier J. J. Le Gall A. Reineix A. [INVITED]
Imaging the Sub-Surface Reflectors: Results from the RANETA/NETLANDER Field Test on the Antarctic Ice Shelf [#6027]

Grant J. A. * Leuschen C. J. Schutz A. E. Rudy J. Bokulic R. S. Williams K. K. [INVITED]
Strata: Ground Penetrating Radar for Mars Rovers [#6009]

12:00 – 1:30 p.m. LUNCH

Monday, February 7, 2005
AFTERNOON SESSION I
RADAR INVESTIGATIONS OF OTHER PLANETARY BODIES
1:30 p.m. Lecture Hall

Rodriguez S. * Le Mouëlic S. Combe J. P. Sotin C. [INVITED]
Complementarity of Radar and Infrared Remote Sensing for the Study of Titan Surface [#6023]

Pett T. * Sechler J. Keller R. Hill D. Cabanas-Holmen M.
High Power Amplifier Design Considerations for Europa Surface Penetrating Radar Application [#6031]

McKinnon W. B. *
Radar Sounding of Convecting Ice Shells in the Presence of Convection: Application to Europa, Ganymede, and Callisto [#6039]

3:00 – 3:15 p.m. BREAK

Monday, February 7, 2005
AFTERNOON SESSION II
RADAR INVESTIGATIONS OF OTHER PLANETARY BODIES (Continued)
3:15 p.m. Lecture Hall

Safaenili A. * Asphaug E. Rodriguez E. Gurrola E. Belton M. Klaasen K. Ostro S.
Plaut J. Yeoman D.

Deep Interior Mission: Imaging the Interior of Near-Earth Asteroids Using Radio Reflection Tomography [#6017]

DAY IN REVIEW DISCUSSION

5:00 – 7:00 p.m.

WELCOME RECEPTION

Tuesday, February 8, 2005
MORNING SESSION I
8:30 a.m. Lecture Hall

REVIEW OF DAY'S AGENDA

A FOCUS FOR WORKSHOP DISCUSSION AND RECOMMENDATIONS

Clifford S. * [INVITED]

Seeking Consensus on a Best-Effort, Two-Mission Approach to Identifying the Global History and the Present Distribution and State of Subsurface Water on Mars

INVESTIGATIONS OF THE MARTIAN POLAR REGIONS AND POLAR ANALOGS

Xu Y. * Cummer S. A. Farrell W. M.

Application of an Orbital GPR Model to Detecting Martian Polar Subsurface Features [#6022]

Nunes D. C. * Phillips R. J.

Propagation of Radar Through the Martian Polar Layered Deposits [#6016]

10:00 – 10:15 a.m. BREAK

Tuesday, February 8, 2005
MORNING SESSION II
INVESTIGATIONS OF THE MARTIAN POLAR
REGIONS AND POLAR ANALOG ENVIRONMENTS (*Continued*)
10:15 a.m. Lecture Hall

Brown S. B. * Weissling B. P. Lewis M. J.
An Ice Thickness Study Utilizing Ground Penetrating Radar on the Lower Jamapa Glacier of Citlaltépetl
(El Pico de Orizaba), Mexico [#6020]

Winebrenner D. P. * Fahnestock M. A. Waddington E. D.
Invertibility of Radar Layers in the Martian North Polar Cap for Flow and Mass Balance Parameters [#6033]

Gogineni S. * Jezek K. Paden J. Allen C. Kanagaratnam P. Akins T.
Radars for Imaging and Sounding of Polar Ice Sheets [#6041]

12:00 – 1:30 p.m. LUNCH

Tuesday, February 8, 2005
AFTERNOON SESSION I
ENVIRONMENTAL COMPLICATIONS TO
RADAR SOUNDING AND INVESTIGATIONS OF NON-POLAR ANALOGS
1:30 p.m. Lecture Hall

Heggy E. * Pommerol A. [INVITED]
Dielectric Map of the Martian Surface [#6028]

Stillman D. E. * Olhoeft G. R. [INVITED]
EM Properties of Magnetic Minerals at RADAR Frequencies [#6029]

Holt J. W. * Blankenship D. D. Morse D. L. Peters M. E. Kempf S. D.
Surface Clutter Removal in Airborne Radar Sounding Data from the Dry Valleys, Antarctica [#6011]

3:00 – 3:15 p.m. BREAK

Tuesday, February 8, 2005
AFTERNOON SESSION II
ENVIRONMENTAL COMPLICATIONS TO
RADAR SOUNDING AND INVESTIGATIONS OF NON-POLAR ANALOGS (*Continued*)
3:15 p.m. Lecture Hall

Dinwiddie C. L. * Clifford S. M. Grimm R. E. Heggy E. [INVITED]
Strategy for Selection of Mars Geophysical Analogue Sites [#6035]

Heggy E. * Clifford S. Grimm R. Gonzalez S. Bannon D. Wyrick D.
Mapping Subsurface Stratigraphy and Anomalies in Iron-rich Volcanoclastics Using Ground-penetrating Radar: Potential for Shallow Sounding on Mars [#6038]

DAY IN REVIEW DISCUSSION

Tuesday, February 8, 2005
POSTER SESSION AND EVENING SOCIAL
5:00 – 7:00 p.m. Great Room

Aly M. H. Klein A. G. Giardino J. R.
SAR Interferometry as a Tool for Monitoring Coastal Changes in the Nile River Delta of Egypt [#6036]

Arokiasamy B. J. Bianchi C. Sciacca U. Tutone G. Zirizzotti A. Zuccheretti E.
Modern Radar Techniques for Geophysical Applications: Two Examples [#6006]

Berthelie J. J. Hamram S. E. Ney R. WISDOM Team
The WISDOM Experiment on the EXOMARS ESA Mission [#6030]

Farrell W. M.
Ionospheric Transmission Losses Associated with Mars-orbiting Radar [#6021]

Necsoiu M. Dinwiddie C. L. Heggy E. Farr T. G.
A Web-based Collaborative Tool for Mars Analog Data Exploration [#6034]

Safaeinili A. Ostro S. Rodriguez E. Blankenship D. Kurth W. Kirchner D.
High-Power Radar Sounders for the Investigation of Jupiter Icy Moons [#6018]

Wednesday, February 9, 2005
MORNING SESSION I
ENVIRONMENTAL COMPLICATIONS TO
RADAR SOUNDING AND INVESTIGATIONS OF NON-POLAR ANALOGS (*Continued*)
8:30 a.m. Lecture Hall

Grimm R. * Heggy E. Clifford S. Dinwiddie C. [INVITED]
Scattering Limits to Depth of Radar Investigation: Lessons from the Bishop Tuff [#6025]

Williams K. K. * Grant J. A. Schutz A. E.
Ground-penetrating Radar in Mars Analog Terrains: Testing the Strata Instrument [#6019]

SAR, POLARIMETRIC RADAR, AND
OTHER ELECTROMAGNETIC INVESTIGATIONS

Paillou Ph. * Lasne Y. Malézieux J.-M. Heggy E. [INVITED]
Simulation of P-Band SAR Performances for Mars Exploration [#6007]

10:00 – 10:15 a.m. BREAK

Wednesday, February 9, 2005
MORNING SESSION II
SAR, POLARIMETRIC RADAR, AND
OTHER ELECTROMAGNETIC INVESTIGATIONS (Continued)
10:15 a.m. Lecture Hall

Campbell B. A. * [INVITED]

Probing the Martian Subsurface with Synthetic Aperture Radar [#6001]

Mouginis-Mark P. J. * Rosen P. Freeman A. [INVITED]

Application of Interferometric Radars to Planetary Geologic Studies [#6014]

Jezek K. * Rodriguez E. Gogineni P. Curlander J. Freeman A. Wu X.

A Design Concept for Spaceborne Imaging of the Base of Terrestrial Ice Sheets and Icy Bodies in the Solar System [#6043]

12:00 – 1:30 p.m.

LUNCH

Wednesday, February 9, 2005
AFTERNOON SESSION I
SAR, POLARIMETRIC RADAR, AND
OTHER ELECTROMAGNETIC INVESTIGATIONS (Continued)
1:30 p.m. Lecture Hall

Campbell D. B. * Carter L. M. Campbell B. A. Stacy N. J.
Planetary Surface Properties from Radar Polarimetric Observations [#6026]

Freeman A. * Campbell B. A. Oh Y.
A Polarimetric Scattering Model for the 2-Layer Problem [#6004]

Lasne Y. * Paillou Ph. Malézieux J.-M.
A Phase Signature for Detecting Wet Structures in the Shallow Subsurface of Mars Using Polarimetric P-Band SAR [#6008]

3:00 – 3:15 p.m. BREAK

Wednesday, February 9, 2005
AFTERNOON SESSION II
SAR, POLARIMETRIC RADAR, AND
OTHER ELECTROMAGNETIC INVESTIGATIONS (Continued)
3:15 p.m. Lecture Hall

Le Gall A. * Ciarletti V. Berthelier J. J. Ney R. Dolon F. Bonaime S.
Experimental Validation of the Mono and Bistatic Operating Mode of a GPR Dedicated to the Martian Subsurface Exploration [#6032]

DAY IN REVIEW DISCUSSION

6:00 – 8:30 p.m. WORKSHOP DINNER

Thursday, February 10, 2005
MORNING SESSION I
SAR, POLARIMETRIC RADAR, AND
OTHER ELECTROMAGNETIC INVESTIGATIONS (Continued)
8:30 a.m. Lecture Hall

REVIEW OF DAY'S AGENDA

Moghaddam M. * Pierce L. Tabatabaenejad A. Rodriguez E.
*A Tower-based Prototype VHF/UHF Radar for Subsurface Sensing: System Description and Data
Inversion Results* [#6042]

Ozorovich Y. R. * Lukomskiy A. K.
*Geoelectrical Markers and Oreols of Subsurface Frozen Structures on Mars for Long-Term Monitoring of Spatial
and Temporal Variations and Changes of Martian Cryolithozone Structure on the Base Ground and Satellite
Low-Frequency Radar Measurements* [#6015]

Espley J. R. * Cloutier P. A. Delory G. T.
*Observations of Low Frequency Low Altitude Plasma Oscillations at Mars and Implications for Electromagnetic
Sounding of the Subsurface* [#6010]

10:00 – 10:15 a.m. BREAK

Thursday, February 10, 2005
MORNING SESSION II
SUMMARY DISCUSSION
10:15 a.m. Lecture Hall

**SUMMARY DISCUSSION: RECOMMENDATIONS FOR A BEST-EFFORT,
TWO-MISSION APPROACH TO IDENTIFYING THE GLOBAL HISTORY AND THE PRESENT
DISTRIBUTION AND STATE OF SUBSURFACE WATER ON MARS**

Moderator: Clifford S.

ANNOUNCEMENT REGARDING WORKSHOP SPECIAL ISSUE OF *JGR-PLANETS*

12:00 noon

WORKSHOP ADJOURNS

Print-Only Abstracts

Aftabi P. Talbot C. Fielding E.
Salt Kinematics and InSAR [#6012]

Jernsletten J. A. Heggy E.
Comparing Transient Electromagnetics and Low Frequency Ground Penetrating Radar for Sounding of Subsurface Water in Mars Analog Environments [#6040]

Yan Y.
In-situ Remote Sensing Reflectance Measurements in Case 2 Water [#6003]

Salt Kinematics and InSAR

Pedarm Aftabi (1&2) Christopher Talbot (2) & Eric Fielding (3)

1-Geological Survey of Iran, Azadi Square, Meraj Street, PO Box 131851-1494, Tehran, Iran., Ped_Aftabi@yahoo.com.

2-Hans Ramberg Tectonic Laboratory, Uppsala University, Villavagen 16, Uppsala, SE 752 36, Sweden.

3-Jet Propulsion Laboratory, Caltech, Pasadena, California 91109, USA.

Abstract:

As part of a long-term attempt to learn how the climatic and tectonic signal interact to shape a steady state mountain monitored displacement of a markers in SE termination and also near the summit of a small viscous salt fountain extruding onto the Central plateau of Iran. The marker displacements relate to the first InSAR interferograms of salt extrusion (980913 to 990620) calculated Earth tides, winds, air pressures and temperatures.

In the first documented staking exercise, hammered wooden stakes vertically through the surgical marl (c.10cm deep) onto the top of crystalline salt. These stakes installed in an irregular array elongate E-W along the c.50 m high cliff marking the effective SE terminus of the glacier at Qum Kuh(Central Iran) , just to the E of a NE trending river cliff about 40 m high. We merely measured the distances between pairs of stakes with known azimuth about 2 m apart to calculate sub horizontal strain in a small part of Qum Kuh. Stakes moved and micro strains for up to 46 pairs of stakes ($\mu \text{ strain} = ((\text{length1} - \text{length2}) / \text{length1}) \times 10^{-1}$) was calculated for each seven stake epochs and plotted against their azimuth on simplified array maps. The data fit well the sine curves expected of the maximum and minimum strain ellipses. The first documented stakes located on the SE where the InSAR image show -11 to 0 mm pink to purple, 0 to 10mm purple to blue, and show high activity of salt in low activity area of the InSAR image (980913 to 990620). Short term micro strains of stake tie lines record anisotropic expansions due to heating and contraction due to cooling. All epochs changed between 7 to 117 days (990928 to 000116), showed 200 to 400 micro strain lengthening and shortening. The contraction and extension existed in each epoch, but the final strain was extension in E-W in Epoch 1 and 6, contraction in E-W direction during epochs 2-3-4-5 and 7. The second pair of stakes hammered about 20 cm deep into the deep soils (more than 1 m) , near summit, where the colors change between 19 to 29mm in InSAR image (980913 to 990620). The horizontal distances between stakes generally shrank as the temperature rose and increased as the temperature fell. The distances between all 3 stake-pairs were large during high air pressure and small during low air pressure (measurements at 9-10 may 2002). This means that salt block in pull apart shape area in the InSAR image is in wedge shape. The wedge shape salt sank during expansion and up build during contraction (rise and fall of temperature respectively). The soil of the wedge shape salt displaced in opposite directions. The active area between 23 to 28mm interpreted as pull apart zone and salt come up from the vent into this pull apart system.

SAR Interferometry as a Tool for Monitoring Coastal Changes in the Nile River Delta of Egypt

Mohamed H. ALY, Department of Geology & Geophysics, Texas A&M University, College Station, TX 77843-3115, aly@tamu.edu

Andrew G. KLEIN, Department of Geography, Texas A&M Univ, College Station, TX 77843-3174, klein@geog.tamu.edu

John R. GIARDINO, Office of the Dean of Graduate Studies and Department of Geology & Geophysics, Texas A&M Univ, College Station, TX 77843-1113, rickg@tamu.edu

Abstract

The Nile River Delta is experiencing rapid rates of coastal change. The rate of both coastal retreat and accretion in the Eastern Nile Delta requires regular, accurate detection and measurement. Current techniques used to monitor coastal changes in the delta are point measurements and, thus, they provide a spatially limited view of the ongoing coastal changes. SAR interferometry can provide measurements of subtle coastal change at a significantly improved spatial resolution and over large areas (100 km²). Using data provided by the ERS-1&2 satellites, monitoring can be accomplished as frequently as every 35 days when needed. Radar interferometry is employed in this study to detect segments of erosion and accretion during the 1993-2000 period. The average rates of erosion and accretion in the Eastern Nile Delta are measured to be -11.64 m yr⁻¹ and +5.12 m yr⁻¹, respectively. The results of this interferometric study can be used effectively for coastal zone management and integrated sustainable development for the Nile River Delta.

Key Words: SAR interferometry, Coastal change, Nile Delta, Egypt.

MODERN RADAR TECHNIQUES FOR GEOPHYSICAL APPLICATIONS: TWO EXAMPLES. B.J. Arokiasamy¹, C. Bianchi², U. Sciacca², G. Tutone², A. Zirizzotti² and E. Zuccheretti², ¹ TRIL Research Fellow, Istituto Nazionale di Geofisica e Vulcanologia, Via di Vigna Murata, 605, 00143, Rome, Italy. b_james_a@ingv.it and ² Istituto Nazionale di Geofisica e Vulcanologia.

Introduction: The last decade of the evolution of radar was heavily influenced by the rapid increase in the information processing capabilities. Advances in solid state radio HF devices, digital technology, computing architectures and software offered the designers to develop very efficient radars. In designing modern radars the emphasis goes towards the simplification of the system hardware, reduction of overall power, which is compensated by coding and real time signal processing techniques. Radars are commonly employed in geophysical radio soundings like probing the ionosphere, stratosphere-mesosphere measurement, weather forecast, GPR and radio-glaciology etc.

In the laboratorio di Geofisica Ambientale of the Istituto Nazionale di Geofisica e Vulcanologia (INGV), Rome, Italy, we developed two pulse compression radars. The first is a HF radar called AIS-INGV; Advanced Ionospheric Sounder designed both for the purpose of research and for routine service of the HF radio wave propagation forecast. The second is a VHF radar called GLACIORADAR, which will be substituting the high power envelope radar used by the Italian Glaciological group. This will be employed in studying the sub glacial structures of Antarctica, giving information about layering, the bed rock and sub glacial lakes if present. These are low power radars, which heavily rely on advanced hardware and powerful real time signal processing.

The AIS-INGV ionosonde is a Radar capable of measuring the virtual height of the ionospheric reflections in the frequency range 1-20MHz. It is based on a 16-bit complementary phase code that gives the system about 30 dB gain as a result of correlation process and coherent integration. The system is completely programmable and a directly interfaced PC supports the control, data acquisition, real time processing and storage of the acquired data. Two Italian Ionospheric stations have been equipped with AIS-INGV at Gibilmanna (Italy) and Terra Nova Bay (Antarctica). Both these stations are remotely programmable and giving real-time ionograms. This first generation system allows future expansions like polarization information, Doppler shifts etc. in the form of add on boards on the main radar unit.

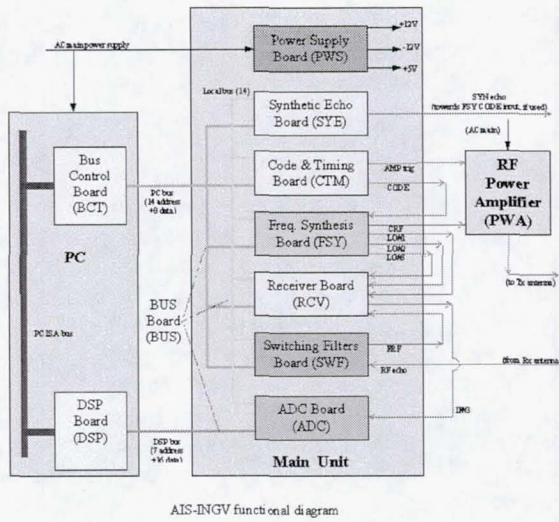
The GLACIORADAR is airborne, working at 60 MHz with 13-bit Barker code encoding the carrier. Although this radar is a single frequency system the design constraints are very challenging; like wide bandwidth of 13.3 MHz, sensitivity of -110 dBm.

These constraints are due to the range resolution of 10-15m and path loss of 165 dB. This phase coded system has a processing gain of about 21 dB, which literally allows a 500W transmitter replacing a 2kW.

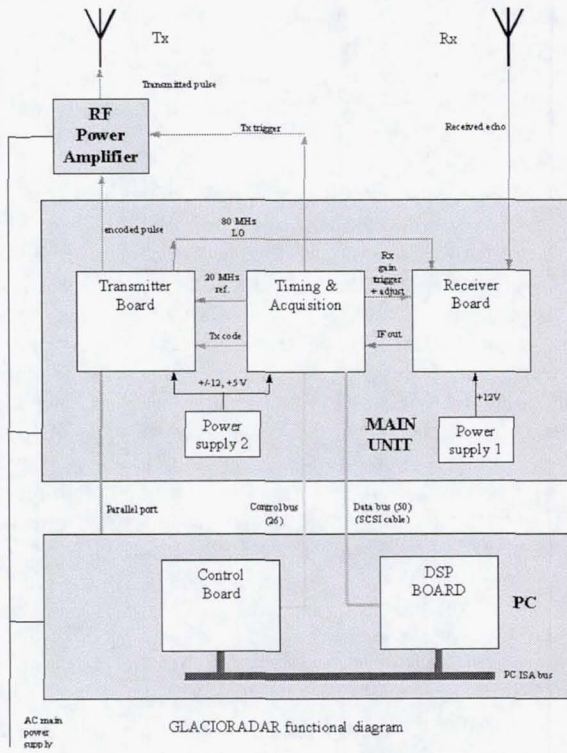
Majority of the functions of these radars are usually implemented digitally and demands high-speed hardware. The carrier, code, control and clock signal generation are implemented digitally. The analog front end of the receiver also plays a major role in improving the signal to noise ratio of the received signal. A special processing care is needed for noise that is inside the information bandwidth of the Radar. The received signal after quadrature sampling would be ready for digital processing. Real time digital processing includes amplitude and frequency filter or limiter, correlation that is a linear detector and coherent integration. The processed data is stored to extract relevant information like position, velocity, reflected energy etc. and displayed.

Concerning the real time signal processing, working in time domain as well as frequency domain is possible. Working in time domain is easier and faster; giving acceptable results in good signal to noise ratio condition. On the contrary changing to frequency domain introduces two more tasks, the Fourier transform and its inverse, but it comes handy when the number of samples increases and above all in poor SNR condition. A good evaluation of the type of coding, kind of noise due to the operating frequency and type of application led to the use of frequency domain processing in these two radars. A trade off between cost, speed and system requirements was done before choosing the type of computing machine. In these two radars the real time signal processing is done by Texas fixed point DSP and PC. This is a cost and computing effective hybrid of fixed and floating-point parallel processing. This hybrid exploits the integration time to run parallel processes. Another highlight of this hybrid is that the calculation/round off noise matches floating point processing.

This poster gives an overview of the two radars and their field results.



AIS-INGV functional diagram



GLACIORADAR functional diagram

References:

- [1] Arokiasamy B.J., Bianchi C., Sciacca U., Tutone G. and Zuccheretti E. (2002), "The new AIS-INGV digital ionosonde design report", *INGV Internal Technical Report* N. 12.
- [2] Zuccheretti E., Tutone G., Sciacca U., Bianchi C. and Arokiasamy B. J. (2003), "The new AIS-INGV digital ionosonde", *Ann. Geophysics*, 46, 647-659.
- [3] Bianchi C., Sciacca U., Zirizzotti A., Zuccheretti E. and Arokiasamy B. J. (2003), "Signal processing techniques for phase-coded HF-VHF radars", *Ann. Geophysics*, 46, 697-705.
- [4] Oppenheim, V., A. Schafer, W. Ronald and J. R. Buck, (1999), "Discrete-Time Signal Processing" (Second Edition), *New Jersey*.
- [5] Skolnik, M.I. (1997), "Radar handbook", *Mc Graw Hill N.Y.*
- [6] Tabacco I.E., Bianchi C., Chiappini M., Passerini A., Zirizzotti A. and Zuccheretti E. (1999), "Latest improvements for the echo sounding system of the Italian radar glaciological group and measurements in Antarctica", *Ann. Geofis.*, 42, 271-276.
- [7] Bianchi C., Sciacca U., Tabacco I.E., Zirizzotti A. and Zuccheretti E. (2003), "On the shape of reflecting surfaces investigated by a 60 MHz radar", *Int. J. Remote Sensing*, 24, 3049-3058.

The WISDOM Experiment on the EXOMARS ESA Mission.

J.J.Berthelier¹ (berthelier@cetp.ipsl.fr) S.E. Hamran² (s.e.hamran@ffi.no) R. Ney¹ (richard.ney@cetp.ipsl.fr) and the WISDOM Team, ¹CETP/IPSL

Introduction: In accordance with the main goal of the PASTEUR payload on the EXOMARS ESA mission, the WISDOM experiment (Water Ice and Subsurface Deposit On Mars) has been proposed to conduct both scientific and engineering investigations of the subsurface. It consists of a set of 3 instruments: a ground penetrating radar (GPR) operating in the UHF and VHF ranges, a permittivity probe (PP) operating at low frequencies and NITON an instrument to determine the radon exhalation from which the water content of the soil down to depths of about 20 meters can be deduced. In this poster we provide a description of the two first instruments that use radio-electric techniques to probe the subsurface.

The WISDOM experiment is primarily focused on observations of the near-subsurface. Although this data will be of interest in and of itself, it will also provide key scientific input for other experiments and essential engineering data to support the mission's drilling operations by returning data on the geology, structure, and physical properties of potential drilling sites, as well as the nature and location of potential targets. In addition to high-resolution measurements of the superficial layers, a more extensive regional survey, extending down to depths of up to a few hundred meters will allow to place the near-subsurface observations in context, whether with regard to understanding the formation and evolution of local terrains or identifying subsurface reservoirs of water. Such observations may provide important clues to understanding the geological and hydrological conditions that may have given rise to life.

The **Ground Penetrating Radar (GPR)** will access to the structure, layering and electromagnetic properties of the subsurface. The primary objective is to probe the first ~ 3 meters of the soil with a very high depth resolution in accordance with the objectives and expected capabilities of the drill exploration. This will be achieved with a radar operating in the UHF range at a central frequency of ~ 2 GHz. The synergy with the Permittivity Probe and also with optical instruments (e.g. spectro-imagers) that observe surface materials, rocks and dust will allow the material identification and a better knowledge of the electrical permittivity which is important for data interpretation. Sounding the subsurface at larger depths is equally important to search for water reservoirs and understand the geology, geomorphology and history of the selected sites

and their environment. To reach larger depths, the GPR will operate in the VHF range. For geology purposes, getting to a depth of 30 to 50 meters appears sufficient and can be achieved using a frequency ~100 MHz. Maximizing the chances to find water reservoirs, in particular liquid water, requires to probe at depths of about ~ 200 meters at least. Due to propagation losses that rapidly increase with frequency, the radar should then operate at about 30 MHz. The GPR design allows to operate both at UHF and at VHF by incorporating two sets of antennas, one for each frequency range. In each frequency range, the GPR will perform polarimetric measurements since these observations add significantly to the ability of the radar to retrieve the properties of the reflectors (dimension, shape, nature,...) and of the interfaces (roughness, ...). To this aim, orthogonal antennas have to be used to measure cross-polarization.

The **Permittivity Probe (PP)** uses the technique of mutual impedance probes to measure the complex electrical permittivity of the soil to a depth of ~3 meters, identical to the GPR range at 1.5 GHz. By using an adapted geometry for the electrodes, PP has also the capability to resolve the electrical permittivity profile with a medium resolution. Using a second set of electrodes located on the drill itself will enhance the capability of the PP instrument by measuring with a very high resolution the permittivity profile along the drill hole. The PP data will provide insight into the nature of the soil material and in particular its water ice and possibly liquid water content mainly through the frequency dependence of the complex electrical permittivity.

Approach

The GPR uses the stepped frequency (SF) technique which is based on the analysis of the system in the frequency domain. In the UHF range, to perform measurements very close to the surface, the GPR will work in a bi-static mode with separate antennas for transmission and reception. To perform polarimetric measurements, two sets of antennas are needed, each one having 2 horizontal orthogonal antennas. With an adequate design (antenna distance, absorbing materials, ...), the transmitting and the receiving antennas can be conveniently decoupled. In the VHF range and due to obvious mechanical constraints there will be only two orthogonal antennas and, when measuring co-polarized echoes, the radar will operate in the

mono-static mode with a single antenna for transmission and reception. In such a configuration the Range Gating (RG) technique can be applied [Hamran et al. 1995].

The GPR electronics is based on a fully digital design that provides greater accuracy and flexibility and may be a significant advantage to optimize the modes of operation. The 2 GHz radar is a stepped frequency unit with a PLL for the signal generation. The 60 MHz signal generation is achieved by a DDS followed by a frequency translation. All functions required to control the radar sequences, the generation of the transmitted signal through an embedded DDS, the data acquisition and processing and the interfaces with the payload CDMS will be performed by a single FPGA. Solid state components, either GaAs or PIN diodes, are considered for the various switches.

The Permittivity probe PP is a simple and light instrument which is based on the measurement of the mutual impedance between two dipoles one used as a transmitter and the other as the receiver. This approach has the advantage of making the measurements independent of the contacts between the electrodes and the soil and thus to allow a precise measurement of the complex electrical permittivity of the underground. Operated over a frequency range extending from 10 Hz to about 100 kHz, the PP will be able to detect an ice concentration in the underground as low as $\sim 2\%$.

An Ice Thickness Study Utilizing Ground Penetrating Radar on the Lower Jamapa Glacier of Citlaltépetl (El Pico de Orizaba), Mexico. S. B. Brown¹, B. P. Weissling² and M. J. Lewis³, ^{1,2,3}Department of Earth and Environmental Science, University of Texas at San Antonio, 6900 N. Loop 1604 W., San Antonio, Texas, 78249, ¹stephen.brown@utsa, ²bweissli@lonestar.utsa.edu, ³mjlewis@satx.rr.com.

Introduction: Citlaltépetl (Pico de Orizaba) is a dormant stratovolcano located at the eastern end of the trans-Mexican Volcanic Belt at approximately 19 degrees of latitude (Figure 1). It is one of the largest stratovolcanos in the world and at 5,630 meters above sea level, the highest mountain in Mexico and the third highest in North America. Situated on the summit cone and north face of the volcano is a permanent ice cap known as the Jamapa Glacier.



Figure 1. Citlaltépetl and the Jamapa Glacier viewed from the northwest.

Recent and historical studies of Citlaltépetl have been based primarily on volcanic risk assessment (Zimbelman, et. al., 2004), in particular stability assessments of the summit cone. Relatively little work has been directed toward the glacial environment of the mountain, possibly due in part to its high altitude, steep slopes, and general inaccessibility. In addition to this glacier's potential to contribute to a better understanding of climate change, the Jamapa glacier and its environmental, cryologic and geologic setting could also serve as a valuable terrestrial analog to studies of Martian geology, hydrology, and subsurface ice.

Methodology: A Geophysical Survey System, Inc. (GSSI) SIR-3000 GPR utilizing a 400 MHz antenna was used to survey three sampling transects on the lower Jamapa Glacier. Twenty-six samples were collected as static points over a run of approximately 1 kilometer. GPR sampling time at each point was approximately 10 seconds. All transect positions were calculated using a Trimble GeoExplorer III Global Positioning System (GPS) receiver collecting autonomous data in a WGS 1984 datum (Figure 2.).

Transect A began at latitude 19.040213431, longitude -97.268328676 at an altitude of 5026 meters

MSL. Transect A ended at latitude 19.039190296, longitude -97.272958227 at an altitude of 5132 meters MSL. The total length of Transect A was approximately 562 meters. Fifteen GPR samples were taken along this transect (Figure 2.).

Transect B, an ascending transect, began at latitude 19.039190296, longitude -97.272958227 at an altitude of 5132 meters MSL. Transect B ended at latitude 19.037365658, longitude -97.272963897 at an altitude of 5206 meters MSL. Five GPR samples were taken along this transect including the end and start points of transects A and C. The total length of Transect B was approximately 184 meters (Figure 2.).

Transect C began at latitude 19.037365658, longitude -97.272963897 at an altitude of 5206 meters MSL. Transect C ended at latitude 19.037136685, longitude -97.269668900 at an altitude of 5219 meters MSL. Eight GPR samples were taken along this transect. The total length of Transect C was approximately 352 meters (Figure 2.). Rapidly deteriorating weather conditions dramatically reduced the number of GPR positions sampled during this study.

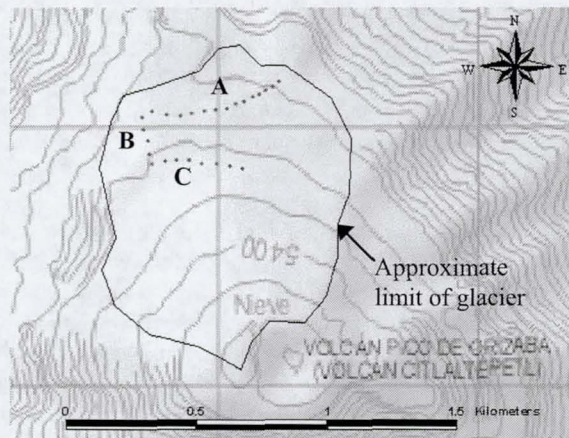


Figure 2. Location of sampling point along transects A, B, And C with approximate limit of the Jamapa Glacier.

Results: The 400 MHz antenna provided a source frequency suitable for ice profiling and was appropriately sized for portability at high altitude. Interpreted GPR results, as ice thickness in meters, based on a dielectric constant of 3.5 are presented in Table 1.

Transect A yielded generally excellent data (Figure 3) with strong ice base/bedrock radar returns up to 21 meters in depth. Transect B and the beginning of transect C (Figure 2) were problematic in that the expected ice base returns were obscured either by a low-frequency "ringing" noise or by strong internal reflections.

GPR Point	Transect	Ice Thickness (m)
1	A	< 0.5
2	A	2.04
3	A	5.02
4	A	(a)
5	A	10.09
6	A	9.30
7	A	13.28
8	A	14.95
9	A	15.65
10	A	15.61
11	A	20.92
12, 13	A	(b)
14	A	13.58
15 - 21	B, C	(b)
22	C	15.36
23	C	17.44
24	C	14.25
25	C	12.87
26	C	15.51

Table 1. Ice thickness in meters at each sampling point along Transects A, B and C. Note: (a) record length was insufficient to reach base of ice, (b) low frequency and "ringing" noise confounded data interpretation.

Discussion: As substantiated in numerous research studies since the mid-century, ground penetrating radar is a superior tool for sub-surface studies in glacial environments. High altitude glacial environments are often difficult to assess due to a number of logistic challenges including unpredictable weather, remote locations, and climbing contingencies. The results of this study indicated surveys performed under these extreme conditions can be used to profile glacial ice and to determine ice thickness. What the authors initially construed as noise in samples along transect B might in fact be legitimate radar returns from a different glacial stratigraphy not seen in transect A and the latter part of transect C, perhaps caused by ash layers from the last recorded eruption in the 17th century. It has long been assumed that the glacier and ice cap of Citlaltépetl was destroyed in the 17th century eruption -

however, it is possible that a portion of the glacier survived and was encapsulated by ash.

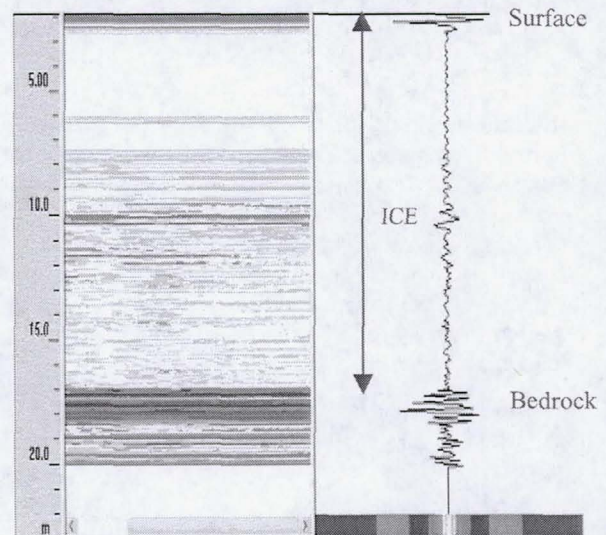


Figure 3. Figure (at right) represents one oscilloscope trace from a collection of scans (at left) recorded at sample point 8. At this location, ice thickness was determined to be 14.95 meters based on an ice dielectric constant of 3.5.

Future Research: A more extensive GPR survey of Citlaltépetl is planned for the Spring of 2005. The 2005 expedition will include surveys of the upper Japapa Glacier and will utilize more traditional continuous surveying techniques rather than the static point system utilized in this study. If logistically feasible, a lower frequency antenna will be used for greater penetration. Of particular interest is whether the glacier is underlain by solid bedrock or by ash deposits and, if the latter, do those deposits conceal a relict ice mass. The logistical and technical experience gained in this and future surveys could well be useful in other high altitude and remote location glacial studies.

References:

Zimelman, D. R., Watters, R.J., Firth, I. R., Breit, G. N., Carrasco-Nunez, G. 2004. Stratovolcano stability assessment methods and results from Citlaltépetl, Mexico. *Bulletin of Volcanology* 66: 66-79.

Acknowledgements: The authors wish to thank the following organizations and individuals for their contributions to this project: Exploration Instruments, American Alpine Club, Trimble Navigation, Arturo Ortiz, Tobin Martin, Subsecretaria de Protección Civil, Estado de Veracruz, Augustine Morales, and Manuel Pallares.

PROBING THE MARTIAN SUBSURFACE WITH SYNTHETIC APERTURE RADAR. B.A. Campbell¹, T.A. Maxwell¹, and A. Freeman². ¹Center for Earth and Planetary Studies, Smithsonian Institution, PO Box 37012, Washington, DC 20013-7012, campbellb@nasn.si.edu; ²Jet Propulsion Lab, 4800 Oak Grove Dr, Pasadena, CA 91109.

Introduction: Many regions of the martian surface are covered by fine-grained materials emplaced by volcanic, fluvial, or aeolian processes. These mantling deposits likely hide ancient channel systems (particularly at smaller scale lengths) and volcanic, impact, glacial, or shoreline features. Synthetic aperture radar (SAR) offers the capability to probe meters below the surface, with imaging resolution in the 10's of m range, to reveal the buried terrain and enhance our understanding of Mars geologic and climate history. This presentation focuses on the practical applications of a Mars orbital SAR, methods for polarimetric and interferometric radar studies, and examples of such techniques for Mars-analog sites on the Moon and Earth.

Modeling of SAR Applications: The major science goals of a Mars-orbital SAR include:

(1) Detecting buried geologic features (i.e., penetrating the mantling material and receiving reflections from a subsurface interface).

(2) Constraining the relative proportion of surface and subsurface components in the radar return (i.e., verifying that the features are, in fact, beneath the surface).

(3) Estimating the thickness of the mantling materials as a guide to their volume and likely emplacement mechanism.

We have carried out a study of the utility of radar backscatter measurements, at a range of wavelengths and polarizations, to satisfy these requirements [1]. Our results show that a radar wavelength in the L- to P-band range (~30 cm) offers the best potential for deep penetration and a relatively strong scattered echo from rough buried terrain.

We also found that the HH/VV ratio provides sufficient information to estimate the fraction of surface and subsurface returns for typical incidence angles of ~40°. Multi-wavelength observations cannot provide a strong constraint on the depth of a mantling layer, due to the large uncertainty in the loss tangent of martian near-surface materials. A more robust thickness estimate may come from the "volume decorrelation" properties of interferometric radar echoes, but the required phase measurement accuracy is challenging.

Terrestrial Radar Studies: Validation of our conclusions from theoretical modeling is an important element of planning for the Mars-orbital radar. To this end, we are using data from the NASA/JPL AIRSAR system (6-, 24-, and 68-cm wavelengths, fully polarimetric) in a variety of Mars-analog settings. These studies are supported by 400-MHz ground-penetrating radar surveys to identify subsurface scattering horizons. Areas of interest include ash deposits in Hawaii, cinder layers in Arizona, sand-covered bedrock in Egypt, and near-surface structural and hydrologic features in Death Valley, CA.

Lunar Radar Studies: We are also using new 70-cm wavelength radar data for the Moon to test models for radar scattering in a dry regolith with highly variable scattering and loss properties. These new data have a spatial resolution of ~450 m, and are collected in both senses of circular polarization (Fig. 1). The radar maps are compared with Clementine multispectral data to study subsurface penetration and the effects of mineralogy on the regolith loss tangent.

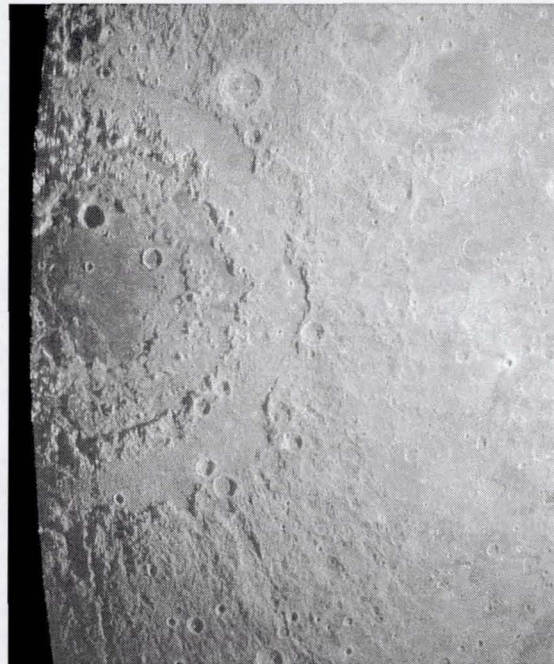


Figure 1. 70-cm radar image of Orientale Basin on the west limb of the Moon.

Work to date reveals significant new detail in the distribution of ancient lunar mare basalts that were buried by highlands material excavated in giant basin-forming impacts. We have also found that large impact craters are surrounded by extensive haloes of low 70-cm radar return, indicating a rock-poor ejecta layer [2]. Differences in polarization properties permit the tracing of Orientale-derived impact-melt materials across the permanently shadowed south polar region [3]. These results all have implications for probing of near-surface materials on Mars.

References: [1] Campbell, B.A., T. Maxwell, and A. Freeman, Mars orbital SAR: Obtaining geologic information from radar polarimetry, *J. Geophys. Res.*, 109, doi:10.1029/2004JE002264, 2004. [2] Ghent, R.R., D.W. Leverington, B.A. Campbell, B.R. Hawke, and D.B. Campbell, Earth-based observations of radar-dark crater haloes on the Moon: Implications for regolith properties, *submitted to J. Geophys. Res.*, 2004. [3] Campbell, B.A., and D.B. Campbell, Surface properties in the south polar region of the Moon from 70-cm radar polarimetry, *submitted to Icarus*, 2004.

PLANETARY SURFACE PROPERTIES FROM RADAR POLARIMETRIC OBSERVATIONS. D. B. Campbell¹, L. M. Carter², B. A. Campbell² and N. J. Stacy³, ¹Cornell University, Space Sciences Bldg, Ithaca, NY 14853; campbell@astro.cornell.edu, ²Smithsonian Institute, Center for Earth and Planetary Studies, MRC315, Washington, DC 20560-0315, ³DSTO, P.O. Box 1500, Salisbury, SA 5108, Australia.

The polarization properties of the reflected radar wave contain information about the physical and electrical properties of the reflecting surface and near sub-surface. Surfaces rough at wavelength scales depolarize the incident wave on reflection, sub-surface reflections modify the linear polarization properties of the incident wave due to the differing surface transmission coefficients parallel and perpendicular to the plane of incidence and, for an incident circularly polarized wave, the circular polarization properties of the reflected wave are very sensitive to the sub-surface propagation loss as demonstrated by the radar reflection properties of low temperature water ice.

Due to the need for dual receiver channels and the consequent doubling of the data rate, only Earth observing aircraft and orbiters have been equipped to measure the full Stokes polarization parameters of the reflected radar echo. The Magellan Venus orbiter carried out some polarization experiments by rotating the spacecraft and the Cassini radar has a similar capability. However, Earth based radars, primarily the Arecibo 13 cm wavelength system, can be used to study the polarization properties of the radar echoes from the Moon and the terrestrial planets, icy satellites of Jupiter and Saturn and small bodies. Full Stokes parameter imaging has been carried out for the Moon, Venus and several near earth asteroids.

The unusual radar scattering properties, high backscatter cross section and circular polarization ratio greater than unity, of low temperature water ice were discovered from observations of the icy Galilean satellites at 13 cm by Campbell et al [1]. These properties have been used to identify probable water ice deposits at the poles of Mercury and to search for evidence of water ice at the poles of the Moon [2], [3], [4]. They will also have a significant impact on the use of a SAR to image the surfaces of the Galilean satellites. Echo strength will be higher than for rocky surfaces but, since almost all of the echo power will be due to sub-surface scatter, it should be relatively insensitive to surface topography potentially making the imagery very difficult to interpret.

The Arecibo S-band radar has been used to image a number of areas on the Moon including the polar regions, Venus and three NEAs in the Stokes polarization parameters. A circularly polarized wave is transmitted and the Stokes parameters of the backscattered signal derived from the complex field related amplitudes of the two senses of received circular polarization. Non zero values for the two linear polarization Stokes parameters combined with a position angle close to the plane of incidence are indicative of sub-surface scattering. We have used this property of the received echo to map the location of mantling deposits on Venus and to detect a regolith on the small NEA, 1998 JM8. We are also attempting to detect a mantling deposit over the ice deposits at the poles of Mercury. The degree of linear polarization can, in theory, be used to provide information about the relative importance of surface and sub-surface scattering and the dielectric properties of the regolith or mantling layer [5], [6]. For high spatial resolution observations, the position angle of the linearly polarized component of the echo can be used to measure local slopes [5].

Stokes parameter imaging of Venus with Arecibo has shown that a substantial fraction of the surface is fully or partially covered by mantling deposits [6]. For much of this mantled terrain the underlying surface features seem to be apparent in the Magellan imagery. Similarly, a long wavelength SAR in orbit about Mars would probe through the surface dust revealing the details of the underlying terrain.

References: [1] Campbell, D.B., et al (1978), *Icarus*, 34, 254-267, [2] Nozette, S., et al (1996), *Science*, 274, 1495-1497, 1996, [3] Stacy, N.J., Campbell, D.B. and Ford, P.G. (1997), *Science*, 276, 1527-1530, [4] Campbell, B.A., et al (2003), *Nature*, 426, 137-138, [5] Stacy, N.J. (1993), PhD Thesis, Cornell University, [6] Carter, L.M., Campbell, D.B. and Campbell, B.A. (2004), *J. Geophys. Res.*, 109, E06009.

IMAGING THE SUB-SURFACE REFLECTORS: RESULTS FROM THE RANETA/NETLANDER FIELD TEST ON THE ANTARCTIC ICE SHELF

V. CIARLETTI, J.J. BERTHELIER, A. LE GALL, A. REINEIX

V.Ciarletti¹, J.J.Berthelier¹, A.Le Gall¹, A.Reineix², ¹CETP/IPSL (ciarletti@cetp.isl.fr), ²IRCOM

Accessing to the geological features which are present in the subsurface of Mars and in particular to the water reservoirs, either in the form of water ice or of liquid water, was one of the main objectives of the NETLANDER project. Model estimates of the permafrost thickness range from 1 to 3 kilometres in equatorial regions, depending on the geothermal heat flow, with liquid water present in the fractured megaregolith under ground ice. Consequently, the NETLANDER ground penetrating radar (GPR) was designed to probe the deep subsurface at depths of a kilometre or more and thus to operate at very low frequencies, from 2 to 4 MHz, in order to minimize the absorption of propagating waves. The normal mode of operation of ground penetrating radars implies a series of measurements made at a number of locations on the surface to achieve the proper determination of the depth (or of the actual position for an adequate 3D network of measurements at the surface) of the reflectors and/or of the interfaces. On NETLANDER, the GPR is operated from a fixed position and we have thus developed an advanced instrument which allows to determine not only the distance of the reflectors, from the propagation delay of the echoes, but also their direction by determining the direction of propagation of the reflected waves. This is achieved by measuring the 2 horizontal components of the wave electric field and the 3 components of the wave magnetic field which are combined to provide the propagation vector.

Field tests of a prototype of the radar were made during the RANETA campaign on the Antarctic ice shelf. The electric antennas were resistively loaded monopoles 35 meters in length disposed at 90° from each other and laid on the ice surface. Two opposite monopoles were associated to form a symmetric dipole for transmission. The horizontal electric component of the co-polarized reflected waves was measured using these two antennas operated either as independent monopoles or associated to form a symmetric dipole. Similarly, the horizontal electric component of the perpendicularly polarized reflected waves was detected using the two other perpendicular electric antennas. Measurement of the 3 components of the wave magnetic field were achieved by a magnetic search coil antenna that can be successively positioned along 3 mutually orthogonal directions. The detailed scheme of operation of the radar involves single pulses of various duration and long coded pulses at transmission and up to

2²⁰ coherent additions at reception to increase the instrument sensitivity.

The RANETA GPR was operated at different locations on the ice-shelf near the Cap Prudhomme station in Terre Adélie and distinctly detected echoes from the reflection of the transmitted waves on the bedrock at depths ranging from 300 to about 1100 meters. In most cases, multiple echoes were detected indicating that reflection occurred from different spots on the bedrock surface. The analysis of the received signals performed as indicated above allowed to disentangle the multiple echoes and provided the position of the reflecting spots. Results of this analysis and of a study of the characteristics of the reflected waves will be presented. We shall also report some preliminary results from a numerical simulation which is presently undertaken to reproduce the experimental results.

In addition, measurements of the electric antenna impedance have been performed over a frequency range from 0.3 to 6 MHz. Based on an accurate numerical model of this mode of operation that takes into account the mechanical structure of the radar and the detailed antenna mechanical and electrical characteristics, such measurements allow to obtain accurate values of the complex electric permittivity of the superficial layers of the ice. Such data are needed to properly determine the direction of the subsurface reflectors. This information would also be of significant interest for a planetary instrument since it provides insight into the nature of the materials in the upper layers of the subsurface.

STRATEGY FOR SELECTION OF MARS GEOPHYSICAL ANALOGUE SITES. C.L. Dinwiddie¹, S.M. Clifford², R.E. Grimm³, and E. Heggy² (¹CNWSA at Southwest Research Institute[®], 6220 Culebra Road, San Antonio, TX 78238-5166; 210-522-5263; email: cdinwiddie@swri.org; ²Lunar and Planetary Institute, 3600 Bay Area Boulevard, Houston, TX 77058; ³Department of Space Studies at Southwest Research Institute[®], 1050 Walnut Street, Suite 400, Boulder, CO 80302.

Introduction: The authors are involved in several efforts to evaluate, using terrestrial analogs, the performance potential of low- to mid-frequency (0.5–1000 MHz) ground-penetrating radar (GPR) and complementary geophysical methods for subsurface investigation of Mars. Our field experience thus far provides insight into selection of appropriate geophysical analogs for investigating the radar sounding characteristics of depositional analogues to the Martian crust.

Evolving Strategy: Our search for analogues began with the understanding that sites best suited to calibrating a suite of geophysical instruments, especially radar sounders, need to be sufficiently characterized to provide an accurate understanding of the local *geologic* context.

Yucca Mountain Vicinity. The availability of more than two decades of geologic, hydrologic, and climatic characterization data¹ from Yucca Mountain, Nevada, led to the selection of nearby sites for initial study.^{2,3} While not cold, this region is relatively arid, and offered complex stratigraphy akin to what might be anticipated for Mars, including highly magnetic cinder cone basalts, pyroclastic ashflow tuffs, aeolian dunes, and alluvium. Transient electromagnetic soundings of the selected sites, which are used to quantify the expected magnitude of GPR signal loss due to absorption, revealed the elevated geoelectrical conductivity of the alluvium-dominated subsurface—a fatal characteristic for deep penetration of radar signals.

Craters of the Moon. A subsequent radar and transient electromagnetic survey at Craters of the Moon National Monument, Idaho, yields additional insight into selection strategy. Stratigraphy at the monument is complex, dominated by basaltic pahoehoe and a lava flows of differing compositions and ages. The potential for correlative analyses between results of radar soundings and ongoing multi- and hyper-spectral imaging by other workers⁴ led the authors to focus on near-surface geophysics in a region where the water table is too deep to image. Unexpectedly, the highly porous subsurface, however, enabled radar penetration to depths of 150 m using a 16 MHz antenna, because the density of the subsurface, rather than the mineralogy, effectively dominated the dielectric^{5,6}. In this area, the 20-m loops for transient electromagnetic soundings should be replaced by 100-m loops for future soundings of the deeper subsurface. Successful use of low-frequency radar at this site keeps it on the

shortlist for further investigation of GPR at frequencies proposed for use on Mars.

Bishop Tuff. Ideally, transient electromagnetic soundings and laboratory analyses of field samples occur in advance of ground-penetrating radar surveys to eliminate geoelectrically unfavorable sites. We took this approach at the Volcanic Tableland, near Bishop, California. Stratigraphy beneath the Volcanic Tableland comprised of heavily faulted airfall deposits and variously welded rhyolitic ignimbrites of the Bishop Tuff. While not ideally cold and dry, the Volcanic Tableland is situated in an arid environment, is easily accessible, and is underlain by a relatively deep water table (>100 m). Initial transient electromagnetic soundings in this area suggested a relatively resistive (approximately 1000 to 5000 ohm-m) near-surface, overlying a conductive (approximately 15 to 40 ohm-m) region at depths ranging from approximately 100 to 180 m, depending on sounding location.⁷ The conductive lower region is interpreted to be the saturated zone because its depth correlates with local surface water elevations. Based on promising resistivity results, it was decided Schlumberger DC resistivity surveys (i.e., vertical electrical soundings) would provide additional constraints on near-surface resistivities and additional confidence during site selection. Subsequently, the authors conducted more comprehensive geophysical surveys in this area, including low-frequency ground-penetrating radar, transient electromagnetic, and vertical electrical soundings. Joint inversions⁸ of DC resistivity and transient electromagnetic data collected from Casa Diablo Road on the Volcanic Tableland suggest the unsaturated zone at this location is 170 m thick, with an average electrical resistivity of 900 ohm-m (preliminary transient electromagnetics alone suggested resistivity as high as 5000 ohm-m). Radar depth of penetration at this site was limited to 70 m, which potentially may be attributed to horizontal scattering by faults. This work will be discussed in greater detail by Grimm et al.⁸ at the workshop.

Future Work and Lessons Learned. The authors have proposed a number of additional sites as potential geological and geophysical Mars analogues.^{9,10} An outcome of our results, reported above, is a new appreciation of the fact that sites best suited to calibrating a suite of geophysical instruments also need to be sufficiently characterized to provide an accurate understanding of the local *geophysical* context.

The NetLander team¹¹ conducted a prototype survey near Bahria Oasis, in the western Egyptian desert, that demonstrated the NetLander radar (0.5–5 MHz) is capable of detecting the Nubian Aquifer at a depth of approximately 900 m beneath a thick layer of highly resistive, dry porous dolomite, illinite, limestone and sandstone, given laboratory-based electromagnetic characterization analyses of field samples for estimating geoelectrical properties of the local crust¹². Data analysis from the initial survey suggests remaining ambiguities associated with identification of lithologic and hydrologic interfaces in this region could be further reduced by acquisition of DC resistivity, transient electromagnetic, multiple low-frequency and broadband ground-penetrating radar data. The location of the original NetLander success, and several other locations in the Eastern Sahara and western Egyptian desert remain of keen interest to the authors as authentic hyper-arid geophysical analogues to Mars.

Cold-climate geophysical analogues to Mars are also sought because of the profound influence that such an environment has on the thermal structure of the crust and the resulting state and distribution of subsurface water. The Permafrost Project¹³ at the Lupin gold mine, Nunavut Territory, Canada, provides an extensive database of relevant climatic, geologic, hydrologic, geochemical and geophysical information, and shafts at the mine completely penetrate the 500 m of continuous permafrost in crystalline rock that is characteristic of the region. Liquid pore-waters are saline, and hydrates are present. The annual mean air temperature is ~262 K. The investigation of such an accessible, well-characterized cold-climate site with broadband ground-penetrating radar and our suite of complementary instruments is our single highest priority.

Thicker permafrost (~1.5 km), approaching that estimated for Mars^{14,15}, is accessible within the Yakutia region of western Siberia and northeast Asia, in the Sakha Republic. The mean annual temperature near Yakutia is ~256 K. Subfreezing conditions may have persisted here for as many as 2 m.y.¹⁶ As with Nunavut Territory, brine inclusions are present in the permafrost. The stratigraphy consists of old Palaeozoic saliferous and calcareous formations (limestones, dolomites) that generally possess very high thermal conductivities. Geophysical soundings of the ~1.5-km thickness of permafrost in the Sakha Republic represents a significant step forward in the thermal and hydrologic reliability of the geological and geophysical Mars analogue environment.

But what of local, more accessible geological and geophysical analogues in the United States? A number of favorable analogue sites with locations in the U.S.

Desert Southwest were recommended in the National Research Council Decadal Study report on Terrestrial Analogues to Mars¹⁷ as potentially offering a substantial amount of scientific and technical return for various lines of inquiry. Many of these geological analogues, however, lack sufficient *geophysical analogy* for testing and calibration of geophysical instruments for Mars exploration. Ideal terrestrial geophysical and geological analogues to Mars combine features such as a hyper-arid and cold climate, a deep water table, saline pore waters, and bedrock dominated by basalt. While sites in the United States cover a wide range of physical properties, and stratigraphic and structural complexity, very few easily accessible sites with local supportive infrastructure approach environmental, and thus geophysical, conditions anticipated for Mars. For example, the Western Great Basin region of California and Nevada is now known, through our own investigations, to be too geoelectrically conductive to enable substantive evaluation of depths of investigation expected in a similar geological environment on Mars.

Potential field sites in the United States remaining on the authors' shortlist for ground-penetrating radar investigation at frequencies proposed for use on Mars include Craters of the Moon National Monument, Idaho, well-drained basalt flows of the high desert south-central Columbia Plateau, Washington, and thick unsaturated basalts overlying seawater on the seasonally dry side of western Maui, Hawaii. Determination of geophysical site suitability will require comprehensive measurements of the electromagnetic properties of the subsurface.

References: [1] DOE. (2002) Yucca Mountain Science and Engineering Report. Las Vegas, Nevada. [2] Heggy E. et al. (2004) *Eos Trans. AGU*, 85(17), Abstract P51A-05. [3] Dinwiddie C. L. et al. (2004) *Eos Trans. AGU*, 85(17), Abstract P53A-03. [4] Khan S. and Gray J. (2004) <http://geoinfo.geosc.uh.edu/GeoRS/Craters.htm> [5] Heggy E. et al. (2004) *Eos Trans. AGU*, 85(47), Abstract P43A-0905. [6] Heggy E. et al. (2005) *Workshop on Radar Investigations of Planetary and Terrestrial Environments*. [7] Gonzalez S. et al. (2004) *Eos Trans. AGU*, 85(47), Abstract GP11A-0826. [8] Grimm, R. E. et al. (2005) *Workshop on Radar Investigations of Planetary and Terrestrial Environments*. [9] Clifford S. M. et al. (2004) Broadband GPR field and laboratory investigations, I. A Proposal to NASA's *Mars Fundamental Research Program*. [10] Dinwiddie C. L. et al. (2004) Broadband GPR field and laboratory investigations, II. A Proposal to NASA's *Mars Fundamental Research Program*. [11] Berthelie J. J. et al. (2000) *Planetary and Space Science*, 48, pp. 1153-1159. [12] Heggy E. et al. (2001) *Icarus*, 154(2), pp. 244-257. [13] Ruskeeniemi T. et al. (2002) Geological Survey of Finland Nuclear Waste Disposal Research Report YST-112. [14] Clifford S. M. (1993) *J. Geophys. Res.*, 98, 10,973-11,016. [15] Clifford S. M. and Parker T. J. (2001) *Icarus*, 154, 40-79. [16] Frolov (2003) *J. Geophys. Res.*, 108(E4) doi:10.1029/2002JE001881. [17] Farr T. et al. (2001) NRC Decadal Study of Terrestrial Analogues to Mars.

OBSERVATIONS OF LOW FREQUENCY LOW ALTITUDE PLASMA OSCILLATIONS AT MARS AND IMPLICATIONS FOR ELECTROMAGNETIC SOUNDING OF THE SUBSURFACE. J. R. Espley¹, P. A. Cloutier¹, and G. T. Delory², ¹Department of Physics and Astronomy, Rice University, Houston, TX, espley@rice.edu, ²Space Sciences Laboratory, University of California-Berkeley, Berkeley, CA.

Introduction: A wide variety of plasma waves have been observed in the near Mars space [1]. The Mars Global Surveyor (MGS) Magnetometer/Electron Reflectometer (MAG/ER) instrument has made observations of magnetic and electron flux oscillations at altitudes as low as 200 km [2]. We report on the characteristics of these oscillations and note their relevancy for the exploration of the deep subsurface using inductive sounding techniques such as those found in magnetotelluric, magnetic gradiometry, and wave tilt methods.

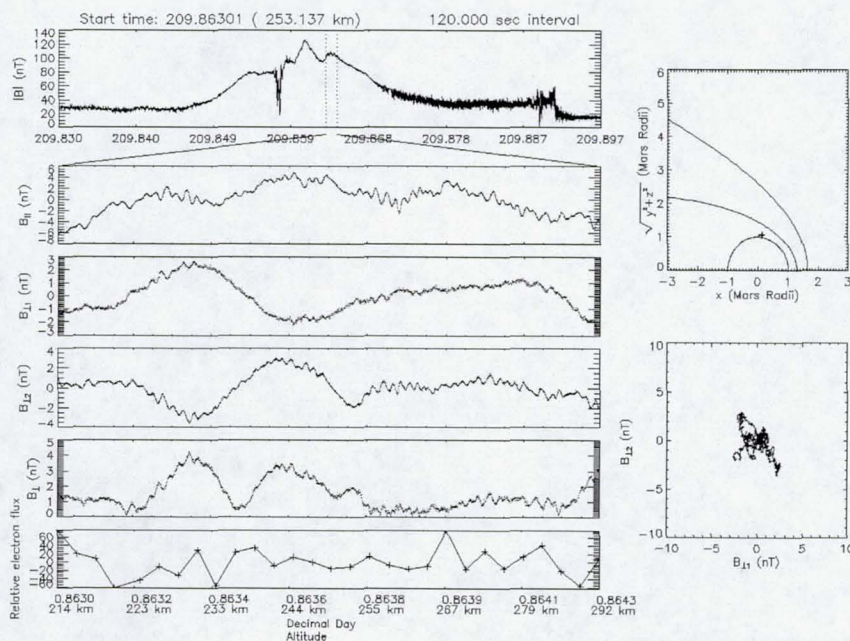
Sample Observations: The figure below shows an example of our observations. In top left panel, the magnetic field magnitude ($|B|$) for the second orbit of July 28, 1998 (decimal day 209) is shown versus time. From second to the top to second to the bottom, the panels below the $|B|$ profile show the magnetic field vector components for the interval of 209.863 to 209.8643 when MGS is nearly at perigee for its orbit. The magnetic components are shown in a coordinate system aligned along the mean magnetic field for the interval. The $B_{||}$ component is parallel to the mean magnetic field, the $B_{\perp 1}$ and $B_{\perp 2}$ components are perpendicular to the mean magnetic field and to each other and $B_{\perp} = B_{\perp 1} + B_{\perp 2}$. The last panel on the left shows the relative omni-directional flux ($\text{cm}^{-2} \text{s}^{-1} \text{sr}^{-1}$

eV^{-1}) of electrons with energies of 191 eV. In the upper right, we show as plus signs the starting and ending locations (which overlap on this scale) of MGS for interval in ecliptic plane coordinates coordinates (the sun is the right in the figure). We also show the best fit locations of the bow shock and MPB [3]. In the lower right panel, we show the perpendicular components of the magnetic field in MF coordinates plotted versus each other (a hodogram).

Distinct oscillations are observed in all components. These oscillations have spectral power at or below the local oxygen gyrofrequency. We note that the altitude range for these observations is below the normal ionopause altitude [4]. In our presentation we report further analyses of this interval including wave-let spectral analysis.

Further Results: We report additional interesting intervals of low altitude oscillations. We also discuss the distribution of such oscillations in terms of solar zenith angle and proximity to crustal magnetic anomalies.

References: [1] Espley, J. R. *et al.* (2004), *JGR* doi:10.1029/2003JA010193. [2] Acuña, M. H. *et al.* (2001), *JGR*, 106, 23,403-23,417. [3] Vignes, D. *et al.* (2000), *GRL*, 27, 49-52. [4] Hanson, W. B. *et al.* (1977), *JGR*, 82, 4351-4363.



IONOSPHERIC TRANSMISSION LOSSES ASSOCIATED WITH MARS-ORBITING RADARS. W. M. Farrell, NASA/Goddard Space Flight Center, Code 695 Greenbelt MD 20771 william.farrell@gsfc.nasa.gov.

Introduction: There are a number of obstacles to radar sounding of the deep Martian subsurface from orbit, including signal losses from the medium conductivity, layer reflective losses, and ground clutter. Another adverse process is signal loss as radio waves propagate through the ionospheric plasma medium.

The ionosphere is a plasma consisting of free electrons, ions and neutrals that can effectively damp/attenuate radar signals via electron/neutral collisions. The effect is most severe for transmissions at lower frequencies, which, unfortunately, are also favorable transmissions for deep penetration into the subsurface.

Calculations: In order to predict the effect of ionospheric losses on the MARSIS and SHARAD radars, a set of MATLAB stubs have been developed to calculate wave loss in the medium. These stubs can be easily incorporated into transmission models that already exist, and will allow a determination of wave attenuation, phase change, and group velocity change as a function of wave frequency and location over the planet.

A description of the stubs will be presented, along with the assumptions applied. It is also demonstrated that the stubs separate the calculation in such a way as to allow the application of new density models derived from the MARSIS ionospheric study and other sources as they are developed.

General Conclusions: The model demonstrates that MARSIS sounding at low frequencies will be affected by the dayside ionosphere, with both strong attenuation and significant pulse dispersion. A meteoric layer near 80 km also has the ability to strongly attenuate radar signals. While these effects have been described before in the literature, medium attenuation is calculated here without approximated index of refraction values, allowing an examination of wave propagation in evanescent regimes. Also, the presentation allows a global perspective on the effects.

The codes and supporting documentation are available to any interested investigator. Forward a request to the e-mail address cited above.

A POLARIMETRIC SCATTERING MODEL FOR THE 2-LAYER PROBLEM. A. Freeman¹, B. A. Campbell², Y. Oh³ 1. Jet Propulsion Laboratory, California Institute of Technology, 4800 Oak Grove Drive, Pasadena, CA 91109, USA, e-mail: anthony.freeman@jpl.nasa.gov; 2. Center for Earth and Planetary Studies, Smithsonian Institution, Washington, DC 20560-0315; 3. Department of Radio Science and Communication Engineering, Hong-ik University, Seoul, Korea

Introduction: In this paper, polarimetric signatures from two layers are examined. In the two layer problem a low-loss dielectric layer sits on top of a shallow subsurface layer of scatterers. Volume scattering within the top surface layer is not considered.

We show that for polarimetric backscatter data acquired from just one incidence angle, no parameter is proportional to the depth of the subsurface layer. We also show that separation of the two components and inversion of the polarimetric backscatter measurements is not possible, in the latter case due to the mismatch between the number of variables that determine the backscatter behavior, versus the degrees of freedom in the measured values.

The interesting results obtained at a sand dune site in SW France courtesy of the group led by Dr. Phillippe Paillou are examined through the prism of this model. It is shown that the model agrees well with results obtained for a subsurface layer at 3 m depth, where the subsurface returns are significant, and that surface scattering alone can account for observations made over a subsurface layer at a depth of 5.8 m, provided the surface slope is adjusted by ~ 10 degrees.

The implications for exploration of the near-surface of Mars, a significant proportion of which is obscured by a dust mantle, are discussed.

Acknowledgement: Part of the research described in this paper was carried out by the Jet Propulsion laboratory, California Institute of Technology, under a contract with the National Aeronautics and Space Administration.

RADARS FOR IMAGING AND SOUNDING OF POLAR ICE SHEETS. S. Gogineni,¹ K. Jezek,² J. Paden¹, C. Allen¹, P. Kanagaratnam¹, and T. Akins¹. ¹Radar and Remote Sensing Laboratory, University of Kansas, 2335 Irving Hill Road, Lawrence, KS 66045-7612, gogineni@ittc.ku.edu. ²Byrd Polar Research Center, The Ohio State University, 1090 Carmack Road, Columbus, OH 43210, jezek.1@osu.edu.

We developed radars for imaging the ice-bed interface, measuring ice thickness, and fine-resolution mapping of internal layers. We developed a synthetic aperture radar (SAR) that operates in bistatic or monostatic modes to generate two-dimensional reflectivity maps of the bed for determining basal conditions. It is designed to operate at 80, 150 and 350 MHz. We developed a compact, wideband, dual-mode radar to measure ice thickness and map internal layers in both shallow and deep ice. The dual-mode radar operates over the frequency range from 50 to 200 MHz for ice thickness measurements and mapping deep layers, and 500 to 2000 MHz for mapping near-surface internal layers.

We collected imaging radar data over 3-km lines at 80, 150, and 350 MHz with HH polarization. We also collected data from parallel paths with offsets ranging from 2 to 10 m to test the feasibility of using an interferometric SAR to obtain additional information on basal topography. We have completed preliminary processing of the 150-MHz monostatic SAR data. The preliminary results show that monostatic SARs operating at incidence angles between 5 and 15 degrees can be used to obtain 2-dimensional reflectivity maps of the ice-bed interface. Figure 1 shows a set of sample images collected along two offset passes. These images are the first and only successful demonstration of imaging the ice-bed interface through 3-km thick ice.

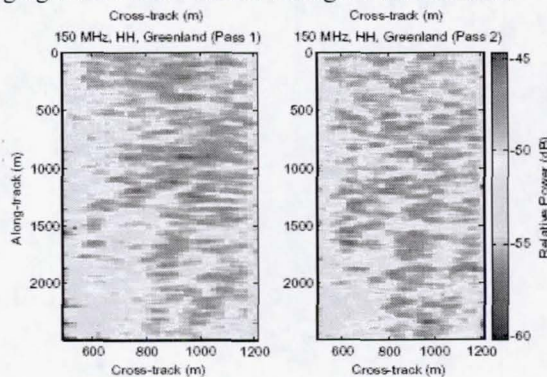


Figure 1: SAR images of ice-bed interface at SUMMIT camp.

Based on the results, we are developing a system that operates over the frequency range from 100 to 300 MHz to image the ice-bed interface with 1-10 m resolution. The wide frequency range and fine resolution will be useful for unambiguous determination of basal conditions. Such a system will be useful for identifying

frozen or liquid water on Mars, and sub-surface characterization of other planets.

We conducted field experiments at the Summit Camp in Greenland during July 2004. We collected data over a 10 km x 10 km grid with the dual-mode radar. The results show that we can sound 3-km thick ice and map deep internal layers with about 2 m resolution and can map near surface internal-layer echoes to depths of about 270 m with about 15 cm resolution as shown in Figures 2 and 3.

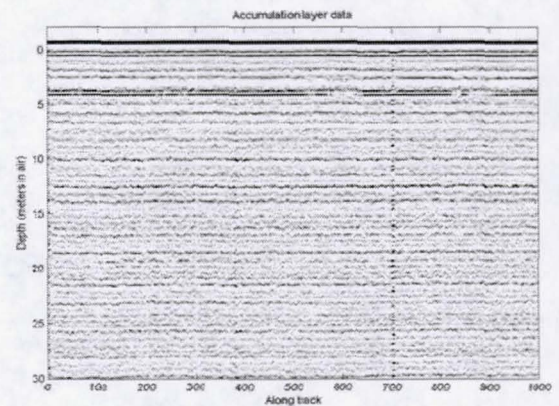


Figure 2: Radar echogram of near-surface internal layers in the top 30 m of firn.

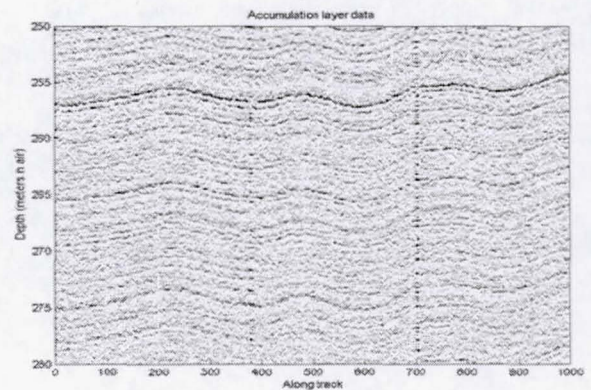


Figure 3: Radar echogram of near-surface internal layers in ice at depths between 250 and 290 m.

In this paper we will present design considerations and system characteristics, and show sample results from the imaging and sounder radars.

STRATA: GROUND PENETRATING RADAR FOR MARS ROVERS. J. A. Grant¹, C. J. Leuschen², A. E. Schutz³, J. Rudy³, R. S. Bokulic², and K. K. Williams¹, ¹Center for Earth and Planetary Studies, National Air and Space Museum, Smithsonian Institution, 6th at Independence SW, Washington, DC, 20560, grantj@nasm.si.edu ²The Johns Hopkins University, Applied Physics Laboratory, 11100 Johns Hopkins Road, Laurel, MD, 20723, Carl.Leuschen@jhuapl.edu, ³Geophysical Survey Systems, Inc., 13 Klein Drive, North Salem, NH, 03073.

Introduction: Ground-Penetrating Radar (GPR) is an efficient means for non-intrusively defining radar properties corresponding to shallow stratigraphy to depths of tens of meters [1] and operates by applying a narrow energy pulse through an antenna placed near a surface of interest. The antenna (either monostatic or bistatic) acts as a band-pass filter and emits a single sine wave cycle that is broadcast into the ground at wavelengths ranging from several meters to centimeters (tens of megahertz to a few gigahertz).

Terrestrial geologic studies with GPR over the past 30 years [1] are varied [2-5] and take advantage of the geometry of radar reflections to characterize shallow stratigraphy and structure associated with a particular depositional setting. These radar reflections serve as diagnostic "fingerprints" (e.g., the number, thickness, orientation, and extent of layers or scale of cross stratification) associated with deposition by different geologic processes in various settings.

Measuring *in situ* radar properties on Mars with GPR [6-10] can similarly identify the shallow stratigraphy, structure, and depositional settings key to defining past habitable environments and the biologic potential of a site.

The Strata Instrument: *Strata* is a low-mass, low-power, and low-volume impulse GPR that uses simple, loaded dipole antennas to radiate and receive signals from the shallow subsurface (Fig. 1). Resultant data can be used to produce images of stratigraphy and structure present beneath the erosionally modified surface of Mars. The instrument is based on a proven commercial design, uses a flight-proven digital processor unit (DPU) and has a mature design easily adaptable to rover accommodation with little or no impact to other instruments or rover resources. For example, the DPU can be placed anywhere within the rover payload module warm electronics box or WEB. Moreover, the antenna assembly is low profile and can be mounted anywhere that has a direct view of the surface (Fig. 1). *Strata* operates at 400 MHz (75-cm wavelength) that best enables defining stratigraphy and structure at the spatial resolution of tens of centimeters, to 10-15 m depth (Fig. 2). The 400 MHz frequency is the perfect tradeoff between penetration and resolution that enables collection of top-quality data even when mounted above the surface (e.g., on the underside of the rover, Fig. 1) and in high-loss settings characterized by iron-rich substrates [9]. *Strata* data volume accumulated along rover traverses totaling 6 to 10 km

will be on order of 1 to 2 Gbits, but will only average 3 to 11 Mbits on typical traverse sols covering distances of 50 to 100 m/sol. These data can be further reduced by lossless compression of up to 8:1 and data from individual or averaged scans collected along traverses will be used to build up 2D profiles and 3D data cubes displaying changing dielectric properties in the near surface corresponding to geologic and/or pe-
dogenic layers and structures.

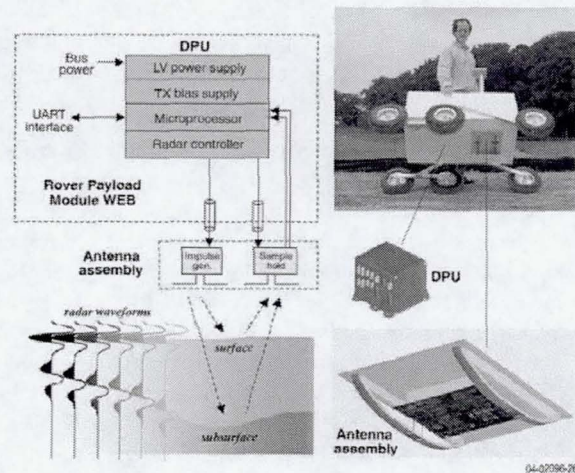


Figure 1. Block Diagram and working prototype of the *Strata* controller and antenna, respectively.

Strata Science: *Strata* is capable of achieving a number of MEPAG goals [11, 12]. For example, *Strata* can define shallow stratigraphy whose geometry and structure can be related to geologic settings that may once have been habitable. It can help search for shallow subsurface ice, water, or water-lain deposits, thereby directly contributing to the definition of the role of water in the geologic history and environments with biologic potential. *Strata* combines the realities of selecting a safe, low relief landing site [13, 14] with the capability to define three dimensional "virtual" outcrops and stratigraphy in the near-surface that can be used to evaluate geologic setting. The ability to quickly determine the nature (e.g., blocky ejecta versus layered) and accessibility (based on dip or structure) of target units, means *Strata* can help establish traverse direction and optimize selection of priority targets.

Information on the subsurface is a missing element in Mars Exploration and a veneer of eolian sediments, impact-derived ejecta, and other surficial deposits of-

ten leads to poorly understood relationships between the nature of near-surface materials and surface landforms. The lack of these data has often dictated the course of landed missions by requiring traverses to locations where subsurface materials can be viewed or accessed.

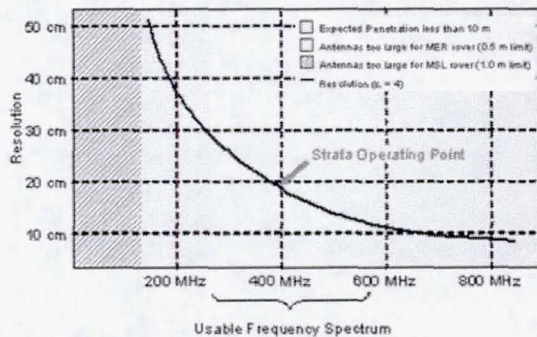


Figure 2. 400 MHz is selected as the optimal operating frequency for *Strata*.

What if MER had *Strata*? Although the MER missions are highly successful by any measure, inclusion of *Strata* in the payload would likely have altered the basic exploration strategy. Vagaries of the surface environment often complicate the definition of exploration strategies and rover traverses. With *Strata*, however, the geologic setting could have been constrained very early in the mission without impacting operations.

In Gusev, *Strata* data would have defined the rubby nature of the substrate after traversing only 10 to 20 m from the lander. These data would have revealed an absence of laterally continuous reflections corresponding to layers, confirmed the discontinuous reflections characteristic of the blocky ejecta, and may have hastened the decision to head towards the Columbia Hills.

At Meridiani Planum, data collected with *Strata* during traverses in Eagle Crater would have shown the scale and complexity of layering beneath the surface. Although these data would not have confirmed an evaporitic origin for the layers, they would have demonstrated that the outcrop was part of a thicker sequence of thinly bedded, laterally extensive rocks better exposed in the walls of Endurance Crater.

In summary, *Strata* would have made defining the presence, extent, and nature of bedrock more straightforward at both MER landing sites and could have helped guide the rovers along traverses best suited to meeting mission objectives.

Operating *Strata* on Mars: Ongoing work in terrestrial analogs to environments on Mars [8, 9] and careful consideration of factors influencing radar performance on Mars instills confidence that *Strata* can achieve 10-15 m penetration with a 400 MHz antenna.

Instrument design is based on consideration of the probable range of complex dielectric properties characterizing the Martian near surface (e.g., electric permittivity, magnetic permeability, and conductivity) and on the likely geometry of scattering/reflecting layers [6]. In general, low ambient temperature and an extremely dry near surface on Mars should reduce electrical losses and mitigate the difficulties related to the presence of fines or salts often encountered in terrestrial field studies [15]. While electrical losses may locally approach ~ 0.3 [16] and magnetic losses may be important in some iron-bearing substrates [7, 17], orbital data from TES on MGS indicate high loss areas (e.g., in Meridiani Planum) are local in extent and can be avoided via landing site selection. Nevertheless, if *Strata* were to operate in Meridiani Planum (or other-potentially high-loss site), the graceful degradation of *Strata*'s performance might mean 5-10 m instead of 10-15 m penetration, easily sufficient for tracing the extent, dip, and layers associated with the outcrops studied in Eagle and Endurance craters.

Recent data collection with the *Strata* prototype antenna in settings including those characterized by iron-rich substrates confirms the instrument can be easily accommodated on a range of rover platforms and will operate effectively in the Martian environment.

References: [1] Ulriksen, C.P.F. (1982) Ph.D. Thesis, Univ. of Technology, Lund, Sweden, 175p. [2] GPR 1994 (1994) Proc. 5th Int'l Conf. on GPR, 1294 p., Waterloo Centre for Groundwater Research, Ontario, Canada. [3] GPR 1998 (1998) Proc. 7th Int'l Conf. on GPR, 786 p., Radar Systems and Remote Sensing Laboratory, Lawrence, KS. [4] GPR 2000 (2000) Proc. 8th Int'l Conf. on GPR, 908 p., SPIE 4084, Gold Coast, Australia. [5] GPR 2002 (2002) Proc. 9th Int'l Conf. on GPR, 734 p., SPIE 4758, Santa Barbara, CA. [6] Olhoeft, G.R., (1998) Proc. GPR'98, 7th Int'l Conf. on GPR, 387-392. [7] Olhoeft, G.R., (1998) Proc. GPR'98, 7th Int'l Conf. on GPR 177-182. [8] Grant, J.A., et al. (2003) *JGR*, 108, 10.1029/2002JE001856. [9] Grant, J.A. et al. (2004) *JGR* 109, 10.1029/2003JE002232. [10] Leuschen, C., et al. (2003) *JGR*, 108, 10.1029/2002JE001875. [11] Greeley, R., et al. (2001) JPL Pub 01-7, JPL, CIT, Pasadena, CA. [12] Taylor, J. et al. (2004) <http://mepag.jpl.nasa.gov/reports/index.html>. [13] Golombek, M.P., et al. (2003), *JGR*, 108, 10.1029/2003JE002074. [14] Grant, J.A., et al. (2004) *Planet. Space Science*, 52, 10.1016/j.pss.2003.08.011. [15] Collins, M.E. and J.L. Kurtz (1998) Proc. GPR'98, 7th Int'l Conf. on GPR. [16] Heggy, E., P. et al. (2001) Conf. Geophys. Detect. Subsurface Water on Mars. LPI, Houston, TX. [17] Paillou, P., et al. (2001) *GRL*, 28, 911.

SCATTERING LIMITS TO DEPTH OF RADAR INVESTIGATION: LESSONS FROM THE BISHOP TUFF. R. Grimm¹, E. Heggy², S. Clifford², C. Dinwiddie³. ¹Southwest Research Institute, Space Science and Instrumentation Division, Space Studies Department, 1050 Walnut St. #400, Boulder CO, grimm@boulder.swri.edu; ²Lunar and Planetary Science Institute, Houston TX; ³Southwest Research Institute, Center for Nuclear Waste Regulatory Analysis, San Antonio, TX.

Summary: Large depths of investigation for ground-penetrating radar (GPR) signals have been previously predicted for the cold near-surface of Mars, leading to orbital-instrument designs in the 2-20 MHz range anticipating penetration of hundreds of meters to kilometers. Although the intrinsic absorption may be low in the total absence of liquid water, scattering due to faults, fractures, and even simple stratigraphic layering may strongly influence achievable depths of investigation. The Bishop Tuff is a terrestrial analog that has low absorption but significant fracture- and fault-induced scattering.

Field Site: A new collaboration between SwRI and LPI seeks to test low-frequency GPRs in terrestrial Mars electrical-analog environments [1]. The Bishop (CA) Tuff was considered a good electrical analog because of the very high resistivity (thousands of $\Omega\text{-m}$) for the unsaturated zone inferred from transient electromagnetic (TEM) soundings [2]. The rapid emplacement of pyroclastic flows, their subsequent partial welding, and the relatively arid environment could have inhibited infiltration and alteration, yielding electrically resistive rocks. Although this site may not be widely representative of Mars geologically, it may be analogous geoelectrically.

The underlying saturated zone at depths of 150-180 m showed relatively low resistivity (tens of $\Omega\text{-m}$). For attenuation rates of ~ 0.1 dB/m expected from ohmic losses (absorption) alone in the vadose zone, radar-range calculations [3,4; Fig. 1] suggested that, if sufficiently sharp, the water table could be detected at at 25 MHz or less. Internal boundaries in the tuff [5] could provide intermediate-depth targets.

Subsequent field and laboratory investigations confirmed that the resistivity of the Bishop Tuff was high, but not as high as indicated in the original TEM soundings. Laboratory measurements of the complex dielectric constant at tens to hundreds of MHz of Bishop Tuff samples [6] yielded equivalent resistivities of 1200-1800 $\Omega\text{-m}$. (One dielectric relaxation was discovered but the overall frequency relations indicated near-constant resistivity). Vertical-electric soundings (VES) acquired at the time of the GPR measurements confirmed near-surface resistivity ~ 1000 $\Omega\text{-m}$. The corresponding attenuation ~ 0.5

dB/m would then limit the depth of investigation to 50-100 m at low frequency (Fig. 1).

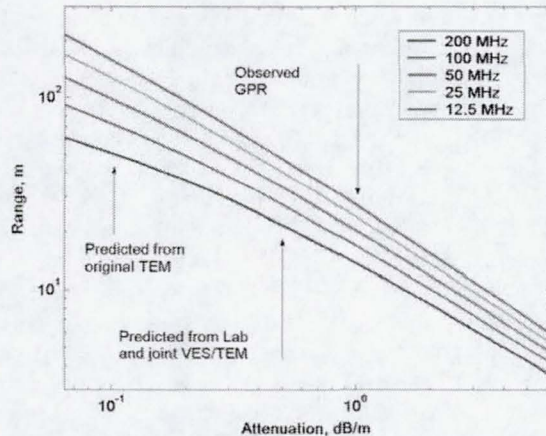


Figure 1. Predicted pulseEKKO GPR depth of detection for a rough, planar interface as a function of total ground attenuation (absorption + scattering). Arrows show absorption predicted for Bishop Tuff using different lab and field methods, and total GPR attenuation observed in the field.

GPR Investigations: Two GPRs were tested at each of three sites at the Bishop Volcanic Tablelands: a Sensors and Software pulseEKKO 100 using 50, 25, and 12.5-MHz antennas and a GSSI Multiple Low Frequency (MLF) system operating at 16-80 MHz. This paper reports only on the former; the latter will also be discussed at the Workshop.

PulseEKKO profiles of 50-100 m length were acquired in standard common-offset geometry, "static" mode, and 128-512 stacks. Limitations in productivity and data quality occurred due to intermittent failure of the receiver to transmit data across an 80-m fiber-optic cable, by coherent noise near ~ 12 MHz, 40-50 dB down from the peak signal (possibly system-related), and by bad transmitter pulses at 12.5 MHz. Common-midpoint (CMP) soundings provided the best control on velocity, which averaged ~ 0.11 m/ns. The useable dynamic range was 50-80 dB.

The three sites were chosen in order of anticipated increasing depth (<70 , <100 , and <180 m, respectively) to the regional groundwater elevation. Specific site locations were constrained by BLM en-

environmental regulations. The profile direction of Site 1 was carefully measured to be perpendicular to a fault scarp about about 150 m away. The Site 2 profile was also approximately normal to the dominant fault strike but could not be as carefully measured because there were no nearby scarps. The Site 3 profile was oblique to local fault strikes because it was constrained to lie along a road.

All profiles show strong hyperbolic scattering patterns from faults and/or block fracture boundaries, as well as traceable faults (e.g., Fig.2). Depths of investigation were visually determined to be 10-20 m. The attenuation was measured by measuring the laterally averaged RMS amplitude in between the direct wave to the noise floor. This approach is valid in the presence of laterally scattered energy (i.e., reflection hyperbolae) assuming horizontal and vertical attenuation is the same. Only low-frequency "wow" was removed in this analysis to preserve all relevant amplitude information.

Measured attenuations were 0.3-0.9 dB/m for Site 1, 0.3-0.6 dB/m for Site 2, and 1.3-1.4 dB/m for Site 3. These values are consistent with the observed depths of investigation in the presence of coherent noise. The frequency dependence was weak, in agreement of the "GPR Plateau" concept [4]. Given an absorption of ~ 0.5 dB/m from the auxiliary field and lab studies, we conclude that an excess attenuation of 0-1 dB/m is present due to scattering.

Discussion: Scattering attenuation of 0.5 dB/m will consume 120 dB of dynamic range in just 120 m. Previous GPR models for Mars [7-10] have used mean layer thicknesses of tens to thousands of meters and no laterally varying structure, so scattering losses have been underestimated [12]. Regardless of whether or not the resistivity of the cryosphere of Mars is large, scattering from fractures, faults, sedimentary or volcanic layering, and ejecta blocks will strongly influence the depth of radar investigation on Mars.

Acknowledgements: R. Grimm and C. Dinwiddie were funded by the Southwest Initiative for Mars (SwIM) internal research program at SwRI. S. Gonzalez, D. Bannon, D. Wyrick, and B. Winfrey acquired the VES/TEM data, D. Farrell analyzed these data, and R. McGinnis assisted with the GPR measurements.

References: [1] Dinwiddie, C., et al., this volume. [2] Gonzalez, S., et al. (2004) EOS Trans AGU, Fall Mtg. [3] Sens. & Soft. Inc. (1996) TM-16. [4] Annan, P. (2003) GPR Workshop Notes, Sens. & Soft. Inc. [5] TUFF PAPER. [6] Heggy, E., et al., this volume. [7] Heggy, E. et al. (2003) *JGR 108*, 2002JE001871; [8] Leuschen, C. et al. (2003) *JGR 108*, 2002JE001875; [9] Shchuko O.B. et al. (2003) *JGR 108*, 2002JE001879. [10] Ciarletti, V. et al. (2003) *JGR 108*, 2002JE001867. [11] Grimm, R.E. (2003) 6th Intl Mars Conf.

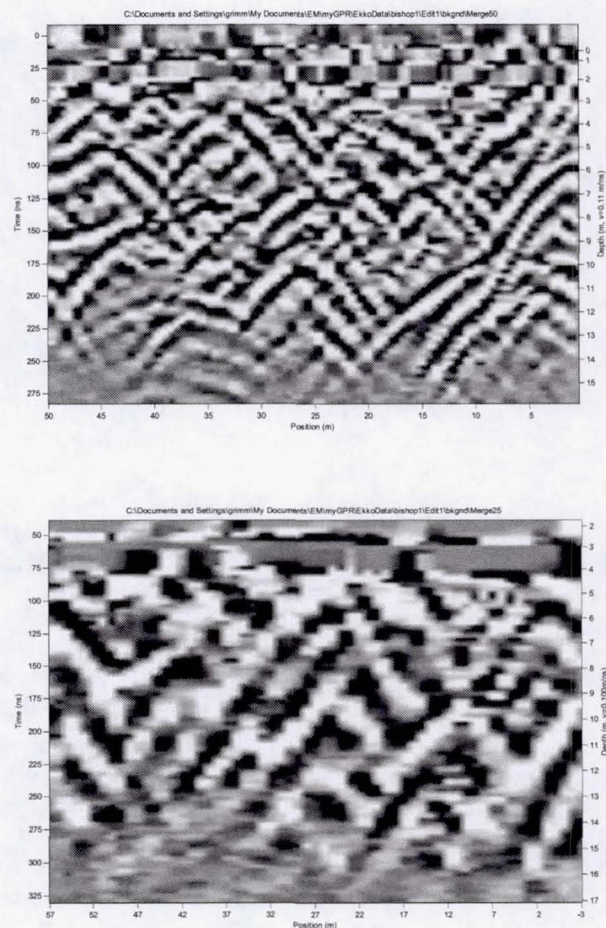


Figure 2. 50-MHz (top) and 25-MHz (bottom) profiles of Bishop Tuff Site 1. Records have low-frequency "wow" and running 5-trace average removed; the latter enhances laterally varying structure.

The Goldstone Solar System Radar: 1988-2003 Earth-Based Mars Radar Observations. A. F. C. Haldemann¹, K. W. Larsen², R. F. Jurgens¹ and M. A. Slade¹, ¹Jet Propulsion Laboratory, California Institute of Technology (JPL M/S 238-420, 4800 Oak Grove Dr., Pasadena, CA 91109-8099, albert.f.haldemann@jpl.nasa.gov), ²Laboratory of Atmospheric and Space Physics, University of Colorado – Boulder.

Introduction: The Goldstone Solar System Radar (GSSR) has successfully collected radar echo data from Mars over the past 30 years. The older data provided local elevation information for Mars, along with radar scattering information with global resolution (e.g. [1,2]). Since the upgrade to the 70-m DSN antenna at Goldstone completed in 1986, Mars data has been collected during all but the 1997 Mars opposition. Radar data, and non-imaging delay-Doppler data in particular, requires significant data processing to extract elevation, reflectivity and roughness of the reflecting surface [3]. The spatial resolution of these experiments is typically some 10 km in longitude by some 150 km in latitude. The interpretation of these parameters while limited by the complexities of electromagnetic scattering, do provide information directly relevant to geophysical and geomorphic analyses of Mars.

Landing Site Assessment with Radar Data: The usefulness of equatorial near-nadir backscatter radar data for Mars exploration has been demonstrated in the past. Radar data were critical in assessing the Viking Lander 1 site [4, 5] as well as, more recently, the Pathfinder landing site [6, 7] and Mars Exploration Rover (MER) landing sites [8, 9, 10]. In general, radar data have not been available to the Mars exploration community at large. We have recently completed submission to the PDS of Hagfors model fits to all delay-Doppler radar tracks obtained since 1988 in aid of landing site characterization for the Mars Exploration Program. The available Level-2 Derived data records consist of Hagfors radar scattering model fits to the delay-Doppler data every 0.1 degrees of longitude. The fit parameters are range (elevation), reflectivity (Fresnel), and surface roughness (RMS slope) for each 10km x 150km resolution cell. We are working on delivering all the individual calibrated delay-Doppler images to the PDS.

Interferometric Delay-Doppler Radar: In both the 2001 and 2003 observations, the reflected radar signal was received simultaneously at four of the Goldstone Deep Space Communications Center telescopes. Delay-Doppler observations map the radar signal reflected from a target into a coordinate system based on time delay and frequency shift imparted by the planets shape and rotation, respectively. Since multiple points on the surface

have the same delay and frequency coordinates, the signal from those regions are merged, and must be deconvolved by other techniques in order to create an unambiguous radar map. Pairs of receiving telescopes are used to create interferometric baselines. The signal from each baseline pair, both complex power-spectra, are multiplied to form a power spectra that contains the radar reflection's magnitude and phase, due to the varied path lengths. An iterated maximum likelihood function algorithm can then unwrap the north-south ambiguity and map the radar backscatter coefficient of the surface, at a resolution of five kilometers per pixel.

Research Perspectives: Three areas of active research apply to the GSSR Mars data.

Solving the conundrum of east-west slope. The fitting routines used for the Hagfors analyses of the sub-Earth delay-Doppler data do not properly account for east-west (or north-south) regional slopes. We have demonstrated in the past [11] that this has minimal effect on landing site analyses where flat areas are desired, but hampers the use of the data for analyses of rougher lava flows on volcanic flanks, where the radar geomorphology could fruitfully compare to terrestrial data. This issue for the time being also applies to the 5 km high-resolution interferometric data. Solving this problem is a high priority of the GSSR team. It will probably require iterative calculation of scattering models using regional MOLA topography, whereas our current algorithm is based on templates fit to a sphere.

Stealth. We are working to develop an improved geomorphic, geologic, and radar understanding of the Stealth region on Mars, known for its very low (lack of) radar backscatter echo. To accomplish this we will use the best spatial resolution GSSR data available to map the boundary of Stealth at ~10x better spatial resolution than previously. In turn, the better definition of the boundary of Stealth will allow us to examine newer high resolution imagery and thermal data to study the nature of Stealth. We expect our new higher resolution approach will allow us to either (i) choose among existing interpretations of Stealth, or, alternatively, (ii) to propose a new, combined, geomorphic, geologic and radar model for this continent-sized Martian region that barely reflects incident centimeter radar energy. At issue is

whether Stealth represents a huge volatile-driven volcanic eruption in recent Martian history [12, 13].

Ground-truthing Earth-based Mars radar. The results from the 2001 and 2003 GSSR interferometric observations and the MER landing sites allow an assessment of the radar slope evaluation. The RMS slope or roughness derived using the Hagfors model on the pre-2001 data indicated a smoother surface at Meridiani than at MPF (3.5 cm wavelength RMS slope of 1.4° vs. 4.5°) and a smoother surface at Gusev than at VL1 (12.6 cm RMS 1.7° vs 6°). Interpretation of all pre-existing radar data predicted that Meridiani Planum would be much less rocky and smoother than the VL 2 site, and that Gusev would have a combination of roughness at decimeter scales similar to or greater than VL 1 and MPF sites, but will be smoother at meter-scales. These predictions appear generally consistent with the generally smooth flat surfaces with moderate and few rocks observed by Opportunity and Spirit, where RMS slopes from MER Front Hazcam (FHAZ) stereo pairs average 3° at 3 m scale for both rovers, but average about 30° at 10 cm scale for Spirit and 20° for Opportunity at the same scale [14]. A small radar mystery arises from the fact that the Hagfors model analysis of the 3.5 cm 5 km x 5 km pixels that contain the MER landing sites have

$$\theta_{\text{rms}}(\text{Gusev}) = 1.6^\circ \pm 0.5^\circ$$

and

$$\theta_{\text{rms}}(\text{Meridiani}) = 2.0^\circ + 1.0^\circ / -0.5^\circ$$

The Hagfors model suggests that these values represent surface roughness at scales 10λ to 100λ . Examination of the FHAZ plots shows that the "best" radar numbers underestimate meter-scale RMS slope for Gusev, and overestimate it for Meridiani. We find this somewhat surprising, since the morphology of Meridiani in particular would intuitively suggest that the "gently undulating" facet terrain conditions required by Hagfors are met. With the plethora of MER data, Mars radar scattering modeling can proceed apace

References: [1] Goldspiel J. M. et al. (1993) *Icarus*, 106, 346-364. [2] Moore H. J. and Thompson T. W. (1991) *LPS XXI*, 812-815. [3] Hagfors T., *JGR*, 102, 3779-3784. [4] Masursky H. and Crabill N. L. (1976) *Science*, 193, 809-812. [5] Tyler G. L. et al. (1976), *Science*, 193, 812-815. [6] Haldemann A. F. C. et al. (1997) *JGR*, 102, 4097-4106. [7] Haldemann A. F. C. et al. (1997) *Eos Trans. AGU*, 78, F404. [8] Golombek M. P. et al. (2003) *JGR*, 108, doi:10.1029/2003JE002074. [9] Larsen, K. W. et al. (2004) *LPS XXXV*, Abstract

#1050. [10] Golombek M. P. et al. (2004) *Nature*, in press. [11] Haldemann A. F. C. et al. (2002) *IGARSS*, Abstract#INT1 A30 04. [12] Edgett K. S. et al. (1997) *JGR*, 102, 21545-21567. [13] Edgett K. S. and M. C. Malin (2000) *LPS XXXI*, Abstract #1065. [14] Haldemann A. F. C. et al. (2004) *Bull. AAS*, 36, 1161.

Acknowledgements: This research described in this publication was carried out at the Jet Propulsion Laboratory, California Institute of Technology, under a contract with the National Aeronautics and Space Administration.

MAPPING SUBSURFACE STRATIGRAPHY AND ANOMALIES IN IRON-RICH VOLCANOCLASTICS USING GROUND-PENETRATING RADAR: POTENTIAL FOR SHALLOW SOUNDING ON MARS.

E. Heggy¹, S. Clifford¹, R. Grimm², S. Gonzalez³, D. Bannon³, and D. Wyrick³. ¹Lunar and Planetary Institute, Houston, TX 77058-1113, USA, heggy@lpi.usra.edu, ²Southwest Research Institute, 1050 Walnut St., Suite 400, Boulder, CO 80302. ³CNWRA at Southwest Research Institute, 6220 Culebra Road, San Antonio, TX 78238-5166.

Introduction: Ground-penetrating radar (GPR) studies conducted in iron-rich volcanoclastics can yield important information for understanding the subsurface stratigraphy that results from lava flows with different compositions and ages. GPR is also helpful for mapping subsurface anomalies that occur in volcanoclastics such as lava flows, rifts, and lava tubes. We conducted a field survey at the Craters of the Moon (COM) National Monument to evaluate the potential use of low frequency GPR for mapping volcanic areas of the Martian subsurface where substantial evidence for underground water can be found¹. We used GPR operating at 16 and 100 MHz to perform structural mapping at several different locations within the Monument. Transient electromagnetic data were acquired simultaneously with the GPR data to assist in assessing the effects of soil conductivity and geochemistry on the identification of subsurface structures.

Site Description: Craters of the Moon National Monument is located in the South Central portion of Idaho, and lies within the northwest margin of the Eastern Snake River Plain (ESRP) where the ESRP abuts the Paleozoic and early Cenozoic Challis volcanic rocks of the Pioneer Mountains. COM is a composite of more than 40 different lava flows erupted from approximately 25 cinder cones and eruptive fissures over eight distinct eruptive periods ranging in age from Late Pleistocene to Holocene². The Monument is approximately 1100 square miles and was established in 1924 to protect the geologic features of the southern Idaho volcanic rift zone³. The monument contains various examples of pahoehoe basalt lava flows, cinder cones, lava tubes, spatter cones, and tree molds. The area is well-characterized geologically, and provides an excellent example of textbook volcanic features.

At COM, most vents are aligned along segments of the north-northwest trending Idaho rift⁴, a tensional feature which extends for a distance of some 50 km, with a strike roughly parallel to that of the Basin and Range type faults north and south of the Snake River Plain. Volcanic features at COM include Inferno cone, fissure vents, and more than 40 lava flows. Unlike most of the ESRP, where the basalts are principally olivine basalts associated with small monogenetic shield volcanoes, the lava flows of COM exhibit a wide range of chemical compositions³. The varied compositions are thought to occur because of crustal

contamination from assimilating older rocks or from crystal fractionation due to prolonged eruptive periods⁴.

We selected three distinct volcanic features to sound for the purpose of evaluating the potential of low-frequency GPR for mapping shallow subsurface structures. These features are a (1) cinder cone, (2) lava tube, and (3) rift.

Survey Setup and Instrumentation Description: In the frequency band between 16 and 100 MHz, GPR can probe the subsurface down to a few tens of meters, depending on geoelectrical ground conductivity. To obtain a confident scientific return from the radar backscattered echoes, resistivity data are crucial for quantifying the penetration depth, identification of subsurface anomalies, and understanding wave losses, propagation, and diffusion mechanisms that constitute the radar tomography of acquired data. Among different techniques to measure geoelectrical ground conductivity, the Transient Electromagnetic Method (TEM) is the best suited for comparison to GPR data in terms of penetration depth, vertical resolution, and sensitivity to subsurface moisture. We give below a brief description of both complementary methods (GPR and TEM) used in this survey to reduce ambiguities regarding the subsurface exploration of COM.

Ground-Penetrating Radar. Radar sounding was performed using pulse repetition ground-penetrating radar. The system was operated with two different antenna configurations covering a broadband from 16 to 100 MHz. Both antennas were coupled to the surface during the data acquisition, and measurements were performed separately to avoid interference. A bistatic shielded 100 MHz antenna was used to acquire data in continuous mode, and an unshielded multiple low-frequency antenna with four frequency configurations (corresponding to central operational frequencies of 16, 20, 40, and 80 MHz) was used to provide monostatic sounding shots at 16 MHz.

Transient Electromagnetic Method. During the field campaign, 20-, 50-, and 100-m loop transient electromagnetic soundings were also performed to explore the geoelectrical ground conductivity. TEM data are used to estimate the extent of absorptive losses during subsequent radar soundings. Current was maintained at 2 A for all transmitter loops at all stations, and one or

more of the pulse repetition rates 285, 75, and 30 Hz were used for each setup. The effective area of the receiver coil is 31.4 m². Data were acquired with the receiver coil at the approximate center of the transmitter loop for all loop sizes; for the 15 and 50 m loops, the receiver coil was also placed 10 m outside the transmitter loop. Results from this survey will be presented at the workshop.

GPR Survey Results: Our results show that even with a relatively large amount of iron-oxides (~14%) penetration depths of 50 m were achieved with the 100 MHz antenna and depths of 150 m were achieved with the 16 MHz antenna. These results are attributed to the high porosity of the soil at the studied areas, which lowered the electrical losses, hence favoring a relatively deep penetration of the radar wave.

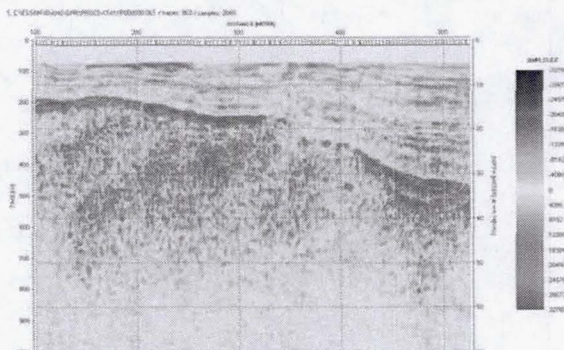


Figure 1: 100 MHz profile of the basalt stratigraphy on the Inferno cinder cone

Both GPR and TEM data confirmed the suitability of the site for shallow subsurface mapping in the presence of relatively Mars-like amounts of iron-oxides. Survey results revealed good data quality in terms of penetration depth and a clear identification of subsurface stratigraphy. The 100 MHz GPR profile obtained from Inferno Cone is illustrated in Figure 1. Analysis of the data suggests an average penetration depth of approximately 40 m was obtained. The cone consists of dry porous basaltic ashes with relatively low dielectric losses. The radar tomography shows a significant layering in the first few meters that could be attributed to different eruptive periods that formed that cone. A clear interface is distinguished at a penetration depth of approximately 15 m. Signal analysis and laboratory dielectric measurements show a reflection like this is mainly caused by the presence of an important dielectric contrast with the surrounding material due to the variation in mineralogical composition of the buried lava flow layer, as suggested by the ESRP geological map. Additional GPR data and results from analyses will be presented at the workshop.

Implications for Shallow Soundings of Mars: In the presence of adequate geoelectrical conditions,^{5,6} shallow subsurface water-saturated zones on Mars, if present, can be sounded and unambiguously resolved from radar echoes. Porous geologic deposits may be a suitable target for shallow and deep radar sounding where density, rather than the mineralogy, may dominate the dielectric behavior of the investigated soil.

References: [1] Clifford, S.M. and Parker, T.J. (2001) *Icarus*. [2] Kuntz et al. (1982); ed. Cenozoic Geology of Idaho, Idaho Bureau of Mines and Geology, Bull. 26. [3] Kuntz et al. (1992); eds., Regional Geology of Eastern Idaho and Western Wyoming: Geological Society of America Memoir 179. [4] Prinz, M., 1970. Idaho rift system, Snake River Plain, Idaho. *Geol. Soc. Am., Bull.*, 81, 941-948. [5] Heggy et al., (2001) *Icarus*, Vol. 154, N2, pp. 244-257. [6] Heggy et al., (2003), *JGR*, Vol. 108, E4, pp. GDS 11-1.

DIELECTRIC MAP OF THE MARTIAN SURFACE. E. Heggy & A. Pommerol, Lunar and Planetary Institute, 3600 bay Area Blvd., 77058-1113, Houston, TX, USA (heggy@lpi.usra.edu); Ecole Normale Supérieure de Lyon, Lyon, France

Abstract: We have undertaken laboratory electromagnetic characterization of the total set of minerals identified by TES [1] on the Martian surface in order to investigate experimentally the dielectric properties of the sediments covering it in the frequency range from 1 to 1000 MHz. Volcanic rocks with a well defined mineralogy and petrology from potential terrestrial analogues sites have also been included in the study. Our primary objective is to evaluate the range of electrical and magnetic losses that may be encountered by the various Radar sounding and imaging experiments dedicated to map the Martian subsurface searching for underground water. The electromagnetic properties of these Mars-like materials will be presented as a function of various geophysical parameters, such as porosity, bulk density and temperature. Using the mineral and soil density distribution provided by TES and THEMIS data we integrated those measurements to form a primary dielectric map of the Martian surface. The secondary objective, is to locate regions where surface dielectric conditions are suitable for subsurface sounding.

Scientific context: The Mars Exploration Program has identified the search for subsurface water on Mars as a key investigation towards understanding the hydro-geologic history of the planet and for identifying potential environments for the survival of primitive life forms [2,3]. During the coming decade three different types of sounding Radars will be used to address this task and to reduce the ambiguities concerning the state, distribution and total abundance of water within the Martian crust [4]. The ability of these radars experiments to detect and identify the presence of liquid water will strongly depend on the physical properties, mineralogy and thermal structure of the Martian subsurface as they define the electrical and magnetic characteristics of the crustal propagation matrix [5,6]. The laboratory characterization of Mars-like volcanic and sedimentary materials in the low frequency range 1-500 MHz (the range covering sounding and imaging radar experiments) is hence a key study in evaluating optimal locations for deep subsurface sounding sites and future data interpretation [7].

Experimental Approach: we perform permittivity measurements using capacitive cells specially designed in order to avoid the resonance that occurs in classical capacitive cells when working with lossy soils. The first one we used machined and compacted

pellet. The second is an open coaxial cell used to measure the dielectric constant of powder-reduced material. Both of the two dielectric cells were connected to an impedance analyser to perform the measurements in the frequency band 1 to 1000 MHz. The analyser was connected to a central command unit to extract data and calculate in real-time the real and imaginary part of the complex dielectric constant and magnetic permeability (μ' and μ''). Samples magnetic permeability was evaluated using the magnetic cell HP16454A, connected to the same analyser described above. Sample density and porosity were controlled using a hydraulic press to compact samples having equal masses. Frequency dependent model was established for each sample and extended to 3 GHz in order to reproduce surface frequency dependent dielectric and loss tangent maps and to compare the map with the current earth based radar observations from the GSSR [9].

Results: We present in this paper only a brief selection of our measurement and modeling data set. More complete results will be exposed in the workshop and an extended paper. Figure 1 show the 2 MHz loss tangent map on a near spherical projection. The loss tangent distribution is derived from the different permittivity measurements of Martian like soils as a function of their density distribution on the surface.



Figure 1: 2 MHz loss tangent map of Mars

In a first step we considered only areas between -60° South and 60° North, as current measurements were performed on ice-free samples. The map shows that 55 % of the surface sediments layer (1 to 10 meters deep) has a loss tangent around 0.07 and the average value is

0.05 at 2 MHz. The loss tangent map results fit with the dust distribution map provided by Mellon [8] from the TES data. Hence, region with the highest dust cover have the lowest loss tangent around 0.02 and vice versa area with low dust cover present higher losses. Comparison with the 3 GHz dielectric map and the earth based radar observation performed near the equatorial regions by Haldemann [9], show an adequate matching between the dielectric values.

Implications for Radar exploration: Measurements on Martian-like minerals and rocks and their possible distribution on the Martian surface have shown an important and expected variation in the Martian surface geoelectrical descriptions. This variation is clearly observed in the low frequency range from 1 to 30 MHz, dielectric contrasts between different areas tend to minimize as we get to higher frequency range. This explains the quite homogeneous dielectric distribution observed from earth based radar observations [9]. Hence, orbital low frequency sounding instruments will encounter a different challenging dielectric configuration; hence such a frequency dependent dielectric map is crucial in order to optimize orbital sounding performances on areas where surface dielectric properties combined with surface roughness may lead to a minimum reflection and losses of the signal from the surface sediments which in term lead to a better penetration depth. Further maps showing the losses and penetration depth will be presented at the workshop.

References: [1] Banfield, J. L., (2002) *JGR*, Vol. 107, E6, pp 9-2. [2] Clifford S.M (1993) *JGR*, 93, 10973-11016. [3] Clifford, S.M., and T.J. Parker (2001) *Icarus*, Vol. 154, pp. 40-79. [4] Clifford, S.M. et al., (2001) Conference on the geophysical detection of subsurface water on Mars, Houston. [5] Heggy et al., (2001) *Icarus*, Vol. 154, N2, pp. 244-257. [6] Olhoeft, G.R., (1998), *7th Int. Conference on GPR*, Lawrence. [7] Heggy et al., (2003), *JGR*, Vol. 108, E4, pp. GDS 11-1. [8] Mellon, M.T., Thermal inertia and rock abundance, Exploring Mars with TES, 2001. [9] Haldemann, A.F. et al., (2000) *Technical Report, JPL, Pasadena*.

SURFACE CLUTTER REMOVAL IN AIRBORNE RADAR SOUNDING DATA FROM THE DRY VALLEYS, ANTARCTICA. J.W. Holt¹, D.D. Blankenship¹, D.L. Morse¹, M.E. Peters¹, and S.D. Kempf¹, University of Texas Institute for Geophysics, The John A. and Katherine G. Jackson School of Geosciences, University of Texas, 4412 Spicewood Springs Rd., Bldg. 600, Austin, TX 78759, jack@ig.utexas.edu

Introduction: We have collected roughly 1,000 line-km of airborne radar sounding data over glaciers, rock/ice glaciers, permafrost, subsurface ice bodies, ice-covered saline lakes, and glacial deposits in Taylor and Beacon Valley. These data are being analyzed in order to develop techniques for discriminating between subsurface and off-nadir echoes [1] and for detecting and characterizing subsurface interfaces.

The identification of features on Mars exhibiting morphologies consistent with ice/rock mixtures, near-surface ice bodies and near-surface liquid water [2,3], and the importance of such features to the search for water on Mars, highlights the need for appropriate terrestrial analogs and analysis techniques in order to prepare for radar sounder missions to Mars. Climatic, hydrological, and geological conditions in the Dry Valleys of Antarctica are analogous in many ways to those on Mars.

A crucial first step in the data analysis process is the discrimination of echo sources in the radar data. The goal is to identify all returns from the surface of off-nadir topography in order to positively identify subsurface echoes. This process will also be critical for radar data that will be collected in areas of Mars exhibiting significant topography, so that subsurface echoes are identified unambiguously.

The positive detection and characterization of subsurface (including sub-ice) water is a primary goal of NASA's Mars exploration program. Our data over the Dry Valleys provides an opportunity to implement techniques we are developing to accomplish these goals.

Data Acquisition Methods: Using a Twin Otter airborne platform, data were collected in three separate flights during the austral summers of 1999-2000 and 2001-2002 using multiple systems, including a chirped 52.5 – 67.5 MHz coherent radar operating at 750 W and 8 kW peak power (with multiple receivers) and 1 - 2 microsecond pulse width, and a 60 MHz pulsed, incoherent radar operating at 8 kW peak power with 60 ns and 250 ns pulse width.

A laser altimeter (fixed relative to the aircraft frame) was also used during both seasons. Precise positioning was accomplished through the use of two carrier-phase GPS receivers on the aircraft and two at McMurdo Station. Post-processing of the positioning data yields accuracies of ~ 0.10 m for samples at ~ 15 m intervals.

Data Acquisition Targets: Flights were undertaken in Taylor and Beacon Valleys in 2000 and 2001. Flight elevation was nominally 500 m above the surface. Radar and laser altimetry data were collected over the following targets in Taylor Valley relevant to Mars: Taylor Glacier, Lakes Fryxell and Bonney, debris flows, permafrost and polygonal terrain. In Beacon Valley, we overflew Friedman rock glacier and polygonal terrain.

Data Analysis: Data analysis so far has concentrated on technique development for discrimination of subsurface echoes from surface echoes due to surrounding topography. For this we have used a 24-km portion of the sole 2001 flight in Taylor Valley. Two techniques were developed for echo discrimination. The first method simulates surface echoes using aircraft position data, the modeled radar antenna pattern, and surface topography from a Lidar-based digital elevation model (DEM) acquired by the USGS and NASA in the Dry Valleys with 2-meter postings [4]. The simulated data are compared with the actual data to reveal to identify echoes that are from the surface (Figure 1).

In the second method, we first identify significant echoes in the radar data and then we migrate them to the surface through range estimation. This uses the measured time delay of the echo, aircraft position and known surface topography. We map the echoes onto both the DEM and optical imagery at the appropriate range in order to identify candidate surface return sources (Figure 2).

Combining the two methods yields the most conclusive echo discrimination. The forward model for simulating surface echoes can also be performed separately for left-side and right-side topography. This helps reduce the problem of left-right ambiguity in the radar sounding data through the quantification of expected surface echo strengths from either side.

Conclusions: Two methods of echo discrimination have been developed and used in order to discriminate apparent subsurface reflectors from off-nadir surface echoes: (1) forward modeling of echoes using aircraft position, antenna pattern and topography, and (2) migration of radar echoes to the surface in the cross-track direction to identify features in the topography that could be echo sources.

One obvious result is that the identification of surface echoes is critically dependent on having a good model of topography.

Acknowledgements: This work is supported by NASA grant NAG5-12693 and the University of Texas at Austin. Data acquisition was supported by NSF grants OPP-9814816 and OPP-9319379.

References: [1] Holt J.W., Blankenship D.D., Peters M.E., Kempf S.D., and Williams B.J. (2003) *Eos Trans. AGU*, 84(46), Abst. P31B-1058 [2] Malin M. C. and Edgett K. S. (2000) *Science*, 288, 2330–2335. [3] Baker V.R. (2001) *Nature*, 412, 228–236. [4] Schenk, T., B. Csatho, W. Krabill, I. Lee, in prep.

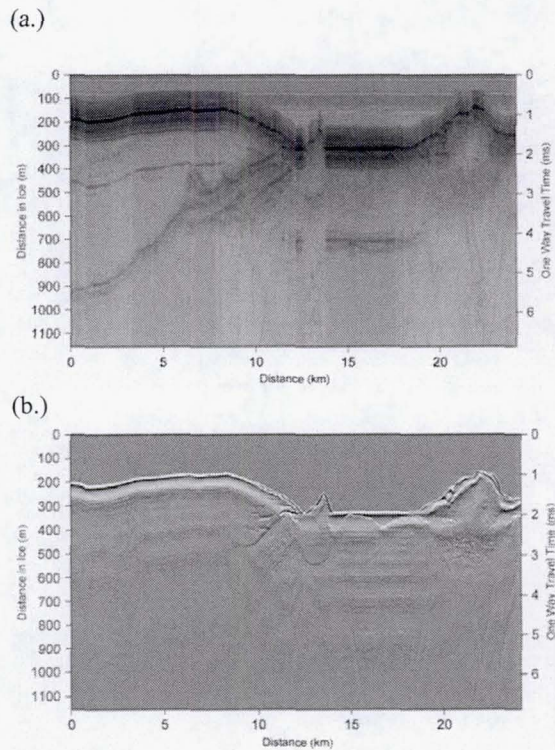


Figure 1. Comparison of (a) airborne radar data and (b) simulated surface-echo data from a portion of the Taylor Valley flight (red line in center of valley in Figures 2b and 2c). Note the prominent echo in (a) that mimics surface topography. This is clearly a double-bounce reflection between the surface and the bottom of the aircraft and is ignored. The simulated data in (b) are derived from a surface elevation model, the aircraft flight path and the antenna pattern. Some of the echoes can be positively correlated with predicted surface echoes, while true subsurface reflectors lie below Taylor Glacier (at left).

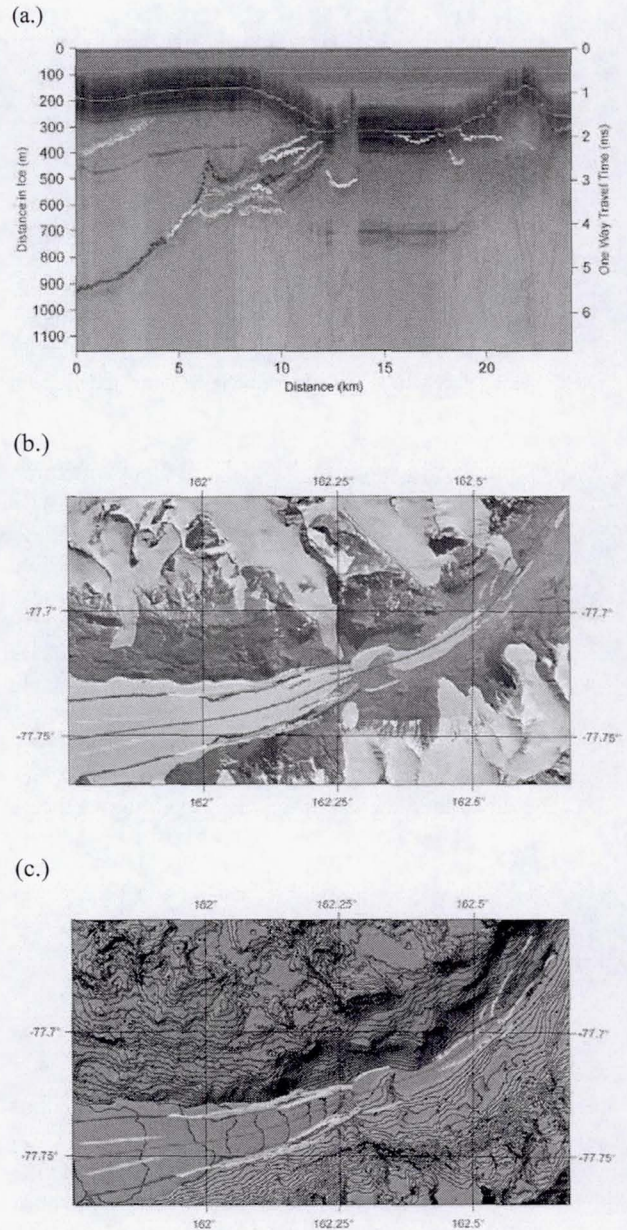


Figure 2. Distinct radar echoes indicated by separate colors (a) are migrated to the surface in the across-track direction using surface topography and aircraft position, and then overlaid on (b) an optical image and (c) the DEM (shown with 50-m contour intervals). This helps in identifying surface features that may be the source of echoes in the radar sounding data. Taylor Glacier flows down the valley from the left side of the image and terminates at Lake Bonney.

COMPARING TRANSIENT ELECTROMAGNETICS AND LOW FREQUENCY GROUND PENETRATING RADAR FOR SOUNDING OF SUBSURFACE WATER IN MARS ANALOG ENVIRONMENTS. J. A. Jernsletten¹ and E. Heggy², ¹1917 Florida Dr., Seabrook, TX 77586, joern@jernsletten.name, ²Lunar and Planetary Institute, Houston, Texas, heggy@lpi.usra.edu.

Introduction: The purpose of this study is to compare the use of (diffusive) Transient Electromagnetics (TEM) for sounding of subsurface water in conductive Mars analog environments to the use of (propagative) Ground-Penetrating Radar (GPR) for the same purpose. To provide a baseline for such studies, and to show how these methods differ and complement each other, we show data from three field studies: 1) Radar sounding data (GPR) from the Nubian aquifer, Baharia Oasis, Egypt; 2) Diffusive sounding data (TEM) from Pima County, Arizona; and 3) Shallower sounding data using the Fast-Turnoff TEM method [11] from Peña de Hierro in the Río Tinto area, Spain. The latter is data from work conducted under the auspices of the Mars Analog Research and Technology Experiment (MARTE) [1-6].

The GPR and TEM methods are discussed and compared in terms of their strengths and weaknesses in the following areas; resolution, sensitivity to highly conductive layers (clay, ore bodies, brines, metal-rich fluids, etc.), depth of investigation, sounding frequencies, logistical efficiency, and appropriate applications.

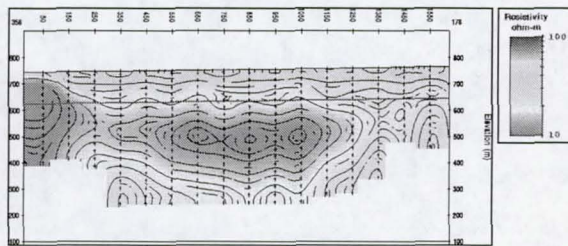


Figure 1. Line 2 TEM Data from Arizona Survey.

Potential of TEM: The TEM method has been used extensively for mapping of groundwater [7-8], and of metal-bearing acid solutions in leaching operations. Fig. 1 shows data from a TEM survey that was carried out in Pima County, Arizona, in January 2003. Data was collected using 100 m Tx loops and a ferrite-cored magnetic coil Rx antenna, and processed using commercial software [8-9]. The sounding frequency used in this survey was 16 Hz, a frequency sensitive to slightly salty groundwater [8, 10].

Prominent features in Fig. 1 are the ~500 m depth of investigation and the ~120 m depth to the water table (horiz. blue line). Note also the conductive (~20-40 Ω m) clay-rich soil above the water table. The blue line marks the ~120 m depth to the water table found in several USGS test wells in the area.

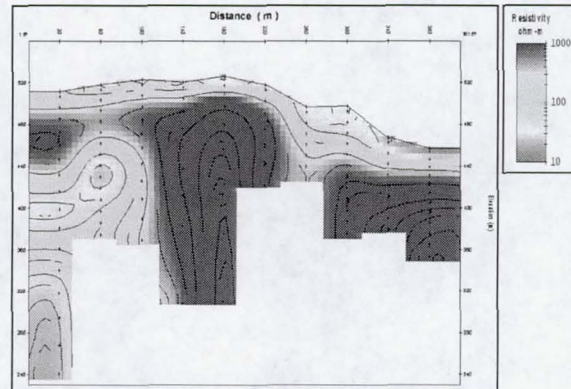


Figure 2. Line 4 Fast-Turnoff Data, Rio Tinto.

Fig. 2 shows data from Line 4 (of 16) from the Río Tinto Fast-Turnoff TEM survey, collected using 40 m Tx loops and 10 m Rx loops, with a 32 Hz sounding frequency [1, 11]. Note the ~200 m depth of investigation and the conductive high at ~80 m depth below Station 20. This is the local water table, with the same 431 m MSL elevation as the nearby pit lake. The center of the "pileup" below Station 60 is spatially coincident with the vertical fault plane located here.

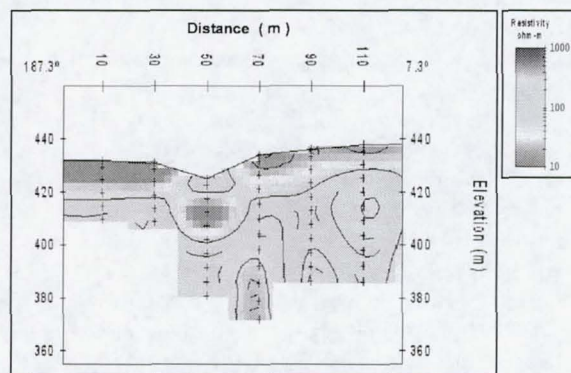


Figure 3. Line 15 Fast-Turnoff Data, Rio Tinto.

Fig. 3 shows Fast-Turnoff TEM data from Line 15 of the Río Tinto survey, collected using 20 m Tx loops and 10 m Rx loops, again with a 32 Hz sounding frequency [1, 11]. Note the ~50 m depth of investigation and the conductive high at ~15 m depth below Station 50, interpreted as subsurface water flow under mine tailings matching surface flows seen coming out from under the tailings, and shown on maps. Both of these interpretations (Line 4 and Line 15) were confirmed by preliminary results from the MARTE ground truth drilling campaign carried out in September and October 2003 [1, 6].

Potential of GPR: Ground Penetrating Radars can probe the subsurface layers to varying depths depending on the sounding geometry and the geoelectrical and geomagnetic properties of the soil at the sounded sites [12]. A Test experiment was carried in February 2003 in the Baharia Oasis in the western Egyptian desert in order to detect the Nubian aquifer water table at depth ranging from 100 to 900 meter, using a 2 MHz monostatic GPR [13]. The geological cross section of the studied area is shown in Fig. 4.

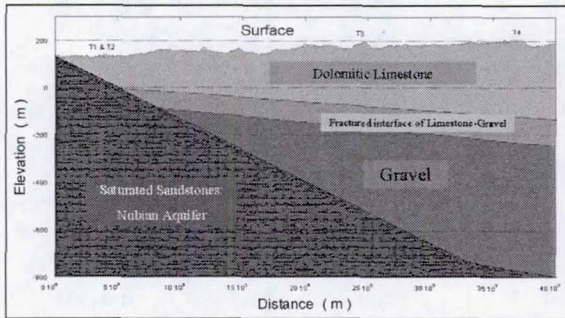


Figure 4. The hydro-geological model along the track of the GPR test experiment in the Baharia test site.

The survey demonstrated the ability of this technique to detect the Nubian Aquifer at a depth around 900 m beneath thick layer of homogenous marine sedimentary quaternary and tertiary structures constituted mainly of highly resistive dry porous dolomite, illinite, limestone and sandstone, given a reasonable knowledge of the local geoelectrical properties of the crust [14].

In the locations where the water table was located at shallower depths of less than 200 meter (cf. Fig. 4; T1 and T2), but with a presence of very thin layers (less than half a meter) of reddish dry clays, the technique fails to probe the moist interface and also fails to map any significant stratigraphy.

Fig. 5 shows an example of the data collected in the site T4 (indicated on Fig. 4) where the water table was located 900 meter deep. The GPR was able to map the first interface between the dolomitic limestone and the gravel (The first reflection occurring around 10 ns in Fig. 5) while the detection of the deep subsurface water table remains uncertain due to the uncertainties arising from some instrumental and geoelectrical problems.

Conclusions: GPR excels in resolution, productivity (logistical efficiency) and is well suited for the shallower applications, but is more sensitive to highly conductive layers (result of wave propagation and higher frequencies), and achieves considerably smaller depths of investigation than TEM.

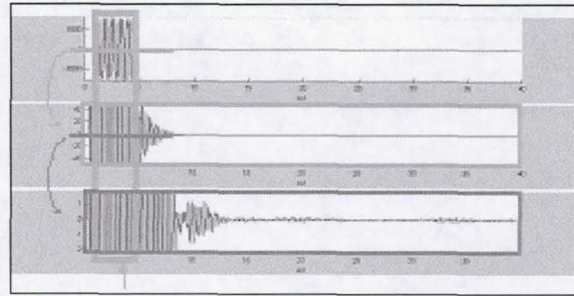


Figure 5. Monostatic radar sounding data collected in Egypt using the 3.5 MHz band of the GPR [15].

The (diffusive) TEM method uses roughly two orders of magnitude lower sounding frequencies than GPR, is less sensitive to highly conductive layers, achieves considerably deeper depths of investigation, and is more suitable for sounding very deep subsurface water. Compared with GPR, TEM suffers for very shallow applications in terms of resolution and logistical efficiency.

Fast-Turnoff TEM, with its very early measured time windows, achieves higher resolution than conventional TEM in shallow applications, and somewhat bridges the gap between GPR and TEM in terms of depths of investigation and suitable applications.

References: [1] Jernsletten J. A. (2003) *Fast-Turnoff Transient Electro-Magnetic (TEM) Geophysical Survey*. MARTE field report. [2] Fernández-Remolar et al. (2003) *JGR*, 108/E7, 16-1 – 16-15. [3] Stoker C. R. et al. (2003) *Drilling Campaign Plan V0.1*. MARTE working document. [4] Stoker C. R. et al. (2003) *Drilling Plan CRS 4-20-2003*. MARTE working document. [5] Stoker C. R. et al. (2003) *LPSC 34*, abstract no. 1076. [6] Stoker C. R. et al. (2003) *Initial Results From the 2003 Ground Truth Drilling Campaign*. MARTE working document. [7] Reynolds J. M. (1997) *An Introduction to Applied and Environmental Geophysics*. [8] Zonge K. L. (1992) *Introduction to TEM*. In: *Practical Geophysics II, for the Exploration Geologist*. [9] MacInnes S. and Raymond M. (1996) *Zonge STEMINV manual*. [10] Palacky G. J. (1987). In: *Electromagnetic Methods in Applied Geophysics, Volume 1, Theory*. Nabighian M. N., editor. [11] Zonge K. L. (2001) *NanoTEM – A Very Fast-Turnoff TEM System*. Zonge Engineering case study. [12] Olhoeft, G.R., (1998), *7th Int. Conference on GPR*, Lawrence. [13] Bertheliet, J.J., and Netlander Team, (2000) *Planetary and Space Science*, 48, pp. 1153-1159. [14] Heggy et al., (2001) *Icarus*, Vol. 154, N2, pp. 244-257. [15] Bertheliet J.J. et al., *CNES technical report*, 2003.

**THE MARSIS RADAR, SIGNAL SIMULATION AND INTERPRETATION
USING MOLA TOPOGRAPHY DATA.**

W. Kofman (1), JF Nouvel (1), A. Hérique (1), J-E. Martelat (2)
(1) Laboratoire de Planétologie de Grenoble, , Fax: (+33) 476 51 41 46;
(2) Laboratoire de Géodynamique des Chaînes Alpines, Grenoble

To study the surface and subsurface , the Mars Express Mission involves a radar sounder equipment called MARSIS, for "Mars Advanced Radar for Subsurface and Ionosphere Sounding", in order to map Martian subsurface dielectric characteristics.

We developed a MARSIS radar signal simulation which will be used to validate the radar echoes processing and to support the interpretation of the future MARSIS data.

This tool simulates all the sounding process steps, and is based on the Facet Method in order to model the Martian surface. We have shown this method is a valuable process to model a smooth surface, such as the Martian one, and noticed this simulator takes a short computation time comparatively to other methods.

We will present simulations results using the MOLA topographic data to model the Martian surface for some chosen orbits of the spacecraft. On examples of the geological structures, we show how the received signal looks like, how it behaves and what physical parameters (dielectric constant, attenuation, geological structures...) can be measured from these echoes. We will underline the possible difficulties (ambiguities) in the interpretations but also the methods how to solve these problems. Some ground constitution models will be advanced and their radar signature simulated and interpreted.

A PHASE SIGNATURE FOR DETECTING WET STRUCTURES IN THE SHALLOW SUBSURFACE OF MARS USING POLARIMETRIC P-BAND SAR.

Yannick Lasne¹, Philippe Paillou¹, J.-M. Malézieux²,
¹Astronomical Observatory of Bordeaux, 33270 Floirac, France, paillou@obs.u-bordeaux1.fr, ²Institut EGID, 33607 Pessac, France.

Introduction: Over the last two decades, remote sensing using polarimetric synthetic aperture radar (SAR) has been widely used to study the earth's surface. One of the main interesting application is the mapping of the near-surface soil moisture from space-borne SAR data (ERS 1/2, JERS1, ENVISAT, and RADARSAT). Several experiments demonstrated that low-frequency radar has penetration capabilities that can be used to map subsurface heterogeneities such as geological interfaces or wet layers. As regards soil moisture, it is well known that the presence of water significantly influences the radar response of a terrain. Nevertheless, very few authors used the phase information from SAR data to detect moisture. In previous studies, we showed that a copolarized phase difference between horizontal (HH) and vertical (VV) channels observed on SAR images is correlated to buried wet layers. It can be used to detect wet subsurface layers down to a larger depth than when only considering HH and HV amplitude signals [1].

As Mars is concerned, recent measurements by the Gamma Ray Spectrometer (GRS) on board the Mars Odyssey spacecraft allowed the mapping of ground-ice (in the form of water or hydrated minerals) in the upper few meters of the southern hemisphere of Mars at mid and high latitudes [2]-[5]. Since the geographic range of ground-ice stability strongly depends on the abundance of atmospheric water, several studies discuss the possible location and occurrence of liquid water on Mars [6]-[7]. Using a general circulation model to calculate ground temperature, Haberle et al. [7] determine the current locations on Mars where pure liquid water or brine solutions could exist, that is where the ambient CO₂ pressure is greater than the water vapor pressure at the local temperature. One could then reasonably assume the presence of liquid water in the few upper meters of the Martian surface, at least temporarily. Since radar is sensitive to dielectric contrasts, the liquid water in the shallow subsurface could lead to easily detectable interfaces because of a high permittivity due to the moisture. Moreover, Mars has been shown to have a wide range of scattering properties in the wavelength range from C-band (3 cm) to L-band (18 cm) including volume scattering from buried terrains, and specific dielectric and magnetic properties due to iron-rich materials [8]. We propose the use of P-band (70 cm) polarimetric SAR system to investigate the presence of wet structures in the first few meters of the Martian soil.

Geoelectrical model of the near subsurface: Numerous studies of ground-ice stability predicted the occurrence of a layered subsurface, in which a dry (ice-free soil) upper layer covers a wet lower layer (ice-cemented soil) [2],[5]. For that reason, we considered a two-layers scattering problem in order to assess the capabilities of a P-band SAR system to penetrate

soil for retrieving information about subsurface, in particular detecting moisture using the radar copolarized phase signal. Since the alpha X-ray spectrometer on the Spirit rover showed that the composition of Gusev soil is similar to the Viking 1/2, and Pathfinder landing sites [9]-[11], we assumed an upper dry layer composed of a mixture of iron oxides, basalts, salts, and meteoritic materials, covering a wet lower layer mainly basaltic in composition, with a variable water content (Fig. 1). Each layer is characterized by its roughness and electromagnetic parameters. Permittivity measurements were performed on several minerals that appear to be good analogs to those observed on the surface of Mars. The permittivity of the mixture for the upper dry layer is derived from the dielectric constant of each mineralogical component using the second formula of Lichteneker [12]. According to our laboratory measurements around 400 MHz, we found a complex permittivity of $\epsilon_1 = 5.87 - i0.141$ for an upper layer mainly composed of basaltic materials mixed with small amounts of iron oxides (goethite, hematite) and meteoritic materials. The permittivity of the underlying basaltic layer is set at $\epsilon_2 = 4.19 - i0.178$ when dry and will increase with respect to the moisture content.

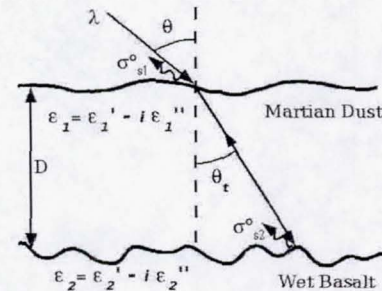


Fig. 1. Geometry of the two-layers scattering problem.

The two-layers scattering IEM model: In order to determine the copolarized phase difference Φ_{HH-VV} , we had to compute the backscattering coefficients for each layer. Since smooth to medium rough surfaces are considered here, the Integral Equation Model (IEM) proposed by Fung [13] can be used. We initially only considered the single- and multiple-scattering terms and neglected volume scattering. The total backscattered power $\sigma_{pp}^o(\theta)$ can be written as:

$$\sigma_{pp}^o(\theta) = \sigma_{S1pp}^o(\theta) + \sigma_{S2pp}^o(\theta) \quad (1)$$

where pp is the polarization state (HH or VV), and $\sigma_{S1pp}^o(\theta)$ is the surface backscattering coefficient from the upper layer

written as the sum of single and multiple terms:

$$\begin{aligned} \sigma_{S1pp}^o(\theta) &= \frac{k}{4} e^{-2k^2 \cos^2(\theta) \sigma^2} \sum_{n=1}^{\infty} |I_{pp}^n|^2 \frac{W^{(n)}(2k \sin(\theta))}{n!} + \\ & \frac{k^2}{4\pi} e^{-3k^2 \cos^2(\theta) \sigma^2} \sum_{n=1}^{\infty} \sum_{m=1}^{\infty} \frac{(2k^2 \cos^2(\theta) \sigma^2)^{n+m}}{n!m!} \\ & \cdot \int \int \text{Re}[f_{pp}^* F_{pp}(u, v)] W^{(n)}(u - k_x, v) W^{(m)}(u + k_x, v) dudv \\ & + \frac{k^2}{16\pi} e^{-2k^2 \cos^2(\theta) \sigma^2} \sum_{n=1}^{\infty} \sum_{m=1}^{\infty} \frac{(k^2 \cos^2(\theta) \sigma^2)^{n+m}}{n!m!} \\ & \cdot \int \int [|F_{pp}(u, v)|^2 + F_{pp}^*(u, v) F_{pp}^*(-u, -v)] W^{(n)}(u + k_x, v) \\ & \cdot W^{(m)}(u - k_x, v) dudv \end{aligned} \quad (2)$$

where θ is the radar incident angle, k the radar wave-number, W^n is the Fourier transform of the n^{th} power of the Gaussian surface correlation function and u, v are the spectral variables from the Green's function. f_{pp} are the Kirchhoff field coefficients while F_{pp} represents the complementary field coefficients. The non-coherent scattering of the lower layer $\sigma_{S2pp}^o(\theta)$ is derived from (2) taking into account the wave attenuation due to the propagation through the upper layer. Since (1) could be represented as the sum of two vectors, the phase difference between HH and VV signals can be written as [1]:

$$\begin{aligned} \Phi_{HH-VV} &= \left| \text{Arctg} \left(\frac{\sigma_{S2HH}^o \sin(\varphi_P)}{\sigma_{S1HH}^o + \sigma_{S2HH}^o \cos(\varphi_P)} \right) - \right. \\ & \left. \text{Arctg} \left(\frac{\sigma_{S2VV}^o \sin(\varphi_P)}{\sigma_{S1VV}^o + \sigma_{S2VV}^o \cos(\varphi_P)} \right) \right| \end{aligned} \quad (3)$$

Results: We performed simulations of Φ_{HH-VV} for several moisture contents of the lower layer at three incidence angles: $\theta = 20^\circ, 30^\circ$, and 40° for a central radar frequency of 430 MHz. The roughness parameters (rms-height σ and correlation length L) are $\sigma_1 = 1.5$ cm and $L_1 = 10$ cm, and $\sigma_2 = 3.5$ cm and $L_2 = 10$ cm for the upper and lower layer respectively. As shown in Fig. 2, Φ_{HH-VV} is very sensitive to the incidence angle. Wet subsurface structures should be more easily detectable at larger incidence. Fig. 2 also shows that for a moisture content of the lower layer leading to a permittivity close to the upper layer, Φ_{HH-VV} decreases to zero, indicating that the phase signal is mainly related to the dielectric contrast at the upper-lower layer interface. Indeed, when $\epsilon_2 = \epsilon_1$, the scattering problem reduces to a single layer problem and only the surface signal contributes to the backscattering. Monitoring changes in Φ_{HH-VV} value could then be an interesting method to map seasonal changes of the subsurface moisture on Mars.

Fig. 3 displays the backscattering coefficient for HH polarization for the subsurface layer σ_{S2HH}^o at $\theta = 40^\circ$. It may be seen that σ_{S2HH}^o strongly decreases when ϵ_2 is close to ϵ_1 that is when only the surface signal contributes to the backscattering, confirming that the phase signal is related to the buried wet structure. Furthermore, when the moisture content of the

lower layer increases, single and multiple scattering occur at the buried wet interface which significantly contribute to the backscattered signal, increasing the backscattering coefficient to an easily detectable level (-25 dB) for P-band SAR even for a 3m deep wet layer.

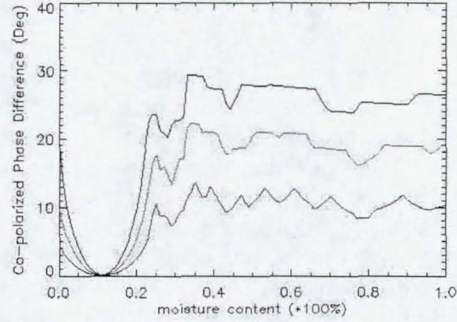


Fig. 2. Φ_{HH-VV} as a function of the moisture content of the lower wet layer for three incidence angles: $\theta = 40^\circ$ (black), 30° (red), and 20° (blue).

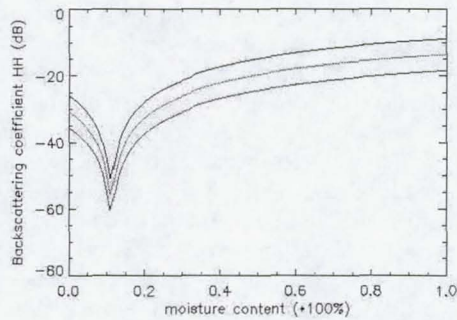


Fig. 3. σ_{S2HH}^o as a function of the moisture content of the lower wet layer for three upper layer thicknesses: $D = 1\text{m}$ (black), 2m (red), and 3m (blue).

Future work: We initially considered single and multiple scattering and limited our study to a pure water case. Further studies will consider volume scattering that could occur inside the dry upper layer because of the presence of rock clasts comparable to the radar wavelength in size. We will also investigate the effects of brine solutions on Φ_{HH-VV} because of the occurrence of small amounts of salts in the Martian crust that could significantly affect the conductivity in the few upper meters of the Martian subsurface. Finally, we shall also test the capabilities of airborne P-band polarimetric SAR on terrestrial sites that could be good analogs to Mars.

References: [1] Lasne Y. et al. (2004) *IEEE TGRS*, 42, 1683-1694. [2] Mellon M. T. et al. (2004) *Icarus*, 169, 324-340. [3] Feldman W. C. et al. (2002) *Science*, 297, 75-78. [4] Mitrofanov I. et al. (2002) *Science*, 297, 78-81. [5] Boynton W. V. et al. (2002) *Science*, 297, 81-84. [6] Möhlmann D. (2003) *Icarus*, 168, 318-323. [7] Haberle R. M. et al. (2001) *JGR*, 106, 23317-23326. [8] Harmon J. K. et al. (1999) *JGR*, 104, 14065-14089. [9] Gellert R. et al. (2004) *Science*, 305, 829-832. [10] Morris R. V. et al. (2004) *Science*, 305, 833-836. [11] Christensen P. R. et al. (2004) *Science*, 305, 837-841. [12] Zakri T. (1997) Physic Thesis from INPG (Grenoble). [13] Fung A. K. et al. (1992) *IEEE TGRS*, 30, 356-369.

EXPERIMENTAL VALIDATION OF THE MONO AND BISTATIC OPERATING MODE OF A GPR DEDICATED TO THE MARTIAN SUBSURFACE EXPLORATION

Le Gall¹ (Legall@cetp.ipsl.fr) V.Ciarletti¹ (ciarletti@cetp.ipsl.fr) J.J.Berthelier¹, R.Ney¹, F.Dolon¹, S.Bonaimé¹
¹CETP/IPSL

In the frame of the NETLANDER project, the CETP (Centre d'étude des Environnements Terrestre et Planétaires) has developed a ground penetrating radar (GPR) aimed at initial observations of the geological features in the deep Martian subsurface and the detection of liquid water underground reservoirs. Contrary to the normal mode of operation of subsurface radars, which can be moved over the soil to be explored, the GPR of NETLANDER operates in a fixed position and aims at performing a 3D imaging of the underground reflecting structures. This is achieved by retrieving not only the distance of the reflectors but also the direction of the backscattered waves by measuring the 2 horizontal electric components and the 3 magnetic components of the reflected waves.

In-situ measurements, on Martian electromagnetic analogues, are crucial to validate the concept of the instrument all the more as its size (antennas of 35 m) forbids tests in laboratory. In February 2004, ground tests at 2, 3 and 4MHz have been successfully carried out on the Antarctic continent with a monostatic GPR prototype. As expected the echoes due to interaction with the bedrock were detected and the magnetic component measurements allowed us to retrieve the position (depth and direction) of the reflecting structures. Since then, complementary ground tests have been performed on the Pyla Dune with the updated version of this instrument. Two GPRs were operated simultaneously in order to test a bistatic mode as well as a monostatic one.

The Pyla Dune is a sand dune nearly 100 m high and 2 km long along the south-west Atlantic coast in France. The two radars were installed on the top of the dune and separated by about 350 m. The horizontal reflecting layer located at the base of the dune together with the known permittivity value of the sand offer the opportunity to test the performance of the device in a rather well-documented and simple environment. As the dune is only 100 m high and thus of the order of the radar blind zone, short (250 ns) pulses were used in the sequence of measurement to lessen the extent of the blind zone. As a consequence we were only able to use 4MHz as the operating frequency. The main goal of this field tests was to ensure that the bi-static GPR mode was operational by checking the synchronization of the driving clocks of both instruments, the synchronization of measurements, and the transmission of a short pulse between the two

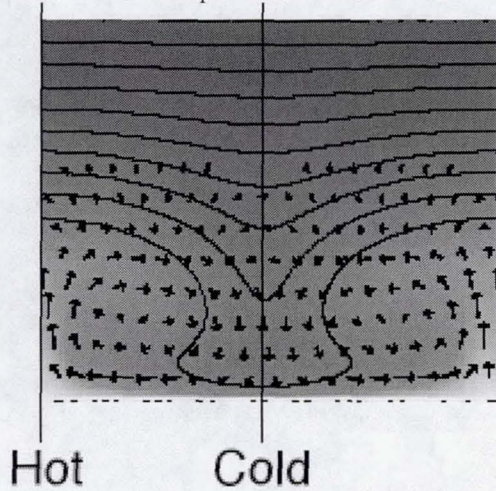
GPRs. We also took advantage of this new operating mode to find out the configuration of operation providing the optimal signal to noise ratio (number of coherent additions, attenuation to avoid receiver saturation, impedance adaptation...).

These experimental results will be presented in the poster. We will focus on the precise measurement of the received electric and magnetic fields and the analysis and comparison of the signals obtained in monostatic and bistatic modes. Comparisons with simulations taking into account the actual environment of the GPR will also be presented.

RADAR SOUNDING OF CONVECTING ICE SHELLS IN THE PRESENCE OF CONVECTION: APPLICATION TO EUROPA, GANYMEDE, AND CALLISTO. William B. McKinnon, Dept. of Earth and Planetary Sciences and McDonnell Center for the Space Sciences, Washington University, Saint Louis, MO 63130, mckinnon@wustl.edu.

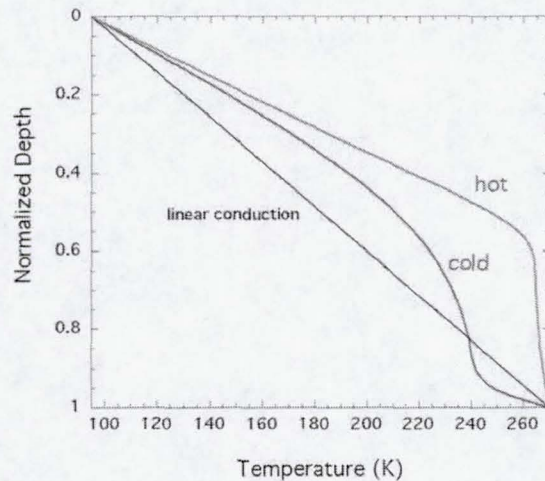
Introduction: Radar sounding is in principle one of the most powerful tools for exploring the third dimension (depth) of ice shell structure and determining shell thickness (depth to ocean), owing to the extraordinary transparency of cold water ice at radar wavelengths [e.g., 1]. Obviously, there are unknowns, and such sounding may be thwarted by contamination (radar absorption) by sulfates, salts, or cometary silicates [1]. Subsurface scattering in a regolith layer is another possible complication [2]. Chyba et al. [1] noted in particular that warm, convecting ice in the lower portion of Europa's shell may impose a severe limit to the possible sounding depth (if convection occurs). Here I reexamine the case of radar sounding in the presence of convection, specifically the case of weak convection near the convective instability threshold [3]. I find that cool downwellings are substantially more radar transparent than hot upwellings, and that in favorable cases the sounding depth on Europa (50 dB loss limit) is 15-20 km. Sounding the much thicker (and dirtier) ice shells on Ganymede and Callisto is more difficult, but with sufficient radar power not impossible. Moreover, if convection is occurring, simply detecting the top of individual upwellings or the convective layer provides a measure of the internal heat flow (otherwise an extraordinarily difficult measurement to obtain).

A European Example: Previous convective calculations [4,5] were used to provide a temperature field. The example below is based on a tidally

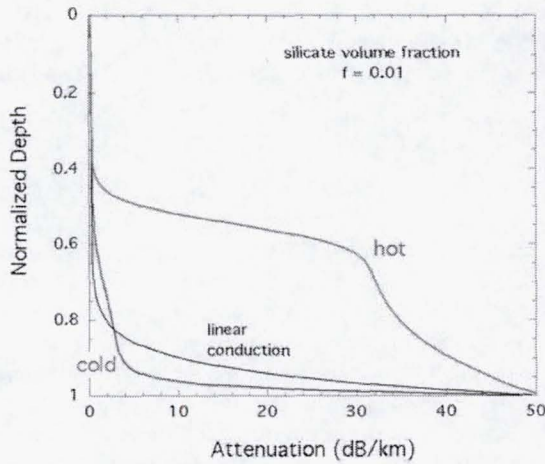


linearized (and therefore Newtonian) GBS rheology. The viscosity range from the cold (~100 K) top to the ice/ocean interface (~270 K) is 2×10^6 , when using the exponential, Frank-Kamenetskii approximation [e.g., 6]. The Rayleigh number (Ra), defined using the bottom viscosity, is 10^6 , near but super-critical. The calculations were done in a 4×1 box for natural scale selection (only a portion is shown), and were bottom heated (to mimic the initial tidal dissipation). Thermodynamic parameters (such as thermal conductivity k) were taken to be constant.

For Ra not too far above the critical value for convection, convection is steady state, with well-spaced upwelling plumes and intervening cold downwellings. There is no stagnant lid penetration in the absence of tidal heating, compositional convection, or perhaps, other unknown physical effects. The average adiabatic, convective temperatures are high, ~255-260 K, in agreement with theory [5]. This is the worst convective case from the perspective of [1], but in the steady-state regime the upwellings and downwellings are distinct. The plot below illustrates the vertical "hot" and "cold" temperature profiles from the calculation at

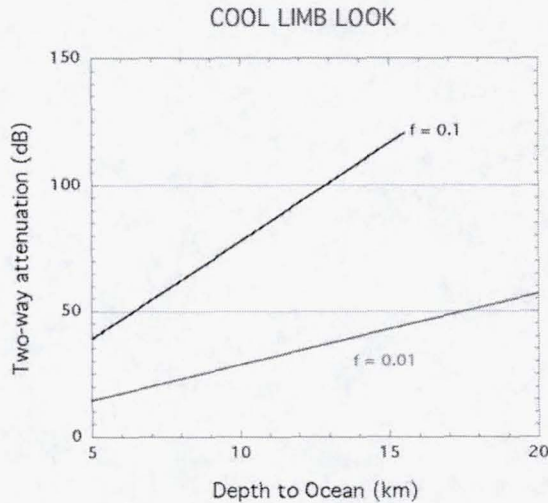


left, compared with the linear, conductive temperature profile that would obtain in the absence of convection. The next figure illustrates the radar attenuation (in dB/km) as a function of depth for all three profiles, for the case of minor silicate contamination (rock fraction $f = 0.01$, using the radar



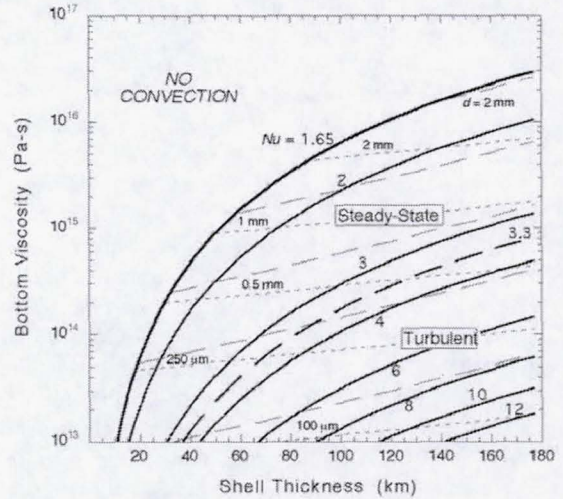
attenuation model of [1] for a 50 MHz [6 m] orbiting system), which is probably most appropriate to Europa. The upwellings are considerably hotter than average and should strongly attenuate the radar signal. In comparison, radar attenuation in the cold limbs is up to ~50% less than that for a conductive temperature profile. Steady-state convection can be an aid to radar sounding!

The total 2-way attenuation for sounding the cool downwelling is shown below as a function of total shell thickness, for two f values. If following [1], a 50 dB loss is considered a good benchmark, then reasonably thick ice shells can *in principle* be sounded. For more powerful radar systems, such as could be flown on the proposed JIMO mission, radar can find even deeper oceans.



Ganymede and Callisto. Neither Ganymede nor Callisto are presently being tidally heated, although Ganymede may have been so in the past.

Nevertheless, both may possess oceans, and both may be undergoing sluggish convection deep in their ice I shells [7]. The following figure illustrates the conductive and convective regimes attainable for Callisto (Ganymede is similar), as a function of total



shell thickness and bottom viscosity. Because of the low buoyancy stresses involved, the creep mechanism is Newtonian volume diffusion, which is grain-size dependent. The fine lines in the figure show the dependence of (bottom) viscosity on ice grain size for two different assumptions regarding the viscosity pressure dependence (activation volume). Also shown are contours of Nusselt number, the dimensionless heat flow (in units of the equivalent conductive value). If convecting, Ganymede and Callisto are likely in the upper right of the figure, implying deep, sluggish convective planforms. In this case the entire shells are colder compared with Europa (other than at the near-surface), and importantly, the convecting portions are <250 K. It is also possible that the deep oceans in these bodies are maintained by salts or even ammonia in solution acting as an antifreeze, making the convecting portions colder still. Whether such temperatures imply greater radar transparency depends on the radar attenuation in cold ice as a function of pressure, which is as yet unmeasured.

References: [1] Chyba C.F. et al. (1998) *Icarus*, 134, 292-302. [2] Eluszkiewicz, J. (2004) *Icarus*, 170, 234-236. [3] McKinnon, W.B. (1999) *BAAS*, 31, 1176-1177. [4] McKinnon, W. B. (1999) *Geophys Res. Lett.*, 26, 951-954. [5] McKinnon, W.B., and Gurnis, M. (1999) *LPS XXX*, Abstract #2058. [6] Solomatov, V. S. (1995) *Phys. Fluids*, 7, 266-274. [7] McKinnon, W.B. (2004) *Icarus*, submitted.

A Tower-based Prototype VHF/UHF Radar for Subsurface Sensing: System Description and Data Inversion Results

Mahta Moghaddam*, Leland Pierce, Alireza Tabatabaenejad, and Ernesto Rodriguez¹

Electrical Engineering and Computer Science Department
The University of Michigan, Ann Arbor, MI 48109
mmoghadd@umich.edu, Tel: 734-647-0244

¹Jet Propulsion Laboratory, California Institute of Technology
Pasadena, CA 91109

Knowledge of subsurface characteristics such as permittivity variations and layering structure could provide a breakthrough in many terrestrial and planetary science disciplines. For Earth science, knowledge of subsurface and subcanopy soil moisture layers can enable the estimation of vertical flow in the soil column linking surface hydrologic processes with that in the subsurface. For planetary science, determining the existence of subsurface water and ice is regarded as one of the most critical information needs for the study of the origins of the solar system.

The subsurface in general can be described as several near-parallel layers with rough interfaces. Each homogenous rough layer can be defined by its average thickness, permittivity, and rms interface roughness assuming a known surface spectral distribution. As the number and depth of layers increase, the number of measurements needed to invert for the layer unknowns also increases, and deeper penetration capability would be required.

To nondestructively calculate the characteristics of the rough layers, a multifrequency polarimetric radar backscattering approach can be used. One such system is that we have developed for data prototyping of the Microwave Observatory of Subcanopy and Subsurface (MOSS) mission concept. A tower-mounted radar makes backscattering measurements at VHF, UHF, and L-band frequencies. The radar is a pulsed CW system, which uses the same wideband antenna to transmit and receive the signals at all three frequencies. To focus the beam at various incidence angles within the beamwidth of the antenna, the tower is moved vertically and measurements made at each position. The signals are coherently summed to achieve focusing and image formation in the subsurface. This requires an estimate of wave velocity profiles.

To solve the inverse scattering problem for subsurface velocity profile simultaneously with radar focusing, we use an iterative technique based on a forward numerical solution of the layered rough surface problem. The layers are each defined in terms of a small number of unknown distributions as given above. An a priori estimate of the solution is first assumed, based on which the forward problem is solved for the backscattered measurements. This is compared with the measured data and using iterative techniques an update to the solution for the unknowns is calculated. The process continues until convergence is achieved. Numerical results will be shown using actual radar data acquired with the MOSS tower radar system in Arizona in Fall 2003, and compared with in-situ measurements.

APPLICATION OF INTERFEROMETRIC RADARS TO PLANETARY GEOLOGIC STUDIES. P. J. Mouginis-Mark¹, P. Rosen², and A. Freeman², ¹Hawaii Institute Geophysics and Planetology, University of Hawaii, Honolulu, HI 96822 (pmm@higp.hawaii.edu), ²Jet Propulsion Laboratory, CalTech, Pasadena, CA 91109.

Introduction: Radar interferometry is rapidly becoming one of the major applications of radar systems in Earth orbit. So far the 2000 flight of the Shuttle Radar Topographic Mission (SRTM) is the only dedicated U.S. radar to be flown for the collection of interferometric data, but enough has been learned from this mission and from the use of foreign partner radars (ERS-1/2, Radarsat, ENVISAT and JERS-1) for the potential planetary applications of this technique to be identified.

A recent workshop was organized by the Jet Propulsion Laboratory and the Southern California Earthquake Center (SCEC), and was held at Oxnard, CA, from October 20th – 22nd, 2004. At this meeting, the major interest was in terrestrial radar systems, but ~20 or the ~250 attendees also discussed potential applications of interferometric radar for the terrestrial planets. The primary foci were for the detection of planetary water, the search for active tectonism and volcanism and the improved topographic mapping. This abstract provides a summary of these planetary discussions at the Oxnard meeting.

Moon: Radar imaging could provide views of the permanently shadowed areas at the lunar poles. Together with interferometrically derived topographic data, such measurements could help in the characterization of potential landing sites at the meter-scale, and enable the determination of lighting geometry of these areas in order to evaluate the availability of solar energy for rovers and human exploration. At the global scale, terrestrial experiments such as the Shuttle Radar Topography Mission (SRTM) have demonstrated the value of having a consistent elevation data set for the Earth [1]. For the Moon, a digital elevation model at a horizontal resolution of 30 – 50 m/pixel would aid in crustal modeling and in quantitative geomorphic studies such as the analysis of impact crater geometry.

Mars: A key question about Mars is the identification of any near-surface liquid water. At a wavelength of 24 cm (L-band) or longer, radar imaging of high latitudes may penetrate the regolith to a depth where the Mars Odyssey neutron spectrometer data [2] indicate high concentrations of hydrogen-bearing materials, which may well be ice-rich regolith. In hyper-arid terrestrial environments, L-band radar signals have been shown to penetrate to a depth of 1 –

2 meters [3, 4], which is the same depth range within which hydrogen-bearing materials exist near to the poles on Mars [2]. The potential exists not only to identify the seasonal position of the boundary between the hydrogen-free and hydrogen.

Significant advances have been made in the terrestrial glaciology community in the use of radar interferometry for investigating ice sheet dynamics [5]. The same application may also hold true for Mars, where the North Polar Cap may experience surface flow over the Martian year. In addition, decorrelation of radar interferograms due to the sublimation of carbon dioxide frosts on the South Polar Cap [6] would be easily identified. Experience with Space Shuttle Radar (SIR-C) has shown that surface changes in the planimetric outline of features can be related to geologic processes [7], and the same technique could be applied to measuring the sublimation rate of ice at the poles.

Topographic mapping on Mars is also possible with radar interferometry but, unlike the Moon, there are other data sets already available (or to be collected on future missions) that make this radar-derived data set non-unique. The Mars Orbiter Laser Altimeter (MOLA) and the Mars Express Stereo Camera have already collected high precision elevation data for Mars. MOLA has provided a global data set [8] while Mars Express has improved spatial resolution of selected sites. Future measurements from the HiRISE instrument on Mars Reconnaissance Orbiter offer the potential for decameter-scale digital elevation models on a local scale. Radar interferometry could play a role in this instance in the collection of regional topographic data at the 10 – 20 m scale. Longer wavelength radar measurements (L-Band and P-Band for example) could provide key information on the topography of subsurface features currently obscured by a layer of dust up to 5 m thick. Such measurements would facilitate the analysis of potential landing sites, geomorphic features indicative of paleo-climates (possible shorelines, valley networks, gullies on the walls of impact craters, etc.).

Venus: Venus represents a fascinating comparison with the Earth, primarily because of its similarity in size and distance from the Sun. But the lack of liquid water on the surface and the thick carbon dioxide atmosphere appears to have been responsible for the lack of plate tectonics on Venus. No direct evidence

has been obtained for active tectonic or volcanic processes on Venus, although high dielectric materials at the summit of Maat Mons suggest that this volcano may have been active in the recent geologic past [9].

Radar interferometry is particularly good at the detection of the deformation fields associated with earthquakes [10, 11], and so would be an excellent way to detect any current tectonic activity on Venus, if it were to occur. Similarly, the same methods that were used to map new lava flows on Kilauea volcano, Hawaii [7] could be used to search for active volcanism on Venus.

The collection of high resolution topographic data for Venus can also be accomplished with an interferometric radar. The Magellan mission collected image data at a spatial resolution of 75 m, but the topographic data from the altimeter had a much lower resolution (~10 km, with ~50 m vertical accuracy). The collection of topographic data at the same scale as the existing image data would greatly facilitate an improved understanding of structural and volcanic features on Venus.

Europa: Radar interferometric studies of any of the Galilean satellites will be a challenge, partly because of the need for small baselines between successive orbits, and partly because of the likely short duration of the missions due to the high energy environment within the Jovian system. However, these experiments offer the exciting opportunity of answering questions related to the thickness of the icy crust on Europa [12, 13], as well as provide detailed topographic information that might be of value for planning future penetrator experiments. Investigating the origin of the cycloid ridges on Europa, and searching for deformation along triple bands, would enable the identification of parts of the crust that are flexing on a daily basis. In particular, if brines were leaking on to the surface at the present time, the decorrelation of the radar interferogram would permit the spatial mapping of this process. Polarimetric radar may also permit determination of the dielectric constant variability in this instance.

The acquisition of high resolution topographic data for Ganymede and Callisto via interferometric radar would also enable the analysis of crustal structure on these moons. Rheological models for the deformation of impact craters of different sizes require knowledge of decameter-scale topography, which could be obtained for selected regions using a short-lived interferometric radar mission.

Technical Developments Needed: The Oxnard Workshop identified several technical issues that need

to be addressed before an interferometric mission could be flown to any of the planets. Highest priority was for the need to develop on-board data processing for the recovery of topographic information. The very large data volumes involved in producing digital elevation models for any planet require that ways to reduce this data volume be devised. Collecting such data from spacecraft at the distance of Jupiter's moons will be particularly challenging. Secondly, navigation of the spacecraft in orbit around a planet or moon may require significant improvement in navigation capability. Baseline separation for the two radar passes needs to be within ~1 km for most applications, so that detailed knowledge of the spacecraft's position and orientation are needed. Radiation shielding for the radar electronics may be required for the inner moons of Jupiter. Imaging a whole planet, particularly one the size of Venus, to search for possible deformation due to earthquakes requires a wide swath width for the radar. In terrestrial studies, most radar interferograms are produced with a spatial resolution of a few tens of meters but a swath width of less than 100 km. A new technique for terrestrial studies, involving SCAN-SAR and Radarsat data, has recently been used experimentally and may offer the potential for routine large-area coverage. Finally, for selected small areas where landers may be sent to the surface of the Moon or Mars, Spotlight techniques for the production of topographic information at the meter-scale may also be possible.

References: [1] Farr, T. G., & Kobrick, M. (2000) *Eos*, 81, 583-585. [2] Feldman W.C. et al. (2002) *Science* 297, 75 – 78. [3] McCauley J.F. et al. (1986) *IEEE Trans Geoscience & Remote Sensing GE-24*, 624-648. [4] McCauley J. F. et al. (1982) *Science* 218, 1004-1020. [5] Bamber, J. L. et al. (2000) *Science* 287, 1248 0 1250. [6] Malin, M.C. et al. (2001) *Science* 294, 2146 – 2148. [7] Zebker, H. A. et al. (1996) *Geology* 24, 495 - 498. [8] Smith, D.E. et al. (2001) *JGR-Planets* 106(E10), 23,753-23,768. [9] Klose, K. B. et al. (1992) *J. Geophys. Res.*, 97, 16,353 - 16,369. [10] Massonnet, D. and K. Feigl (1998) *Revs. Geophys.* 36(4), 441 – 500. [11] Peltzer, G. et al. (2001) *Geology* 29, 975 – 978. [12] Carr, M. H. et al. (1998) *Nature* 391, 363 – 365. [13] Buck, L. et al. (2002) *Geophys. Res. Ltrrs.* 29 (22) doi. 10.1029/2002GL016171.

A WEB-BASED COLLABORATIVE TOOL FOR MARS ANALOG DATA EXPLORATION.

M. Necsoiu¹, C.L. Dinwiddie¹, E. Heggy², and T.G. Farr³ ¹CNWR, Southwest Research Institute®, San Antonio, TX 78238, mnecsoiu@swri.org, cdinwiddie@swri.org, ²Lunar and Planetary Institute, 3600 Bay Area Blvd., Houston TX 77058, heggy@lpi.usra.edu, ³Jet Propulsion Laboratory, Pasadena, CA 91109, tom.farr@jpl.nasa.gov.

Introduction: Solving today's complex research and modeling challenges are dependent on our ability to discover, access, integrate, and share information from multiple sources. The planetary sciences community is no exception¹; over the last few years, the need for data mining and exploration tools that can expedite comparative studies between Martian and terrestrial analogs sites and aid the interpretation of Mars data sets has become evident. Data sharing maximizes scientific return from studies and data sets.

General Description: Functionalities that allow for comparative studies between Martian and terrestrial analogs are incorporated into a prototype system under development at Southwest Research Institute®. The system architecture is based on Olympus DISS^{®2,3}, a data information and sharing system successfully used to manage a large volume of geospatial data at the Center for Nuclear Waste Regulatory Analyses.

The web-based Mars Analog Data Explorer tool (MADE) uses established data and metadata standards and provides a flexible mechanism from which to build new applications. The system supports a wide variety of ground-based (e.g., ground-penetrating radar, transient electromagnetic soundings, and vertical electrical soundings) and orbital and aerial (i.e., multi-, hyper-spectral, and radar) datasets. The system can also provide access to existing GIS data such as geologic, hydrologic, and topographic maps. Metadata facilitates identification of data by search and retrieval mechanisms based on the user's selection criteria, and assists the user to fully understand the data content and evaluate its usefulness. Each metadata entry contains a brief description of the dataset, the location and date of its acquisition, its status, its file size and format, data type, data attributes (e.g., spatial, temporal, and spectral resolution depth of investigation), principal investigator contact information, and the link(s) to the data source (either residing on a local or remote server).

A graphical user interface (Fig. 1) enables the available data to be searched spatially, temporally, or by keywords. Spatial searches are done either by drawing a box around a map location, selecting predefined locations, or by entering geographic coordinates. Temporal searches are conducted by searching for specific data acquisition or release dates. Keyword searches are conducted by searching for keywords (e.g., data or feature types) in the geological, geophysical, and hydrological analogue datasets.

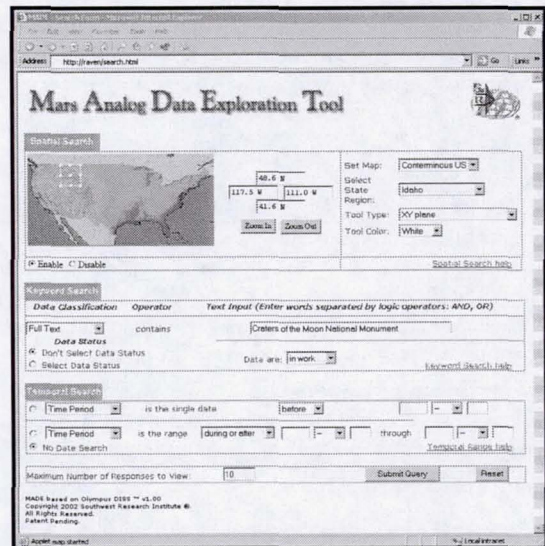


FIGURE 1: MADE Graphical User Interface

One possible use for this tool is the evaluating and selecting potential terrestrial analog sites to Mars for testing future Mars mission instruments. The system also provides a mechanism for testing blind interpretations of data from radar and EM soundings at similar resolutions as Mars data. NASA's Office of Space Operations may also find this tool valuable.

Conclusions: The flexible design of this system enables continued incorporation of newly available field and airborne/satellite remote sensing datasets. Our integrated data-access system will help unify community efforts toward improved testing and evaluation of potential new planetary exploration instruments and human exploration techniques by identifying and providing basic information on analog study sites, allowing collaborating investigators access to available data.

References: [1] Farr et al. (2001) NRC Decadal Study on Terrestrial Analogs to Mars; [2] Necsoiu M. et al., (2002), *Eos Trans. AGU*, 83(47), Fall Meet. Suppl., Abstract U61A-04; [3] Necsoiu M. (2003), *Technology Today*, Spring issue, SwRI (<http://www.swri.org/3pubs/today/spring03/Mapping.htm>)

Additional Information: MADE software will be controlled according to the requirements of CNWR Technical Operating Procedure.

PROPAGATION OF RADAR THROUGH THE MARTIAN POLAR LAYERED DEPOSITS. D. C. Nunes¹ and R. J. Phillips², ¹Lunar and Planetary Institute, Houston, TX 77058, ²Dept. of Earth and Planetary Sciences and McDonnell Center for the Space Sciences, Washington University, St. Louis, MO 63130. (nunes@lpi.usra.edu)

Introduction: The Martian polar caps are among the primary targets for orbital radar sounders scheduled to acquire data in the next few years (e.g., SHARAD [1]). Several factors bolster the case for radar sounding of the caps. One is the enhanced spatial coverage provided by the nearly polar orbits of the spacecraft. Another is the relatively low dielectric constant and loss tangent values of H₂O ice, the primary cap component, which should lessen signal attenuation. The polar caps also contain other species. CO₂ ice overlies the Polar Layered Deposits (PLD), permanently at the Southern cap and seasonally at the Northern cap [e.g., 2]. Silicate inclusions are also present in the ice and are likely the source for the PLD dark layers [2]. Fig. 1 shows a section of a Northern PLD (NPLD) scarp. Two units are clearly distinguishable: the upper is bright and smooth, and the lower is rough and dark. Interpretations commonly assert that the upper unit is composed of relatively clean ice, while the lower unit is rich in sand [3].

The objectives of this work are (i) to determine to what degree the PLD strata can be resolved by SHARAD, (ii) to assess the contribution of the layering to signal attenuation via path and transmission losses, and (iii) to evaluate the effect of cap composition on the predicted radar reflections.

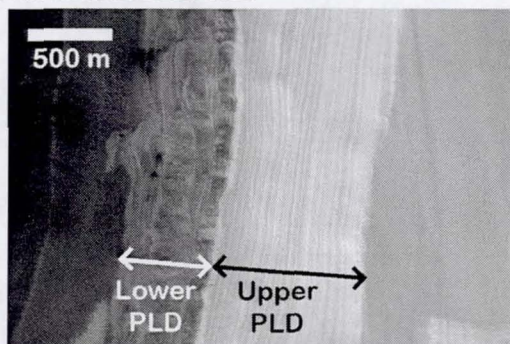


Figure 1. Section of MOC frame E0300889 showing the Upper and Lower units of the Northern PLD.

Propagation Model: We model the 1-D propagation of normally incident plane waves through a layered medium by solving the full wave equation, including the electrically diffusive losses due to medium conductivity [4]. The solution consists of an effective, complex impedance Z , which describes the full electromagnetic response of the subsurface and yields an effective reflection coefficient R at the surface. Coefficient values, however, are frequency dependent and collectively form a reflection spectrum. The convolution of the reflection spectrum with the radar

flexion spectrum with the radar spectrum and the subsequent inverse Fourier transformation to time domain produce the time history of the radar reflections, or “radargram”. The radar signal has a center frequency of 20 MHz, bandwidth of 10 MHz, and consists of a 85- μ s chirped pulse. Applying a Hanning window to the radar pulse reduces side-lobe amplitude substantially. The numerical layers in the model are smooth, horizontal, and have a uniform thickness of 2.5 m throughout the model domain, which is finer than and properly resolves the albedo variations that define the PLD strata.

Dielectric PLD Profile: The essence of modeling the dielectric profile of the PLD lies in (i) estimating the volumetric fraction v of silicate inclusions in the ice, a free parameter, as a function of depth from the variations in brightness across the PLD strata, and (ii) using mixing formulae to obtain an effective dielectric constant for each v value. We used the upper 250 m of the brightness-depth profile illustrated in [5], which derived from a trough in the NPLD. The ice in this trough section shows an overall darkening with depth, which could result from effects other than dust content [e.g., 6]. We subtract this darkening trend and, consequently, maximize the variation in dust content. We linearly scale the resulting brightness profile to the range in measured albedo and then use the delta-Eddington approximation to radiative transfer of [7] to obtain plausible depth profiles for inclusion fraction. The resulting dielectric profile derives from the Tinga-Voss-Blossey mixing formula for two phases [8], ice and silicates. The adopted values for the dielectric constants of ice and silicates are $3.15 + i 2.2 \times 10^{-4}$ [e.g., 9] and $8.8 + i 0.017$ (from average shergottites, [10, 11]), respectively. This 250-m profile is repeated to a depth of 2 km so as to produce a model for the upper unit of the NPLD. The lower unit of the NPLD is more difficult to model because of its rough, platy structure, and we only represent it as uniformly sand-rich ($v = 50\%$).

Results: Fig. 2 shows radargrams for the NPLD model and different ranges in inclusion fractions in the upper NPLD. The vertical dashed line represents the sensitivity threshold imposed by SHARAD’s dynamic range. The fine stratigraphic structure of the NPLD is detectable if dust fractions are larger than 1%, as the resulting variations in dielectric constants are sufficiently large to produce observable reflections. The repetition of the 250-m section is also evident, as the strong reflectors are easily seen at $\sim 6 \mu$ s, $\sim 13 \mu$ s, and $\sim 20 \mu$ s. Weaker reflectors are harder to pick out be-

cause of multiple reflections, especially at later times. Greater silicate content also delays reflections because of the overall higher dielectric constant of the upper PLD. The unconformity between the upper and lower units of the NPLD (Fig. 1) also produces strong reflections in the cases illustrated, between 24 μs and 27 μs . The simulations in Fig. 2 adopt a sand-rich composition for the lower NPLD unit ($v \sim 50\%$), as suggested by [3], but the main point is that enough radar energy returns from the unconformity even when the upper unit is rich in silicates. Note also that the boundary between the PLD and a basaltic crust produces a strong reflection at $\sim 40 \mu\text{s}$.

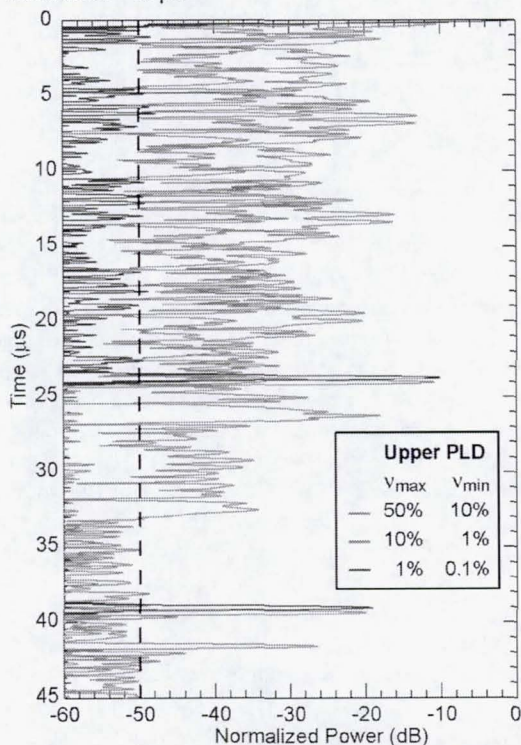


Figure 2. Radargrams for different compositions of the upper NPLD for a SHARAD type of signal.

Performing the same simulations as the ones in Fig. 2 with only the real portion of the dielectric constants serves to illustrate the relative contributions of path and transmission losses to signal attenuation. Not surprisingly, the greatest difference occurs for the $v = [10, 50]\%$ case, as it has the largest effective loss tangent ($\tan\delta = \epsilon_{\text{real}}/\epsilon_{\text{imag}}$) of all of the cases illustrated. Omitting path losses incurs in an increase of 8 dB in the power of the reflection generated at the unconformity (26 μs), and causing all strong reflections to be at the -10 dB level; path and transmission losses are each responsible for $\frac{1}{2}$ of the attenuation in this case. Finally, placing a 10-m layer of CO_2 frost on top of the NPLD model has a noticeable effect on the simulations. The

dielectric constant of dry ice depends heavily on its density and can be obtained via Raleigh mixing [12]. At 910 kg m^{-3} [13], the dielectric constant of CO_2 frost is $1.59 + i 9.78 \times 10^{-7}$, which is lower than that of water ice (pure or with silicate inclusions) and serves to reduce the power of the surface reflection. Consequently, subsurface reflections are relatively stronger when an upper dry ice layer is present. Fig. 3 shows an enhancement of nearly 10 dB for the case of $v = [0.1, 1.0]\%$, in which the strongest reflections from the upper PLD are barely detectable without the dry ice.

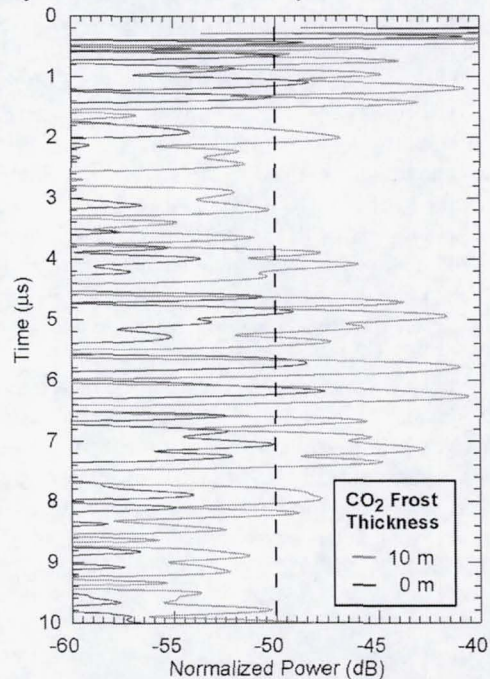


Figure 3. Radargrams illustrating the effect of a surficial layer of CO_2 frost using a SHARAD-like radar pulse.

Synopsis: Mapping of the stratigraphic structure of the PLD appears to require dust fractions of at least 1% under optimal conditions. Path and transmission losses may not, a priori, prevent the mapping of the unconformity in the NPLD, provided that the silicate content in the lower unit is significantly greater than that of the upper unit. The presence of a dry ice layer at the surface may help in the detection of weaker subsurface reflectors.

References: [1] Seu R. et al. (2004), *Planet. Space Sci.*, 52, 157-166. [2] Thomas P. et al. (1992) *Mars*, U. of Arizona Press, 767-795. [3] Byrne S. and Murray B. C. (2002) *JGR*, 107(E6), 5044. [4] Wait J. R. (1962), *Electromagnetic Waves in Stratified Media*, MacMillan. [5] Laskar J. et al. (2002) *Nature*, 419, 375-377. [6] Arthern R. J. et al. (2000) *Icarus*, 144, 367-381. [7] Kieffer H. H. (1990) *JGR*, 95(B2), 1481-1493. [8] Ulaby F. T. (1986), *Microwave Remote Sensing*, Artech House. [9] Picardi G. et al. (2004), *Planet. Space Sci.*, 52, 149-156. [10] Olhoeft G. R. and Strangway D. W. (1975), *EPSL*, 24, 394-404. [11] Lodders K. (1998) *MAPS*, 33, A183-A190. [12] Pettinelli E. et al. (2003) *JGR*, 108(E4), 10.1-10.11. [13] Smith D. E. et al. (2001) *Science*, 294, 2141-2146.

Geoelectrical markers and oreols of subsurface frozen structures on Mars for long-term monitoring of spatial and temporal variations and changes of martian cryolitozone structure on the base ground and satellite low-frequency radar measurements. Y. R. Ozorovich, A. K. Lukomskiy, Space Research Institute, Russian Academy of Sciences, 84/32 Profsoyuznaya st., Moscow, 117997, Russia Tel:7-095-3333177; Fax:7-095-9133040; e-mail: yozorovi@iki.rssi.ru.

Choosing right methods and instruments for Mars' cryolitozone structure research is the present-day task for future missions on Mars. Data analysis of Mars' near-surface element composition (Mossbauer spectrums from Mars Exploration Rovers) shows magnetic materials presence on the surface. In some extent it confirm the "theory of meteorite Mars' upper crust evaporating". At the same time crust structure will develop under any frequency- or time-domain sounding methods in additional induced polarisation effects.

This geoelectrical subsurface structure of Mars is complicated enough to make us searching methodical and instrumental ways to reveal real Mars' frozen structure.

One way seems to be establishing geoelectrical markers of specific subsurface layers that will help us getting certainty structure of Mars subsurface layers as the result of direct measurements from Mars' surface or from the base satellite low-frequency radar for regional distribution of martian cryolitozone. Basing on established markers and oreols more accurate geoelectrical structure measurements of frozen subsurface structure can be done.

Solving one of previously mentioned tasks a comprehensive expedition near Tambov area have been made. Finding similar geoelectrical markers reference measurements using TDEM method have been done. These allow us building spatial geoelectrical structure using given approach.

These results shows necessity of further experimental and methodical research studies on Mars analog field sites to find out adequate experiment strategy on Mars' surface.

References:

[1] Ozorovich Y.R., Linkin V.M., Smythe W., "Mars Electromagnetic Sounding Experiment – MARSSES", Proceedings of LPI Conference, Houston, 1999. [2] Ozorovich Y.R., et al. "Geomonitoring shallow depth structure and groundwater by MARSSES TEM instrument", Proceedings of SEG Conference, Houston, 1999. [3] Ozorovich Yu.R., et al, "Operational system for groundwater, salt/water intrusion and pollution determination and monitoring", July 2001, Proceedings of the Conference New Paradigms for the Pre-

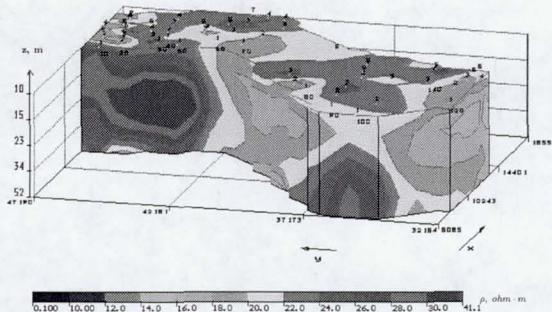


Figure 1: 3D geoelectrical subsurface structure of the field site (titanium-zircon deposit near Tambov). (x,y – distance in m, vertical component z – the depth in m). Geoelectrical markers reflections of thin geological structure in this deposit.

diction of Subsurface Condition – EuroConference on the Characterisation of the Shallow Subsurface: Infrastructure and Assessment, Spa, Belgium. [4] Ozorovich Yu., et al, "Operational system for groundwater and pollution determination and monitoring", "A New Hydrology For the A Thirsty Planet", Proceedings of IAHS Scientific Assembly, Maastricht, The Netherlands, 18-27 July 2001, Workshops 7. [5] Ozorovich Yu. R., et al, "Operational system for groundwater and pollution determination and monitoring into the coastal zones", Proceedings of the SWIM17 - 17th Salt Water Intrusion Meeting, Delft May, 2002. [6] Ozorovich Yu. R., et al, "Operational System for Groundwater, SaltWater Intrusion and Subsurface Pollution Determination and Monitoring into Coastal Zone", Proc. Internatl. Conf. On Soil and Groundwater Contamination & Clean-up in Arid Countries. Muscat, January 20-23, 2003. Part II, pp.35-36. Al-Nahda Press. [7] Lobkovsky L.L., Kontar E.A., Garagash I.A. and Ozorovich Y.R. (2003). Monitors and Methods for Investigation of Submarine Landslides, Seawater Intrusion and Contaminated Groundwater Discharge as Coastal Hazards. Kluwer Publishers., Volume NATO "Risk Science and Sustainability: Science for Reduction of Risk and Sustainable Development of Society" edited by T. Beer and A. Ismail-Zadeh, pp. 191-207. [8] Kon-

tar, E.A., Yu.R. Ozorovich, A. Salokhiddinov, and Ye.B. Azhigaliyev (2002). Study of Groundwater-Seawater Interactions in the Aral Sea Basin. Proceedings of the International Conference on Low-lying Coastal Areas - Hydrology and Integrated Coastal Zone Management, 9-12 September 2002, Bremerhaven, Germany, 225-230. [9] Ozorovich Yu., Kontar E., Babkin F., Lukomsky A., "Geophysical survey spatial and temporal variations of the saltwater interface, vadose zone flow processes into the coastal zone", Proceedings of IUGG 2003, Sapporo, Japan, June 30-July 11, 2003.

SIMULATION OF P-BAND SAR PERFORMANCES FOR MARS EXPLORATION. Ph. Paillou¹, Y. Lasne¹, J.-M. Malézieux², E. Heggy³, ¹Astronomical Observatory of Bordeaux, 33270 Floirac, France, paillou@obs.u-bordeaux1.fr, ²Institut EGID, 33607 Pessac, France, ³Lunar and Planetary Institute, Houston, 77058, USA.

Introduction: MOC images indicate that much of the surface of Mars has been intensely reworked by aeolian processes, and key evidence about the history of the Martian environment (craters, faults, paleo lakes and rivers) seems to be hidden beneath a widespread layer of debris [1]. The subsurface of Mars is also very likely to contain water in the form of ice [2]. Most of future Mars exploration missions then focus on sounding the planet's subsurface, for which radar systems proved to be efficient tools. In particular, space borne imaging radar (SAR) allows a unique access to subsurface information down to several meters for L-band in arid regions [3], depending on the electromagnetic characteristics of geological materials [4]. We realized the first global radar mosaic of Eastern Sahara using more than 1600 SAR scenes of the JERS-1 L-band radar instrument [5]. It reveals the near-surface geology hidden by the superficial sand layer (cf. Figure 1): it will help discovering unknown subsurface structures (paleo rivers and lakes, faults, impact craters [6,7]) and will contribute to answer several key questions about the climatic, geological, and hydrological history of Eastern Sahara. In a same way, a P-band imaging radar could be a unique tool to reveal the past history of Mars [8]. We developed a radar simulator that allows predicting penetration performances of long wavelength imaging radars for various models of the Martian subsurface. First results indicate that a P-band SAR could detect buried structures down to at least 5 meters.

A two-layers model for the Martian subsurface:

We already proposed several electromagnetic models for the Martian subsurface that were used to simulate penetration performances of low-frequency sounding radars such as MARSIS instrument on-board MARS EXPRESS and SHARAD on-board the future MRO platform [9,10]. We consider here a two-layers model for the shallow subsurface of Mars constituted of an overlying dust layer hiding a basaltic substratum. Laboratory measurements of permittivity and magnetic permeability were performed on representative minerals and rocks that are likely to be present on the Martian surface, derived from last results of Mars Exploration Rovers [11,12,13]. A typical Martian dust was simulated using a mixture of iron oxides, basalts, salts and meteoritic materials with a permittivity of 5.87-0.14j. The dust layer was considered as rather smooth with roughness parameters $\sigma=0.55\text{cm}$ and $L=10\text{cm}$ [14]. The dust layer covers a basaltic substratum simulated using a Djiboutian basalt of permittivity 4.19-0.18j,

with a surface roughness characterized by $\sigma=5\text{cm}$ and $L=10\text{cm}$. Both layers were considered to present a Gaussian autocorrelation function. No volume scattering was simulated, assuming that the dust layer is homogeneous.

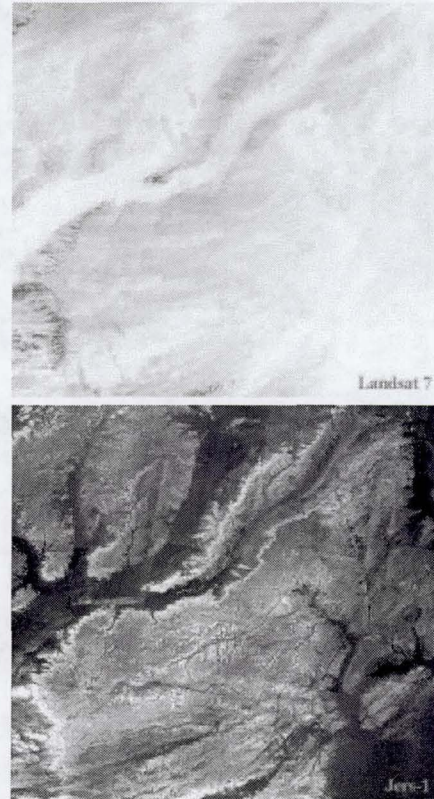


Figure 1: LANDSAT-ETM image (top) and JERS-1/SAR image (bottom) of northern Sudan showing an unknown ancient river network hidden under sandy sediments.

A subsurface basaltic topography was represented using a DEM as shown in Figure 2 (top), the deepest structures being located 10m under the surface. We then covered this substratum with a 4m thick dust layer, resulting in the landscape simulated in Figure 2 (bottom).

The electromagnetic model: Simple simulations of SAR backscattering usually make use of small perturbation model, which presents limited validity with respect to roughness parameter values [15]. We used here a two-layer integral equation model [16] that is widely considered in the radar remote sensing community and proved to accurately reproduce both surface and subsurface scattering [17,18,19].



Figure 2: Digital elevation model simulating the subsurface basaltic structures (top) and landscape simulation when covered with a 4 meters thick dust layer (bottom).

The total backscattered power can be expressed by the sum of a surface component and a subsurface component:

$$\sigma_{pp}^0(\theta) = \sigma_{S1pp}^0(\theta) + \sigma_{S2pp}^0(\theta),$$

the surface component being in the form:

$$\sigma_{S1pp}^0(\theta) = \frac{k}{4} e^{-2k^2 \cos^2(\theta) \sigma^2} \sum_{n=1}^{\infty} |I_{pp}^n|^2 \frac{W^{(n)}(2k \sin(\theta))}{n!}$$

and the subsurface component being expressed by:

$$\sigma_{S2pp}^0(\theta) = \frac{\cos(\theta)}{\cos(\theta_t)} T_{1tp} T_{t1pp} e^{-\frac{2\kappa_e d}{\cos(\theta_t)}} \sigma_{Spp}^0(\theta_t).$$

We generated a P-band (central frequency of 435 MHz) SAR image using the two-layer IEM model combined to radar geometry simulation, applied to the DEM presented in Figure 2 for an incidence angle of 30° and a HH polarization. The resulting simulated SAR image is presented in Figure 3. A log-scale was used to better show that the P-band SAR is able to reveal subsurface basaltic structures down to a 4m deep. While outcrop-

ping structures correspond to a backscattered power between -10dB and -12dB , buried structures return a signal between -18dB and -28dB , which is in the range of what can be detected using orbital radars. The JPL radar team performed a feasibility study that have shown that a P-band SAR can be designed for Mars exploration. Such an instrument could map the Martian subsurface down to 10m with a resolution of 50m [20]. Further modeling has to be conducted in order to take into account other models of the Martian subsurface (possibly in the presence of moisture) and also consider the effect of volume scattering due to rock clasts that can be found in the first meters of the Martian subsurface.

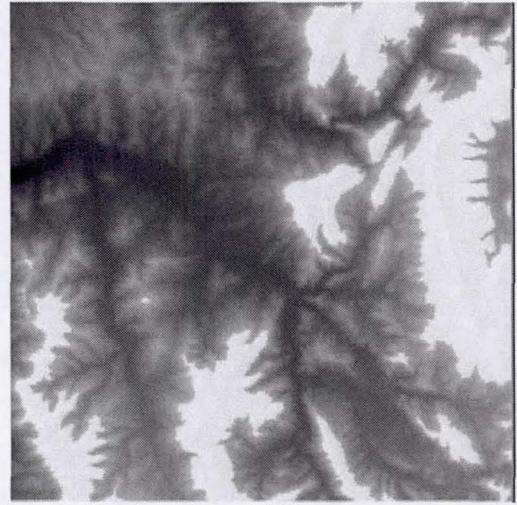


Figure 3: Simulated P-band SAR image using a two-layer IEM model of the Martian subsurface.

- References:** [1] Metzger S. M. (1999), *5th Int. Conf. Mars*, Pasadena, USA. [2] Clifford S. M. (1993) *JGR*, 98, 10973–11016. [3] Elachi Ch. et al. (1984) *IEEE TGARS*, GE-22, 383–388. [4] Paillou Ph. et al. (2001) *GRL*, 28, 911–914. [5] Paillou Ph. et al. (2003) *IGARSS'03*, Toulouse, France. [6] Paillou Ph. et al. (2003) *C.R. Geoscience*, 335, 1059–1069. [7] Paillou Ph. et al. (2004) *C.R. Geoscience*, 336, in press. [8] Paillou Ph. et al. (2001) *Conf. Water on Mars*, Houston, USA. [9] Heggy E. et al. (2001) *Icarus*, 154, 244–257. [10] Heggy E. et al. (2003) *JGR*, 108, GDS 11–1. [11] Squyres S. W. et al. (2004) *Science*, 305, 794–799. [12] Gellert R. et al. (2004) *Science*, 305, 829–832. [13] Morris R. V. et al. (2004) *Science*, 305, 833–836. [14] Dierking W. (1999) *IEEE TGARS*, 37, 2397–2412. [15] Campbell B. A. et al. (2004) *JGR*, 109, 11p. [16] Fung A. K. et al. (1992) *IEEE TGARS*, 30, 356–369. [17] Grandjean G. et al. (2001), *IEEE TGARS*, 39, 1245–1258. [18] Paillou Ph. et al. (2003), *IEEE TGARS*, 41, 1672–1684. [19] Lasne Y. et al. (2004), *IEEE TGARS*, 42, 1683–1694. [20] Team X (2000), *Mars SAR*, JPL.

High Power Amplifier Design Considerations for Europa Surface Penetrating Radar Application.

T. Pett, J. Sechler, R. Keller, D. Hill and M. Cabanas-Holmen; Ball Aerospace & Technologies Corp., 1600 Commerce Street, Boulder, CO 80301 tpett@ball.com

Introduction: Surface penetrating radar has been identified as an important tool for the investigation of planetary geology, ice thickness/characterization, water detection and distribution measurements. During the high capability instrument feasibility study for the Jupiter Icy Moons Orbiter (JIMO) [1], a radar sounder was identified as an important instrument candidate to investigate the ice layer structure of Europa and to search for a possible ice/liquid interface. Europa stretches the capabilities of sounding radar due to the expectation of thick, non-homogenous ice layers possibly overlaying a subsurface ocean. Top level instrument performance objectives include the capability to provide 100 meter and 10 meter minimum vertical resolutions within ice depth ranges of 2 km – 30 km and 100 m – 2 km respectively.

Deep sounding necessitates operation at low frequencies to minimize signal attenuation. However, sub-jovian radio frequency noise severely limits radar sensitivity at frequencies below approximately 5 MHz. As a result the feasibility study identified five channels in a band spanning 5 MHz – 50 MHz to meet sounding depth and ambiguity resolution requirements. The resulting long operating wavelengths at the lowest frequencies limit the gain achievable from a practical antenna (dipole) to ~ 2 dB in the 5 - 10 MHz range and when combined with a maximum expected orbital altitude approaching 400 km, the *average* transmit power required at 5 MHz to meet the desired sounding depth approaches 10 kW assuming a minimum signal-to-noise ratio (SNR) of ~10 dB.

The requirement for such a high RF power level at the lowest measurement channel necessitates incorporation of design innovation in the high power amplifier (HPA) subsystem. The HPAs and power supplies must be designed for high efficiency to control thermal dissipation and demands on the spacecraft bus power. Additionally, the proximity to Jupiter presents a harsh radiation environment which must be accommodated through the selection of radiation hardened parts and appropriate shielding. Using the JIMO feasibility study performance recommendations for a Europa radar sounder as the foundation, this paper will discuss design challenges and present a trade space of design considerations specific to a HPA for this sounding application.

References:

- [1] The Aerospace Corporation (2004), *Report No. TOR-2004(2172)-3232*, 139-144.

SHARAD: RADAR SOUNDER ON THE 2005 MARS RECONNAISSANCE ORBITER. R. J. Phillips¹, R. Seu², and the SHARAD Team, ¹Dept. of Earth and Planetary Sci. & McDonnell Center for the Space Sciences, Washington Univ., CB 1169, One Brookings Drive, St. Louis, MO 63130 USA (phillips@wustite.wustl.edu), ²INFOCOM Department, University of Rome La Sapienza, Via Eudossiana, 18-00184 Rome, Italy (robseu@infocom.uniroma1.it)

Introduction: SHARAD (SHAlLOW RADar) is a subsurface sounding radar provided by ASI (Agenzia Spaziale Italiana) as a Facility Instrument for the 2005 Mars Reconnaissance Orbiter (MRO) mission. It is designed to characterize the upper several hundred meters of the martian subsurface. As of this writing, the instrument has been integrated into the payload on the spacecraft undergoing assembly at Lockheed Martin Aerospace in Denver, CO. The protoflight model has met all of its design requirements, including a dynamic range of 50 dB (in essence, detection of a subsurface signal 50 dB weaker than the strong surface reflection).

The properties of the SHARAD instrument are given in Table 1 below.

Frequency band	15-25 MHz chirp
Vertical resolution, theoretical, reciprocal bandwidth, $\epsilon_r = 4$	7.5 m
Transmitter Power	10 W
Pulse length	85 μ s
Receive window	135 μ s
PRF	750/375 (nom.) Hz
Antenna	10-m tip-to-tip dipole $G^2 = -5.7$ to 0.2 dB
Post-Processor SNR (worst-best)*	50-58 dB
Horizontal resolution (along track \times cross track)	0.3-1 km \times 3-7 km

Table 1. SHARAD instrument parameters. *Biggest source of uncertainty is antenna gain.

SHARAD Objectives: The primary objective of the SHARAD experiment is to map, in selected locales, dielectric interfaces to several hundred meters depth in the martian subsurface and to interpret these results in terms of the occurrence and distribution of expected materials, including competent rock, soil, water and ice [1].

This is a cautious set of objectives, making no promises about the unique detection of any specific material (e.g., water). The chief obstacles to the success of the SHARAD experiment are (i) subsurface loss tangents larger than anticipated, and (ii) inability to mitigate the effects of surface clutter. Surface clutter can be dealt with in a variety of ways including: (a) operating in areas of smooth terrain, (b) forward mod-

eling of scatter from DEMs, and (c) the use of stereo techniques, as was successfully implemented in Apollo Lunar Sounder Experiment (ALSE) data analysis [2].

Uniqueness of interpretation will be another issue with SHARAD data. The best approach to this problem lies in the integration of SHARAD data with geologic information and with other remote sensing data sets.

Some SHARAD Targets: There are a plethora of potential subsurface targets for SHARAD; two are described below. Mapping of the Polar Layered Terrain with SHARAD is described in another abstract [Nunes and Phillips, this meeting].

Mapping ice depth with SHARAD. The Neutron and Gamma-Ray Spectrometers on the Mars Odyssey spacecraft discovered abundant evidence for subsurface ice [e.g., 3]. While the top of the ice is predicted by theoretical models [4], which are in good agreement with the Neutron Spectrometer data set [5], depths to the bottom of the ice are poorly known. If the ice in the shallow subsurface is just that in equilibrium with the atmosphere, then the equilibrium depth to the bottom of the ice is estimated to be in the range of 10-20 m when the thermal conductivity of ice in the pore spaces is taken into account (M. Mellon, personal communication, 2004). Estimating, or at least constraining, the subsurface ice volume is extremely important in understanding the present-day global water inventory of Mars.

Given SHARAD's vertical resolution, detecting dielectric interfaces in the 10-20 m depth range seems feasible. However, resolution close to the theoretical limit can only be achieved when resolving signals of equal strength, which is not the case when attempting to detect a relatively weak signal from the base of the ice in the presence of a strong surface reflection.

Figure 1 shows the range-focused (chirp compressed) model results for a 15-m depth to the bottom of the ice. The two major points to be made are that choice of data processing parameters matters and that the likelihood of detection depends on the porosity of the soil. A confident interpretation of a shallow reflection in terms of the dielectric interface at the bottom of the ice layer could depend on the integration of other parameters that might control the ice-bottom depth. These include latitude, albedo, thermal inertia, and

local slope. Further, the equilibrium calculations resulting in Figure 1 involve a sharp boundary at the base of the ice; the actual occupation of pore spaces by ice depends on the transient movement of water vapor in the subsurface. Calculations are currently underway to address this issue (M. Mellon, personal communication, 2004).

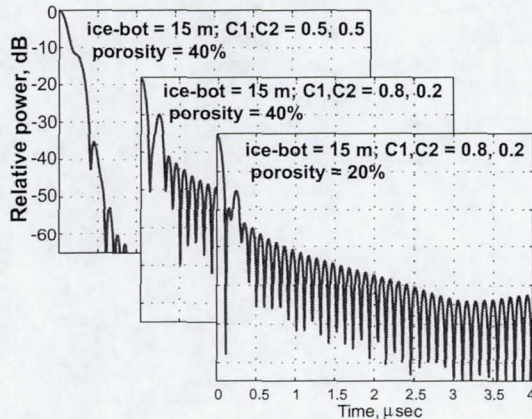


Figure 1. Model detection of an ice bottom at 15 m depth. $w(t) = C_1 - C_2 \cos(2\pi t/T)$ describes the chirp weighting function for pulse length T , and $C_1 + C_2 \equiv 1$. Nominal data processing for best sidelobe control is a Hanning function ($C_1 = C_2 = 0.5$). It is not the best choice here.

Mapping the Etched terrain with SHARAD. The rover Opportunity landed at a hematite-rich region in Terra Meridiani. Earlier geomorphic mapping showed that the hematite occurrence was part of an extensive stack of Noachian layered deposits [6]. An important multi-layered member of this group is a differentially-eroded unit that is high in both thermal inertia and albedo [6,7], termed “etched” terrain. At the Opportunity landing site, hematite spherules weather out of a sulfur-rich bedrock [8] that is in fact the upper layers of the etched terrain [9]. Etched terrain is exposed over at least $3 \times 10^5 \text{ km}^2$ in the Meridiani and western Arabia Terra regions [9], yet is seen to disappear under younger units (Figure 2). As this sulfate-rich unit, in places hundreds of meters thick, is likely indicative of a large standing body of water, mapping the extent of the etched terrain is fundamental to estimating the magnitude of Noachian surface water occurrence. Of course, this is where SHARAD comes in. As a guide to the reflective properties of the top of the etched terrain, we note that the dielectric constant of anhydrite is about 6. Further, the large thermal inertia of this unit implies that it is a relatively highly indurated geological material. Thus SHARAD has a good probability of mapping subsurface occurrences of the etched terrain. Further, because this unit is exposed at the surface, it can be “followed” from there into the subsur-

face, giving confidence to its identification in SHARAD radar returns.



Figure 2. Thermal inertia map of a portion of the Terra Meridiani - W. Arabia Terra region of Mars derived from THEMIS data [10]. Etched terrain and hematite bearing unit are indicated [9]. Etched terrain is buried to the north, but is exposed in some craters. Adopted from [9].

Data Processing and Products: The ~28 Tb of processed SHARAD data holds the potential for a number of important discoveries. Of interest to the Mars science community are the data products to be available. The SHARAD-EDR product is a collection of radar echoes at full resolution, time ordered, with duplicates and transmission errors removed, and located in space and time. The SHARAD-RDR product consists of SHARAD-EDR data that have been converted to complex voltages, Doppler filtered and range compressed, and contains proper engineering and spacecraft information. The SHARAD-DDR product is a radargram, i.e., a 2-D (ground distance, time delay) image of individual sounding profiles (SHARAD-RDR) that have been collated and stacked along track in a way that is similar to that used in terrestrial GPR data displays.

References: [1] Seu, R., *et al.* (2004) *Planet. & Space Sci.*, **52**, 157-166. [2] Peeples, W. J., *et al.* (1978) *JGR*, **83**, 3459-3468. [3] Boynton, W. V., *et al.* (2002) *Science*, **297**, 81-85. [4] Mellon, M. T., and Jakosky, B. M. (1995) *JGR*, **100**, 11781-11799. [5] Mellon, M. T., Feldman, W. C., and Prettyman, T. H. (2004) *Icarus*, **169**, 324-340. [6] Hynek, B. M., Arvidson, R. E. & Phillips, R. J. (2002) *JGR*, **107**, doi: 10.1029/2002JE001891. [7] Arvidson, R. E., *et al.* (2003) *JGR*, **108**, doi:10.1029/2002JE001982. [8] Squyres, S. W., *et al.* (2004) *LPS XXXV*, Abstract # 2187. [9] Hynek, B. M. (2004) *Nature*, **431**, 156-159. [10] Putzig, N. E., *et al.* (2004) *LPS XXXV*, abstract # 1863.

THE MARSIS SCIENCE MISSION. J. J. Plaut¹, G. Picardi², and the MARSIS Team. ¹Jet Propulsion Laboratory, California Institute of Technology, Mail Stop 183-501, Pasadena, CA 91109, plaut@jpl.nasa.gov, ²University of Rome La Sapienza, Infocom Dept., via Eudossiana 18, 00184 Rome, Italy, picar@infocom.ing.uniroma1.it.

The Mars Advanced Radar for Subsurface and Ionospheric Sounding (MARSIS) [1, 2] is an integral component of the Mars Express mission. A low-frequency sounding radar was carried on the Russian Mars 96 spacecraft, and in keeping with the concept of re-flying the science experiments lost on that mission, a call for a radar sounder was part of the Announcement of Opportunity for the 2003 ESA Mars Express mission. MARSIS is the only totally new instrument on Mars Express. The instrument was developed, delivered and operated as a joint effort between the Italian Space Agency and the U.S space agency NASA. The MARSIS science mission has been delayed due to concerns about the safety of the antenna deployment.

As a testament to the importance placed on the MARSIS experiment by ESA and the Mars Express project, the mission was designed to include several phases in which the solar illumination was favorable for low frequency penetration through the night side ionosphere. The first of these phases occurred in 2004. The second is from March through May, 2005. This night side phase in 2005 combines favorable illumination, extensive coverage of the northern hemisphere, and high downlink data rates. MARSIS observations during this period will address key questions on Mars polar deposits, the nature of the northern plains (are they remnants of an ocean?), outflow deposits, and the crustal dichotomy boundary. As solar elevation angles increase later in 2005, MARSIS will focus on ionospheric measurements. Early in the proposed extended mission, MARSIS will have the opportunity to observe the southern hemisphere, including the polar region, on the night side.

MARSIS is unique among instruments on Mars Express; it is the only instrument capable of probing the subsurface of Mars to significant depth. The experiment has the potential to revolutionize concepts about water, climate and the geologic evolution of the planet.

References: [1] Picardi, G. et al. (2003). *Planetary and Space Sci.* 52, 149-156. [2] Nielsen, E. (2004) *Space Sci. Rev.*, 111, 245-262, 2004.

COMPLEMENTARITY OF RADAR AND INFRARED REMOTE SENSING FOR THE STUDY OF TITAN SURFACE. S. Rodriguez¹, S. Le Mouëlic¹, J.P. Combe¹, and C. Sotin¹. ¹ Laboratoire de Planétologie et de Géodynamique de Nantes, Sciences et Techniques, 2 rue de la Houssinière, B.P. 92205, 44322 Nantes, France, email: sebastien.rodriguez@chimie.univ-nantes.fr

Introduction: Earth observations from space highly contribute to the monitoring and discrimination of natural surfaces, as well as to the study of environmental processes such as the water cycle. Among the remote sensing instruments onboard satellite platforms, the most commonly used are the visible/infrared sensors. Indeed, visible/infrared sensors have demonstrated their potential for surface imaging and geophysical investigation since the 1970s. The last decade has also been characterized by the systematic use of active microwave sensors for Earth remote sensing observation, thanks to a great improvement in hyper-frequency technology and the always higher spatial resolution available. Both types of instruments are now often used to cover the same Earth area and derive complementary information on surface properties.

Infrared remote sensing techniques have been implemented for studying the surface of atmosphere-free (or with light atmosphere) planets and satellites such as the Moon, the jovian satellites (Galileo mission) or Mars (missions ISM/Phobos, OMEGA/Mars Express, CRISM/Mars Reconnaissance Orbiter). SARs have been implemented for planetary bodies coated with a dense atmosphere, without infrared complement in the case of Venus (mission Venera, followed by Magellan), but in addition to infrared remote sensing for Titan (Cassini-Huygens mission).

After a brief description of the interest of each type of instrument for planetary surfaces geology, we present the implications that their combined use over the same surface regions could have on images interpretation in general, and on our comprehension of Titan geology in particular.

Complementarities of active radar and infrared remote sensing:

Infrared imagers and spectrometers [1]. As passive sensors, satellite infrared imagers and spectrometers observe the solar light scattered by planetary surfaces. In the case of infrared instruments with spectroscopic capabilities, such as multispectral or hyperspectral cameras, it is possible to retrieve geological key parameters such as the mineralogical composition and the grain sizes of the observed surface. In this wavelengths domain, these instruments are also sensitive to surface temperature and thermal inertia. Due to the short wavelengths used, infrared remote sensing is limited to the study of the very first microns of the

surface, and is highly disturbed by atmospheric absorption or emission. Infrared instruments are quasi-inoperant when the target surface is coated by a dense atmosphere or a large cloud coverage, such as Venus.

Active radars [2]. Compared to infrared instruments, active microwaves sensors have two major advantages: (1) active sensors like SARs are independent of solar radiation fluctuations, (2) in their operating wavelengths range, SARs are not disturbed by atmospheric components such as clouds, droplets, aerosols, molecules of gas, and can probe surfaces in many meteorological conditions. SARs are primarily sensitive to surface geometry and relative humidity (in particular surface dielectric properties, roughness, and relative slope) and are able to penetrate the ground down to a depth of a few wavelengths (typically few centimeters for SAR applications), in a dry geological context like Earth sand desert or Mars dust layer.

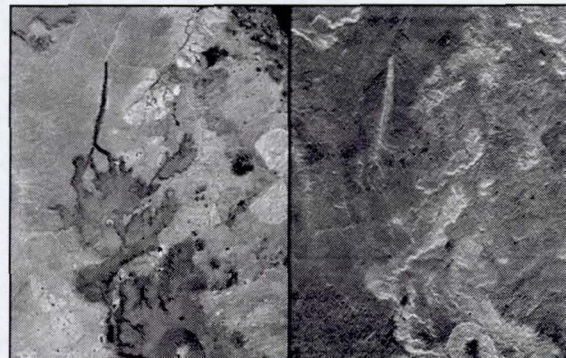


Figure 1: Lavaflows region in Patagonia (Argentina). Infrared Landsat 7 (left) and SRTM Radar (right) images comparison (width: 21 km) - (not copyrighted, courtesy of NASA Visible Earth website).

Example for combined Earth surface remote sensing. Figure 1 shows an example of SRTM (Shuttle Radar Topography Mission) C-band radar image of lavaflows in Patagonia (right) compared to an image of the same region acquired by the Landsat 7 satellite in an infrared wavelength around 2.2 μm (left). In infrared light (left), the image brightness reflects mineral chemistry and both lava flows appear dark. Generally, the upper flow sits atop much lighter bedrock, providing good contrast and making the edges of the flow distinct. However, the lower flow borders some rocks

that are similarly dark, and the flow boundaries are somewhat obscured. In the radar image (right), image brightness corresponds to surface roughness (and topographic orientation) and substantial differences between the flows are visible. Much of the top flow appears dark, which indicates that it is fairly smooth. Consequently, little or no contrast is found with the smooth and dark surrounding bedrock and thus the flow virtually vanishes. However, the lower flow appears rough (and therefore bright) and contrasts well with the adjacent bedrock, in such a way that the flow is locally more distinct here than in the infrared Landsat view. The various differences among these two images illustrate the importance of illumination wavelength in image interpretation and the complementarities between the two techniques in terms of geological characterization.

Implications for spatial exploration of Titan:

The joint NASA-ESA-ASI Cassini-Huygens mission reached the saturnian system on July 1st 2004. It has started the observations of Saturn's environment including its atmosphere, rings, and satellites (Phoebe, Iapetus and Titan). Primary target of the mission, Titan is veiled by an ubiquitous thick haze [3]. Its surface is unreachable to visible wavelengths, except for some infrared atmospheric windows and for greater wavelengths, in the case of an unclouded low atmosphere [4,5]. Onboard the Cassini spacecraft, two instruments are expected to pierce the veil of the hazy moon and successfully image its surface, the first in the infrared (1), and the second one in centimetric wavelengths (2): (1) the VIMS instrument (Visual and Infrared Mapping Spectrometer) that takes hyperspectral images in the range 0.4 to 5.2 μm [6], (2) the RADAR experiment that can operate as Ku-band SAR (2.7 cm wavelength) [7].

On October 26th 2004 Cassini spacecraft flew 1200 km over Titan surface and acquired infrared and SAR data for the first time, but not at the same location. Figure 2 (left) shows the infrared image recorded by the VIMS instrument at 2.03 μm a few minutes before closest approach. This high contrasted image is likely to show high resolution feature coming from Titan surface. In particular at the centre of the image a bright feature clearly shows up. This circular feature is about 30 km in diameter with two elongated features extending westwards. It can be seen in each of the infrared spectral windows. Later the same flyby, Cassini RADAR experiment acquired SAR images of other regions of Titan surface. One of these images is shown on Figure 2 (right). As on VIMS picture (Figure 2 – left), a wide variety of geologic terrain types can be seen on this image. Brighter areas may correspond to

rougher terrains and darker areas are thought to be smoother, probably made of radar-absorbing materials, and sloped away from the direction of illumination. A large dark circular feature is seen at the western end of the image (left of the SAR image), but very few features resembling fresh impact craters are seen. This suggests that the surface is relatively young. Enigmatic sinuous bright linear features are visible, mainly cutting across dark areas. Different interpretations are envisaged for the infrared image (atmospheric feature, cryo-volcanic dome, ...), as well as for the SAR image (lavaflows, ...) but there is at this time no unambiguous argument to discriminate between all of them.

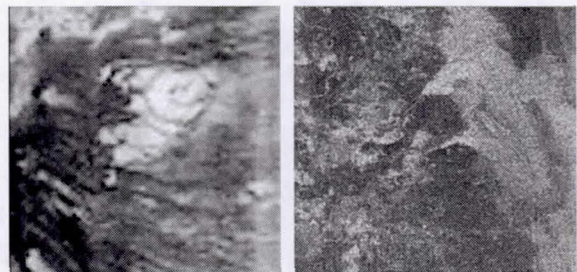


Figure 2: Titan VIMS (left, with kilometeric resolution) and RADAR (right, under kilometeric resolution) images recorded by Cassini during Titan's first flyby on October 26th 2004 (NASA/JPL).

Perspectives: For now, no overlap between Cassini infrared and SAR observations is available, causing difficult interpretation of separate VIMS and RADAR images. But this should happen soon during the planned 44 flybys of Titan. We plan to investigate this information to improve, as it is done for Earth, our understanding of Titan surface processes and global history. In a similar way, it would be very interesting to implement a SAR (in C or L band) in a forthcoming Mars mission in order to complement the currently operating OMEGA/Mars Express instrument (and planned CRISM instrument on MRO) infrared data sets.

References: [1] Rencz A. N. (1999) *Manual of Remote Sensing*, vol. 3, R. A. Ryerson Editor. [2] Henderson F. M. and Lewis A. J. (1999) *Manual of Remote Sensing*, vol. 2, R. A. Ryerson Editor. [3] Lorenz R. D. and Mitton J. (2002) *Lifting Titan's veil: Exploring the giant moon of Saturn*, Cambridge University Press. [4] Smith P. H. et al. (1996) *Icarus*, 119, 336. [5] Rodriguez S. et al (2003), *Icarus*, 164, 213. [6] Brown R. H. et al (2003), *Icarus*, 164, 461. [7] Elachi C. et al (1991), *Proceedings of the IEEE on Geoscience and Remote Sensing*, 79, n.6, 867.

Deep Interior Mission: Imaging the Interior of Near-Earth Asteroids Using Radio Reflection Tomography

A. Safaeinili¹, E. Asphaug², E. Rodriguez¹, E. Gurrola¹, M. Belton³, K. Klaasen¹, S. Ostro¹, J. Plaut¹, and D. Yeomans¹

¹Jet Propulsion Laboratory, California Institute of Technology, Pasadena, CA, ²Earth Science Dept., University of California, Santa Cruz, ³Belton Space Exploration Initiatives

Near-Earth asteroids are important exploration targets since they provide clues to the evolution of the solar system. They are also of interest since they present a clear danger to Earth. Our mission objective is to image the internal structure of two NEOs using radio reflection tomography (RRT) in order to explore the record of asteroid origin and impact evolution, and to test the fundamental hypothesis that some NEOs are rubble piles rather than consolidated bodies. Our mission's RRT technique is analogous to doing a "CAT scan" of the asteroid from orbit. Closely sampled radar echoes are processed to yield volumetric maps of mechanical and compositional boundaries, and to measure interior material dielectric properties.

The RRT instrument is a radar that operates at 5 and 15 MHz with two 30-m (tip-to-tip) dipole antennas that are used in a cross-dipole configuration. The radar transmitter and receiver electronics have heritage from JPL's MARSIS contribution to Mars Express, and the antenna is similar to systems used in IMAGE and LACE missions. The 5-MHz channel is designed to penetrate >1 km of basaltic rock, and 15-MHz penetrates a few hundred meters or more. In addition to RRT volumetric imaging, we use redundant color cameras to explore the surface expressions of unit boundaries, in order to relate interior radar imaging to what is observable from spacecraft imaging and from Earth. The camera also yields stereo color imaging for geology and RRT-related compositional analysis. Gravity and high fidelity geodesy are used to explore how interior structure is expressed in shape, density, mass distribution and spin.

Ion thruster propulsion is utilized by Deep Interior to enable tomographic radar mapping of multiple asteroids. Within the Discovery AO scheduling parameters we identify two targets, S-type 1999 ND43 (~500 m diameter) and V-type 3908 Nyx (~1 km), asteroids whose compositions bracket the diversity of solar system materials that we are likely to encounter, from undifferentiated to highly evolved. The 5-15 MHz radar is capable of probing more primitive bodies (e.g. comets or C-types) that may be available given other launch schedules. 5 MHz radar easily penetrates, with the required SNR, >1 km of basalt (a good analog for Nyx). Basalt has a greater loss tangent than expected for most asteroids, although iron-rich M-types are probably not appropriate targets. 15 MHz radar penetrates the outer ~100 m of rocky 1 km asteroids and the deep interiors of comets. Laboratory studies of the most common NEO materials expected (S-, C- and V-type meteorite analogs) will commence in 2005.

This work was supported by the Jet Propulsion Laboratory, California Institute of Technology under a contract with National Aeronautic and Space Administration and by CalSpace and the University of California, Santa Cruz.

High-Power Radar Sounders for the Investigation of Jupiter Icy Moons

A. Safaeinili¹, S. Ostro¹, E. Rodriguez¹, D. Blankenship², W. Kurth³, D. Kirchner³

¹ Jet Propulsion Laboratory, 4800 Oak Grove Dr., Pasadena, California,

² Institute for Geophysics, John A. and Katherine G. Jackson School of Geosciences, The University of Texas at Austin, Austin, TX 78759

³Dept. of Physics and Astronomy, University of Iowa, Iowa City, Iowa.

The high power and high data rate capability made available by a Prometheus class spacecraft could significantly enhance our ability to probe the subsurface of the planets/moons and asteroids/comets. The main technology development driver for our radar is the proposed Jupiter Icy Moon Orbiter (or JIMO) mission due to its harsh radiation environment. We plan to develop a dual-band radar at 5 and 50 MHz in response to the two major science requirements identified by the JIMO Science Definition Team: studying the near subsurface (<2 km) at high resolution and detection of the ice/ocean interface for Europa (depth up to 30 km). The 50-MHz band is necessary to provide high spatial resolution (footprint and depth) as required by the JIMO mission science requirements as currently defined. Our preliminary assessment indicates that the 50-MHz system is not required to be as high-power as the 5-MHz system since it will be more limited by the surface clutter than the Jupiter or galactic background noise. The low frequency band (e.g. 5 MHz), which is the focus of this effort, would be necessary to mitigate the performance risks posed by the unknown subsurface structure both in terms of unknown attenuation due to volumetric scattering and also the detection of the interface through the attenuative transition region at the ice/ocean interface. Additionally, the 5-MHz band is less affected by the surface roughness that can cause loss of coherence and clutter noise. However, since the Signal-to-Noise-Ratio (SNR) of the 5-MHz radar band is reduced due to Jupiter noise when operating in the Jupiter side of the moon, it is necessary to increase the radiated power. Our challenge is to design a high-power HF radar that can function in Jupiter's high radiation environment, yet be able to fit into spacecraft resource constraints such as mass and thermal limits. Our effort to develop the JIMO radar sounder will rely on our team's experience with planetary radar sounder design gained during our participation in the MARSIS radar sounder implementation.

This work was supported by the Jet Propulsion Laboratory, California Institute of Technology under a contract with National Aeronautics and Space Administration.

EM Properties of Magnetic Minerals at RADAR frequencies. D. E. Stillman and G. R. Olhoeft, Department of Geophysics, Colorado School of Mines, 1500 Illinois St, Golden, CO 80401 (dstillma@mines.edu).

Introduction: Previous missions to Mars have revealed that Mars' surface is magnetic at DC frequency [1,2]. Does this highly magnetic surface layer attenuate RADAR energy as it does in certain locations on Earth [3]? It has been suggested that the active magnetic mineral on Mars is titanomaghemite and/or titanomagnetite [4]. When titanium is incorporated into a maghemite or magnetite crystal, the Curie temperature can be significantly reduced [5]. Mars has a wide range of daily temperature fluctuations (303K – 143K), which could allow for daily passes through the Curie temperature. Hence, the global dust layer on Mars could experience widely varying magnetic properties as a function of temperature, more specifically being ferromagnetic at night and paramagnetic during the day. Measurements of EM properties of magnetic minerals were made versus frequency and temperature (300K-180K). Magnetic minerals and Martian analog samples were gathered from a number of different locations on Earth.

Experimental Method: The majority of the samples were already in a soil form, although several rock specimens had to be crushed into soil using a nonmetallic mortar and pestle. Once the magnetic samples were in a soil form, they were dried in a vacuum at 3×10^{-4} mbar until the weight of the sample did not appreciably change with time (0.005% in 24 hours). The sample was then loaded into a GR-900 sample holder that was connected to an HP 8753 vector network analyzer via two phase matched cables. The sample holder and part of the cables were loaded into a So-Low Ultra-Low freezer where the temperature was adjusted from 303K-180K. The network analyzer recorded data every 5K – 10K. This data was then converted into complex dielectric permittivity and complex magnetic permeability versus frequency [6] and temperature.

Analysis: Most samples showed low losses at RADAR frequencies. However, a grey hematite sample from Keweenaw Peninsula, Michigan possessed a strong temperature dependent dielectric permittivity relaxation, Fig. 1. A nonlinear inversion was used to find the best fit Cole-Cole parameters at each temperature [7]. Only the time constant of relaxation changed as a function of temperature. This variation in time constant of relaxation with temperature was modeled by a generalized Boltzmann temperature dependence [8]. Using an Arrhenius plot, the activation energy of the relaxation was found to be 0.145 eV. The general-

ized Boltzmann temperature dependence was then substituted into the Cole-Cole equation. The equation below is a model of the complex dielectric permittivity versus frequency and temperature, where ϵ^* is the complex relative dielectric permittivity, ϵ' is the real part of the relative dielectric permittivity, and ϵ'' is the imaginary part of the relative dielectric permittivity, k is the Boltzmann constant of 8.6176×10^{-5} eV/K, T is temperature in Kelvin, ω is angular frequency in Hz, and i is the $\sqrt{-1}$.

$$\epsilon^* = \epsilon' - i\epsilon'' = 7.162 + \frac{17.101}{1 + (i\omega(2.56 \times 10^{-13} e^{0.145/kT}))^{0.861}}$$

This temperature dependent dielectric relaxation of grey hematite indicates that RADAR depth of penetration varies with temperature. To demonstrate its effect, the complex permittivity was converted into attenuation at MARSIS and SHARAD frequencies at Sinus Meridiani where grey hematite concentrations range up to 15% [9]. Since Sinus Meridiani does not contain 100% grey hematite, the Bruggeman, Hanai, Sen mixing formula was used (Sen, 1981). The grey hematite was assumed to be mixed into lossless basaltic sediments having a real part of the relative dielectric permittivity of 3. Once the mixed complex permittivity was found, it was then converted into attenuation. Figure 2 shows that the temperature and percentage of grey hematite can have huge effects on the attenuation of RADAR.

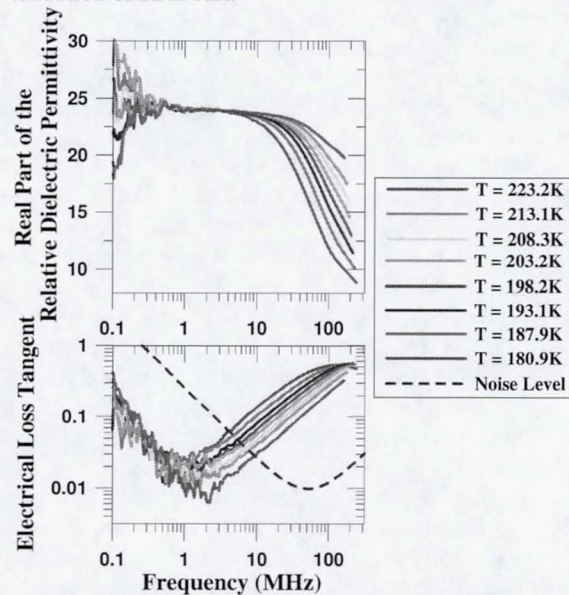


Figure 1. The grey hematite data as a function of temperature and frequency.

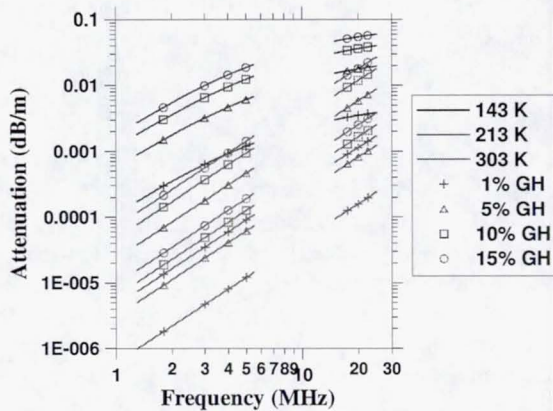


Figure 2. Attenuation at Sinus Meridiani at MARSIS and SHARAD frequencies assuming the only loss mechanism is the grey hematite dielectric relaxation loss (conductivity, scattering, geometrical spreading, and other losses were not included in this calculation). The color of the line represents its temperature while the symbol represents its percent of grey hematite. The symbols are marked at the center frequencies of MARSIS and SHARAD.

Conclusions: Most dry magnetic minerals have low loss in the RADAR frequency range. However, grey hematite contains a significant temperature dependent dielectric relaxation. This loss mechanism should be seen in MARSIS and SHARAD data from Sinus Meridiani. This frequency and temperature dependent loss mechanism could be used to find areas of subsurface grey hematite. This loss mechanism could also be used to estimate heat flow in the upper Martian subsurface if multiple measurements could be made at the same location at different temperatures.

Acknowledgements: This project is funded by NASA Grant 20119458 NAG5-12754. We appreciate the help of Steve Sutley of the USGS who conducted our XRD measurements. Thanks also for the experimentation assistance provided by Justin Modroo, Brianne Douthit, Beau Winters, Andy Kass, Ross Wagle, Matt Hergert and Paul Schwering from Colorado School of Mines.

References: [1] Hargraves R. B. et al. (1979) *JGR*, 84, 8379-8384. [2] Hviid S. F. et al. (1997) *Science*, 278, 1768-1770. [3] Olhoeft G. R. and Capron, D.E. (1993) USGS Open File Report, 93-701, 214p. [4] Morris R.V. (2001) *JGR*, 106, 5057-5083. [5] Hunt C.P. (1995) in *Rock physics and phase relations*, p. 189-204. [6] Canan, B., (1999) PhD thesis Colorado School of Mines, 332p. [7] Cole, K.S. and Cole R.H., (1941) *The Jour. Chem. Phys.*, 9, p 341-351. [8] Olhoeft, G.R. (1976) in *The physics and Chemistry of Rocks and Minerals*, p. 261-278. [9] Christensen,

P.R. et al. (2001), *JGR*, 106, p, 23873-23885. [10] Sen, P.N. et. al. (1981), *Geophyscis*, 46, p. 781-795.

GROUND-PENETRATING RADAR IN MARS ANALOG TERRAINS: TESTING THE STRATA INSTRUMENT. K.K. Williams¹, J.A. Grant¹, and A.E. Schutz², ¹Center for Earth and Planetary Studies, MRC 315, National Air and Space Museum, Washington, DC 20013-7012, williamsk@nasm.si.edu, ²Geophysical Survey Systems, Inc., 13 Klein Drive, North Salem, NH, 03073.

Introduction: Ground-penetrating radar (GPR) has been recognized as a time-saving tool for non-invasive exploration of subsurface structures and radar properties [1]. Whereas GPR has been employed for a variety of geological, archaeological, and engineering problems on Earth, its potential usefulness onboard future Mars rovers has also been discussed [2-7]. In support of development of the *Strata* GPR instrument for Mars rovers [8], prototype and commercial antennas were used to collect data in several Mars analog environments. Field testing was conducted in volcanic, cratered, and fluviually modified environments in northern Arizona (Fig. 1a) [9], ice-rich and ice-poor locations in the Canadian arctic (Fig. 1b) [10], and a paleo glacio-deltaic environment in southern Maine. Data collected at these locations demonstrate the ability of the *Strata* prototype to reproduce accurately the results of commercial antennas, which can reveal subsurface stratigraphy to depths of 10s of meters, depending on the substrate.

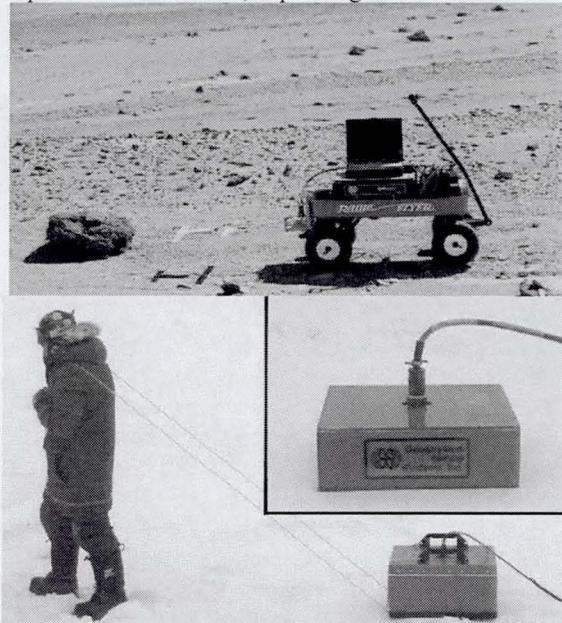


Fig. 1. a) Top: Early *Strata* prototype at 2002 FIDO site. b) Bottom: GSSI antenna in arctic setting. Inset shows mature *Strata* antenna.

Instrumentation: Field data were collected with commercially available Geophysical Survey Systems, Inc. (GSSI) radar controllers and antennas. Antennas used in various parts of this study operated at peak frequencies of 200, 400, 500, 900, and 1500 MHz.

Strata prototypes, also designed and built by GSSI, are low-mass, low-power, low-volume simple, loaded dipole antennas that operated at 600 and 400 MHz. An early, unshielded version was used at the Arizona sites and a mature, low-profile antenna was tested in the extreme environment of the Canadian arctic and was used to collect 3-D data over a deltaic deposit in Maine. As a complement to GPR data, seismic profiles were collected at several sites in Arizona and resistivity data were collected in the arctic.

Field Operations: This study complements others that employed GPR in Mars analog terrains in Egypt and other arid areas [4, 7, 11]. Those studies showed the ability of GPR to constrain local geologic setting and history in extremely arid areas, and this work reports on data collected in moderately arid, frozen, and moist environments. At each location, data were collected along traverses at several different frequencies using commercial antennas. Data were also collected with the prototype *Strata* instrument in different configurations, depending on the location. At the Arizona locations, an early prototype was suspended 20-25 cm above the ground. A more mature prototype was used at the arctic and Maine sites where data were collected with the antenna at ground level and elevated 50 cm above the surface. In addition, data were collected with the prototype 1 m above the ground at some locations in the arctic. Data collection with the prototype antenna above the ground was meant to mimic a likely configuration of a Mars rover-mounted GPR where the antenna would be mounted to the rover underside to minimize risk to rover operations. At the Maine site, a data grid was collected to demonstrate the ability to assemble GPR data profiles into a 3-dimensional representation of dipping layers in the subsurface

Results: As expected, the performance of the commercial and prototype instruments depended on subsurface properties, but penetration in excess of 5-10 meters was achieved at most locations. A summary of results from different locations follows.

Northern Arizona. Testing of the *Strata* instrument took place at iron-rich volcanic, cratered, and fluviually modified sites including Sunset Crater, Meteor Crater, and the 2002 FIDO test site near Cameron. The greatest penetration among these sites in Arizona was at Sunset Crater where up to 5 meters of loose cinders overlaid basalt flows. GPR data collected with the *Strata* and commercial antennas reveal details of

layering within the cinders while revealing interface between cinders and basalt flow (Fig. 2). Interesting stratigraphic relationships were also revealed at Meteor Crater, though signals penetrated less deeply because of the higher dielectric properties. Data showed continued dipping of the southern ejecta blanket beneath an alluvium cover, which had a relatively high permittivity of 5. This interface could be followed to a depth of almost 3 meters, and has been confirmed by excavation [12]. At the FIDO site, GPR data confirmed the stripped nature of the surface and absence of a buried channel.

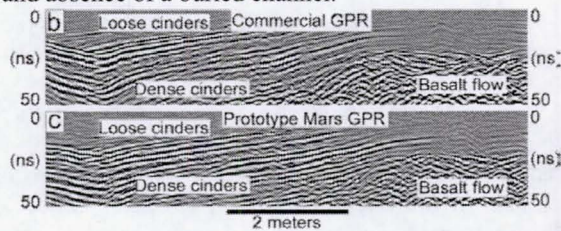


Fig. 2. GPR data collected at Sunset Crater. Top is using commercial antenna, bottom is using prototype antenna.

Canadian arctic: Fieldwork took place in the Mackenzie Delta, Northwest Territories in March 2004 when air temperatures dipped to -40 and the ground had been constantly frozen for more than 5 months. Coordinated data collection with GPR and resistivity provided complementary datasets where locations of buried ice bodies detected in resistivity data could be compared to radar properties revealed in GPR data. Analysis of the two geophysical datasets shows that GPR signals are affected by material property differences between frozen ground and massive ice (Fig. 3). GPR profiles were also effective at detecting the base of the active layer (region that undergoes thaw in the summer) even though it was completely frozen when data were collected. Results from permafrost are especially relevant to Mars studies in light of the detection of near surface ground ice at moderate latitudes on Mars [13, 14].

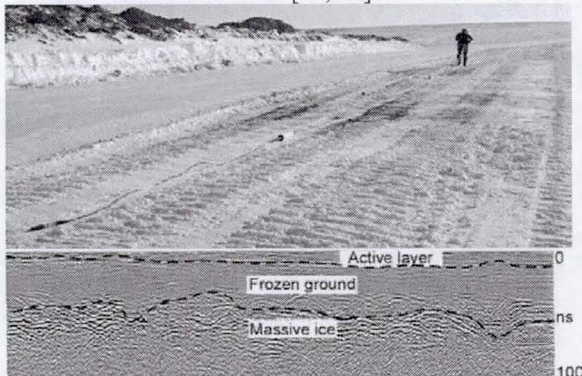


Fig. 3. Area in Mackenzie Delta where geophysical data were collected. Bottom: 400 MHz *Strata* profile of ice interfaces.

Deltaic deposit. Southern Maine contains many areas where dipping, layered strata were deposited in deltas during the Pleistocene [15]. A 400 MHz GSSI antenna and the *Strata* prototype were used to collect data in parallel profiles that could be assembled into a 3-D data cube to add a new dimension to visualization of the subsurface (Fig. 4). The dipping foreset deposits are easily resolved, and horizontal slices through the data cubes show the strike of the dipping layers.

Summary: During development of the *Strata* GPR for Mars rovers [8], data were collected in a variety of Mars analog settings and effectively constrain subsurface layers even when the *Strata* antenna was mounted 50 cm or 1 m above the surface. The ability to reveal subsurface structure and properties remotely without drilling or excavating has proven invaluable on some applications on Earth and would add a new dimension to rover-based investigations on Mars or other solid bodies in the solar system

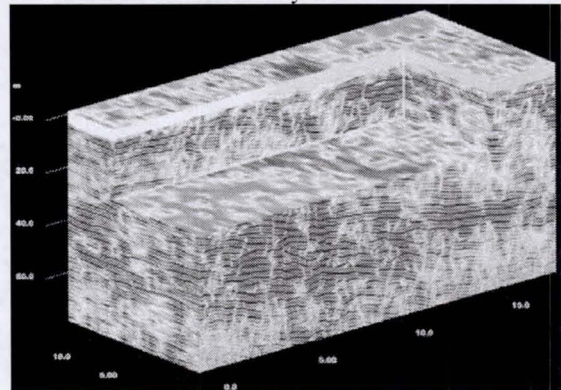


Fig. 4. 3-D data cube of deltaic deposit in SW Maine. Data collected with 400 MHz *Strata* antenna mounted 50 cm above the surface.

- References:** [1] Ulriksen, C.P.F. (1982) *Applications of Impulse Radar to Civil Engineering*: Ph.D. Thesis, Sweden. [2] Olhoeft, G.R., (1998) *Proc. GPR'98*, 177-182. [3] Olhoeft, G.R., (1998) *Proc. GPR'98*, 387-392. [4] Paillou, P. et al. (2001) *GRL*, 28, 911. [5] Grant, J.A. et al. (2003) *JGR*, 108. [6] Leuschen, C. et al. (2003) *JGR*, 108. [7] Grant, J.A. et al. (2004) *JGR* 109. [8] Grant, J.A. et al. (2005) *this volume*. [9] Williams, K.K. et al. (2004) *LPSC XXXV*, Abstract #1563 [10] Williams, K.K. et al. (2004) *EOS Trans. AGU*, Spring Meet. Suppl. [11] Maxwell, T.A. et al. (2002) *GSA*, 34, 174. [12] Grant, J.A. and P.H. Shultz (1993) *JGR*, 98, 15,033. [13] Boynton, W.V. et al. (2002) *Science*, 297, 81. [14] Feldman, W.C. et al. (2002) *Science*, 297, 75. [15] Tary, A.K. and D.M. Fitzgerald (2001) *GSA Boston*, #113-0.

Invertibility of Radar Layers in the Martian North Polar Cap for Flow and Mass Balance Parameters. D.P. Winebrenner¹, M.A. Fahnestock², E.D. Waddington³, ¹University of Washington, Applied Physics Laboratory and Department of Earth and Space Sciences, Box 355640, Seattle, WA 98195 USA, dpw@apl.washington.edu, ²Institute for the Study of Earth, Oceans and Space, University of New Hampshire, Durham, NH 03824 USA, mark.fahnestock@unh.edu, ³University of Washington, Department of Earth and Space Sciences, Box 351310, Seattle, WA 98195 USA, edw@ess.washington.edu.

Introduction: Understanding the present and past states of the Martian residual polar caps is critical to understanding climate and volatile-cycling on Mars [1,2].

The MARSIS and SHARAD radar sounders offer a near-term prospect not only of measuring ice cap thickness and basal topography, but also of observing internal structure, and in particular englacial layering. Observations of englacial layers in terrestrial ice caps have been exceptionally valuable for inferring current and past accumulation rates and ice flow [cf. 3-5].

The Martian polar caps and the terrestrial ice caps differ substantially in many ways. The Martian north polar cap, however, may be least dissimilar to ice caps on Earth. Although accumulation rates and flow speeds probably differ between the two by about 2 and 3 orders of magnitude, respectively, sophisticated modeling now offers some guidance as to the likely situation (modulo significant uncertainties in material parameters, subglacial topography, and possible disequilibrium with the current Martian climate) [6,7]. It is therefore of interest to explore the implications of terrestrial experience for what we might expect to learn from englacial layer observations in the Martian north polar cap, and for what difficulties might be expected.

A preliminary comment about the roles of physical sophistication and complexity in forward vs. inverse modeling may be in order. As a rule, greater realism and accuracy is achieved in forward modeling of ice sheets when the full, 3-dimensional (3-D) and time-varying behavior of an ice sheet is taken into account. Thus forward modeling of ice sheets on Earth and Mars has progressed from 1-D, steady-state models toward 2- and 3-D, non-equilibrium models. The inversion of observations to diagnose, for example, time variation in ice sheet parameters clearly relies on such realistic forward models. However, in our experience, crucial initial insights can be obtained from relatively simple data inversions based on 1-D, steady-state forward models, even in cases where some 3-D and temporal variation surely occurs. We therefore adopt the latter approach in this first investigation.

Experience in Greenland: Englacial radar layers in terrestrial ice sheets are surfaces of constant age, i.e., isochrones (with rare, if any, exceptions). Perhaps the simplest generally useful model for isochrones of

age t_i (before present), at heights y_i from the base of an ice sheet of thickness H (constant in space and time), whose surface accumulation rate λ_H m of ice per year, is the 1-D, steady-state Dansgaard-Johnson model [4,8]:

$$t_i = \frac{(2H - h)}{2 \cdot \lambda_H} \ln \left(\frac{2H - h}{2y_i - h} \right), \quad h = y_i = H, \quad (1)$$

$$t_i = \frac{(2H - h)}{2 \cdot \lambda_H} \left(\frac{h}{y_i} - 1 \right) + t_h, \quad 0 = y_i = h, \quad (2)$$

where h is the shear layer thickness at the bottom of the ice sheet (which typically ranges from 0 to a few hundred meters in terrestrial ice sheets), and t_h is the age of a layer at height h according to equation 1. These equations can be modified in the cases of basal sliding and basal melting. The simplest modification for the case of melting is to use equation 1 alone, set $h=0$, and replace λ_H by $\lambda_H - \lambda_M$, where λ_M is the basal ablation rate in meters of ice per year (which yields the so-called Nye-with-melt model) [5].

Equations 1 and 2 result from consideration (in the simplest approximations) of the horizontal strain necessary to remove ice deposited on the surface (in steady state), and the corresponding vertical strain rates required by the incompressibility of the ice and conservation of mass within the ice sheet [8]. These latter properties of the ice are responsible for the transmission of information about shear layer thickness and basal conditions up to heights well above the bed.

Point knowledge of the t - y (i.e., age/depth) relation, as well as accumulation rate fields, are available in Greenland. Fahnestock and co-workers have fit equations 1 and 2 (and their variations) to dated englacial layers which were tracked by airborne radar sounding, and thus inferred accumulation rates over large areas with useful accuracy [4], and revealed areas of basal ablation [5] (see Figure 1) which were unexpected [9]. This is notable in view of converging and diverging flow, as well as variation since the last glacial maximum, in regions of the ice sheet where the inversion was performed.

Prospective Application to Mars: There is some question as to whether englacial radar layers (i.e.,

abrupt dielectric or magnetic variations) in the Martian north polar cap are sure to be isochronous. However, present understanding of Martian climate variation

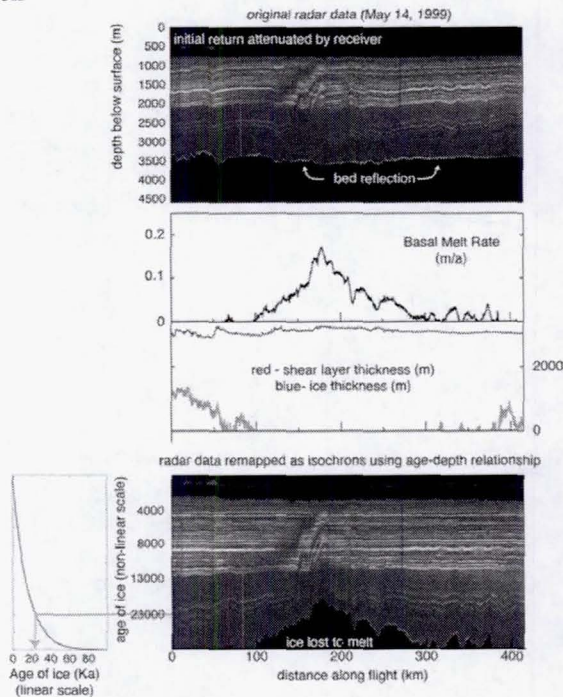


Figure 1. (After[5]) Greenland radar profiles, and the same data mapped versus a “standard” age-depth function using the derived age-depth function at each profile. The horizontal character of the layers mapped by age fits; the self-similarity of the layer patterns along the radar profiles displayed in this manner demonstrates their isochronous nature. Also plotted are the derived basal melt rate, the ice thickness H , and the shear layer thickness h .

and the north polar cap suggests that buried englacial layers would result from effectively isochronous, ice-cap wide variations in dust or volatile deposition [2,10], both of which would have dielectric expressions. We therefore provisionally assume that englacial radar layers in the Martian north polar cap will be isochrones. We also assume that radar observations will show the ice sheet bed, and thus the heights of layers above the bed.

Observations of the seasonal retreat of the north polar seasonal cap suggest that water ice accumulation on the residual cap may be concentrated in summer and near the pole [11,12]. Thus, for example, the segment of the meridian in Hvidberg’s model [7] nearest the pole may flow similarly to terrestrial ice domes,

and may be a good candidate for inversion using englacial layers. Prospective accumulation and strain rates are likely small compared to those in terrestrial ice domes, but the key difference from Earth will be the lack of an age/depth scale, at least for the foreseeable future. This lack precludes a simple application of methods developed for Greenland [4,5].

Instead, we propose to examine, in place of (t,y) -pairs on layers, the variations in layer height along several (presumed-isochronal) layers as functions of the distance x from the ice divide (i.e., dome center), stopping well short of the first trough faces [7]. For a given layer i , heights y_{ik} at distances from the divide $\{x_k\}$, $k = 1, \dots, j, \dots, m, \dots, K$, share a common age, t_i . For simplicity consider only layers above any shear layer, and assume (provisionally) no basal melting or sliding, and that the surface accumulation rate, λ_H , varies according to some specified form over the limited range of x . Then from equation 1

$$\frac{(2H-h)}{2} \cdot \ln \frac{2H-h}{2y_{ij}-h} = \frac{(2H-h)}{2} \cdot \ln \frac{2H-h}{2y_{im}-h}$$

The equations for several layers with several points on each layer appear to be invertible for h and the ratios $\lambda_{Hm}/\lambda_{Hj}$. The inversion would seek to characterize strain thinning of layers with increasing depth due to ice flow. If, however, no plausible values of λ_H and h provide a good fit to the data (within errors), we would conclude that an alternative ice flow model, e.g., a model that is non-steady-state, is required. Successively in this way, we could delineate some sets of flow and accumulation regimes and parameters allowed and disallowed by the observations. In view of the present lack of knowledge, such a delineation would almost surely be valuable.

References: [1] Zuber, M.T. (2004) *Science* 302, 1694-1695. [2] Clifford, S.M. et al. (2000) *Icarus* 144, 210-242. [3] Conway, H., et al. (1999) *Science* 286, 280-283. [4] Fahnstock, M.A. et al. (2001) *J. Geophys. Res.* 106, 33789-33797. [5] Fahnstock, M.A., et al. (2001) *Science* 294, 2338-2342. [6] Greve, R. (2000) *Icarus* 144, 419-431. [7] Hvidberg, C. (2003) *Ann. Glac.* 37, 363-369. [8] Dansgaard, W., and S.J. Johnsen (1969) *J. Glac.* 8, 215-223. [9] Dahl-Jensen, D., et al. (1997) *J. Glac.* 43, 300-306. [10] Laskar, J. et al. (2002) *Nature* 419, 375-377. [11] Aharonson, O. et al. (2004) *J. Geophys. Res.* 109, doi:10.1029/2003JE002223. [12] Kieffer, H.H., and T.N. Titus (2001) *Icarus* 154, 162-180.

APPLICATION OF AN ORBITAL GPR MODEL TO DETECTING MARTIAN POLAR SUBSURFACE FEATURES. Y. Xu,¹ S. A. Cummer,¹ and W. M. Farrell,² ¹Electrical and Computer Engineering Department, Duke University, PO Box 90291, Durham, NC 27708 (ybxu@ee.duke.edu, cummer@ee.duke.edu), ²NASA/Goddard Space Flight Center, Code 695, Greenbelt, MD 20771 (william.farrell@gssc.nasa.gov).

Introduction: There are numerous challenges in successfully implementing and interpreting planetary ground penetrating radar (GPR) measurements. Many are due to substantial uncertainties in the target ground parameters and the intervening medium (i.e., the ionosphere). These uncertainties generate a compelling need for meaningful quantitative simulation of the planetary GPR problem. An accurate numerical model would enable realistic numerical GPR simulations using parameter regimes much broader than are possible in laboratory or field experiments. Parameters such as source bandwidth and power, surface and subsurface features, and ionospheric profiles could be rapidly iterated to understand their impact on GPR performance and the reliable interpretation of GPR data.

Model: We present initial orbital GPR simulations from a 2.5D model that computes fully 3D fields scattered from 2D subsurface and surface inhomogeneities and propagated through an arbitrary ionospheric profile. This model is based on finite difference time domain methods and splits the computational volume into two pieces; one treats the near surface and subsurface fields and the other treats the ionospheric propagation. The computational volume the propagation in the near vacuum between the ground and ionosphere is treated with simpler but accurate plane-wave decomposition methods to maximize computational efficiency. The simulated return signals can be any field component and are automatically calibrated in absolute power and field strength. By accounting for essentially all of the important GPR effects that can be difficult to compute analytically, this model enables accurate numerical experimentation with realistic instrumental and environmental parameters.

Application: We apply this model towards answering the question of whether key Martian polar subsurface targets are likely to be visible using orbital GPR. There are a number of obstacles to MARSIS radar sounding of deep basal lakes and inter-glacial aquifers in the Martian polar subsurface, including signal losses from the ionospheric medium, subsurface ice conductivity, and reflective losses in the strongly layered subsurface. Using our planetary GPR model, we attempt to realistically assess the impact of all of these effects on the ability to detect these critical water-based features in the Martian

polar subsurface. We model the subsurface using a set of MGS/MOC images of the exposed icy and dusty polar layered deposits to identify the layering structure. While the composition of these layers (particularly their permittivity) is unknown, assumptions are made to associate a permittivity to each layer and we scale the image to determine the layer vertical spatial dimensions. Using this set of physically realistic subsurface parameters and an empirical range of ionospheric parameters, we bound the environmental and instrumental conditions under which these deep polar water features might be detectable.

IN-SITU REMOTE SENSING REFLECTANCE MEASUREMENTS IN CASE 2 WATER. Yuhu Yan¹, ¹Water Resources Science, University of Minnesota (356 MWAH, UMD, Duluth, MN, 55812, yanx0057@d.umn.edu).

For testing and improving atmospheric correction algorithms and in-water algorithms for retrieving the concentration of substance in Case 2 water, we have to measure in-situ remote Sensing reflectance (R_{rs}) precisely. However reflectance from rough water-surface introduces uncertainty in the measurements of R_{rs} . To alleviate this problem we used 5 different methods for determination of R_{rs} of West Lake Superior by combination of above-surface, below-surface and polarization measurements of radiance. The results provide consistent values of R_{rs} and indicate that our methods are practical and helpful for reliable determination of R_{rs} (Figure 1).

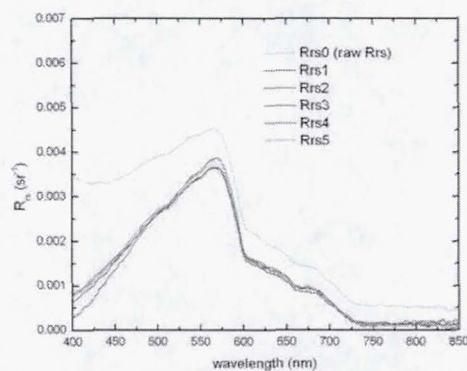


Figure 1. The comparison of R_{rs} from Method I to V

Notes

Notes
